



BUREAU OF ECONOMIC GEOLOGY • W.L. Fisher, Director  
The University of Texas at Austin • Austin, Texas 78712

1979

Report of Investigations No. 93  
**Landsat Analysis  
of the  
Texas Coastal Zone**

by Robert J. Finley



Report of Investigations No. 93

# Landsat Analysis of the Texas Coastal Zone

by Robert J. Finley

assisted by Robert W. Baumgardner, Jr.



*BUREAU OF ECONOMIC GEOLOGY • W.L. Fisher, Director  
The University of Texas at Austin • Austin, Texas 78712*

1979



**Part 1: Evaluation of Unenhanced Landsat Imagery  
for Land Cover and Land Use Delineation of the Texas Coast**

**CONTENTS**

Abstract .....	3	Analysis of test site 3 .....	15
Introduction .....	3	Site description .....	15
General remarks .....	3	Mapping results .....	17
Project objectives .....	3	Change detection .....	21
Background .....	4	Analysis of test site 5 .....	22
Mapping techniques for image interpretation .....	4	Site description .....	22
Coastal Zone applications of remote sensing .....	4	Mapping results .....	22
Methods and approach .....	4	Analysis of test site 4 .....	24
Updating the Coastal Atlas to provide a regional base for the Texas coast .....	4	Site description .....	24
Data acquisition package for image interpretation .....	5	Mapping results .....	25
Development of image-interpretation techniques ..	7	Dredge-spoil detection .....	30
The optical-interpretation procedure .....	7	Change detection .....	30
An image-analysis schedule .....	7	Discussion of test site results .....	32
Development of change-detection techniques .....	7	Evaluation of map products .....	33
Development of a land cover - land use classification scheme .....	8	Procedures .....	33
Results .....	11	Results .....	33
Test site overview .....	11	Conclusions .....	35
Analysis of test site 2 .....	11	Acknowledgments .....	35
Site description .....	11	References .....	36
Mapping results .....	12	Appendices	
		A—Wind velocity and direction time histories at the time of each image .....	38
		B—Accuracy evaluation for each scene, by category	40

**FIGURES**

1. Environmental geology map update .....	6	13. Wind-tide effects at Pass Cavallo .....	19
2. Example of line boundary map .....	7	14. Guadalupe River delta area .....	20
3. Change-detection procedure .....	8	15. Site 5 line boundary map .....	22
4. Coastal Zone precipitation and temperature data .....	10	16. Brazos Santiago Pass area .....	23
5. Test site locations .....	12	17. Geographic features in site 4 .....	24
6. Site 2 line boundary map .....	13	18. Site 4 line boundary map, February 25, 1975 ....	25
7. San Luis Pass area .....	13	19. Site 4 line boundary map, July 10, 1975 .....	26
8. Freeport area .....	14	20. Site 4 line boundary map, February 2, 1976 ....	27
9. Geographic features in site 3 .....	15	21. Site 4 line boundary map, December 16, 1972 ...	28
10. Site 3 line boundary map, March 29, 1974 .....	16	22. Aransas Pass area .....	29
11. Site 3 line boundary map, February 25, 1975 ....	17	23. Summary of dredge-spoil additions .....	31
12. Pass Cavallo area .....	18	24. Sequence of dredge-spoil additions .....	31
		25. Radiance changes in site 4 .....	31

**TABLES**

1. Suggested imagery package .....	5	5. San Antonio Bay area vegetation .....	21
2. Image-interpretation schedule .....	8	6. Images used in dredge-spoil study .....	30
3. Land cover and land use classification .....	9	7. Map accuracy, all maps .....	34
4. Pass Cavallo area vegetation .....	21	8. Map accuracy, first map of each site .....	34

**MAPS—LANDSAT IMAGERY - DERIVED LAND COVER - LAND USE**

Freeport - San Luis Pass area .....	in pocket	South Padre Island - Laguna Madre area .....	in pocket
San Antonio - Espiritu Santo Bay area .....	in pocket	Harbor Island area (February 25, 1975) .....	in pocket
Harbor Island area (July 10, 1975) .....	in pocket		



## Part 2: A Guide to Visual Interpretation of Texas Coastal Features from Landsat Imagery

### CONTENTS

Abstract .....	45	Woodland or dense chaparral .....	57
Introduction .....	45	Water .....	57
Satellite system characteristics .....	45	Wetland .....	58
Standard Landsat data products .....	47	Topographically low marshes .....	58
The Landsat coastal project .....	48	Topographically high marshes .....	58
Coastal Zone applications of Landsat imagery .....	48	Tidal flats .....	59
Classification modification and development .....	48	Sea grass and algal flats .....	59
Mapping techniques .....	49	Vegetated dredge spoil .....	59
Recognition of land cover - land use classes .....	49	Barren land .....	59
Urban and built-up land .....	51	Beaches .....	59
Industrial .....	51	Dunes .....	59
Extractive—hydrocarbons .....	51	Barren dredge spoil .....	60
Transportation .....	51	Undifferentiated barren land .....	60
Mixed urban .....	51	Evaluating the map product .....	60
Agricultural land .....	51	Conclusions .....	60
Cropland .....	51	Acknowledgments .....	60
Grassland/rangeland .....	52	References .....	64
Range-pasture .....	52	Appendix	
Vegetated dunes .....	57	C—Annotated bibliography on the application	
Vegetated barrier flat .....	57	of aerial photographs and Landsat imagery	
Brushland .....	57	to coastal regions .....	65
Forest land .....	57	Glossary .....	71

### FIGURES

26. Locations of Landsat investigation test sites for the Texas coastal region .....	46	28. Hoskins Mound and High Island salt domes imaged on Landsat band 5 .....	52
27. Locations of Landsat false-color composite segments shown in plate 1 .....	50	29. Band 5 imagery and interpretation of turbidity plume, Aransas Pass, Texas .....	58

### TABLES

9. Spectral bands of the Landsat multispectral scanner products .....	45	11. U. S. Geological Survey land use and land cover classification system .....	49
10. Formats of standard Landsat image products .....	47	12. Summary of map-interpretation characteristics .....	61

### PLATE 1—ANNOTATED SEGMENTS OF LANDSAT FALSE - COLOR COMPOSITE IMAGES

A — Freeport area, May 8, 1973 .....	53
B — Freeport area, February 2, 1976 .....	53
C — Matagorda Island - Espiritu Santo Bay area .....	53
D — South Padre Island area .....	53
E — Kenedy County inland dune area .....	53
F — Harbor Island - Corpus Christi Bay area .....	53

## Part 1

---

# Evaluation of Unenhanced Landsat Imagery for Land Cover and Land Use Delineation of the Texas Coast





## ABSTRACT

Mapping based on Landsat imagery was initiated along the Texas coast for four test sites selected for contrasting vegetation, environmental geology, and levels of economic development. Standard Landsat transparencies of part of a 1:1,000,000 band 7 image were optically enlarged to fit an existing 1:125,000 map base. Land-water, cropland, and other distinctive boundaries were extracted from the enlargement and compiled on an overlay on which additional unit boundaries from other bands and from the false-color composite of bands 4, 5, and 7 were added.

Each resulting map unit was then classified according to a bilevel scheme modified from published systems to meet the priorities of this study. These priorities are, in order of greatest emphasis, the inventorying and monitoring of wetlands, land use, beaches and dunes, and bay systems. Primary classes include urban and built-up land, agricultural land, grassland, rangeland, woodland, water, wetland, and barren land. Twenty-three secondary categories include five wetland classes: topographically low marshes, topographically high marshes, tidal flat, submerged sea-grass beds and algal flats, and vegetated dredge spoil. Water was separated into four classes on the basis of turbidity to emphasize flow pattern and suspended-sediment distribution rather than water-body type.

Change detection was accomplished by overlaying enlarged positive and negative transparencies. Areas of radiance change were caused by seasonal growth stage of wetland vege-

tation, burning of rangeland, and status of cropland. Multiple transparencies in bands 5 and 7 were used to map the addition of barren dredge spoil, a unit that was easily detected as a result of its extremely high reflectance. Band 5 images provided a synoptic view of the turbidity plume issuing from Aransas Pass and indicated that turbid water was derived from both the inlet and the surf zone adjacent to the jetties.

The test sites mapped were the Freeport - San Luis Pass area, the upper San Antonio Bay - Espiritu Santo Bay vicinity, southern Padre Island - Laguna Madre, and the Harbor Island area. Substantial variation in areal extent and species content of wetlands was found. The limits of delineation of all categories depended on the size of the map unit relative to Landsat's limit of resolution, reflectivity contrast with surrounding units, and unique characteristics of each image. Mapping of the Harbor Island site from three successive scenes showed significant variations in the detectability of urban and transportation features.

An evaluation of the Landsat mapping was made by a random-point comparison with aerial photographs. A mean accuracy of 87.4 percent was obtained for the 806 points checked; within each category, results varied from 64.9-percent accuracy for undifferentiated barren land to 93.1-percent accuracy for cropland. The results indicate that Landsat offers a valuable source of current information on coastal resources for use in conjunction with the existing data base on Texas coastal resources.

## INTRODUCTION

### GENERAL REMARKS

The use of remotely sensed data for mapping purposes varies from oblique aerial photographs collected from a small airplane through conventional and high-altitude vertical photography to imagery from manned and unmanned orbital craft. Resolution commonly decreases, whereas the area covered by a single image increases through this sequence; the product from each platform offers a unique vantage point. The use of Landsat multispectral scanner (MSS) imagery in four bands permits the mapping and interpretation of Earth resources over a 10,000 n mi<sup>2</sup> area of synoptic coverage for each scene. Each Landsat satellite scans this same area every 18 days, and even with data losses caused by cloud cover and variations in sensor function, a substantial amount of excellent coverage is being obtained. Compilations by Freden and others (1973a, 1973b), Smistad and others (1975), Williams and Carter (1976), and Short and others (1976) demonstrate the wide variety of applications being made of Landsat data, including those in the Coastal Zone.

### PROJECT OBJECTIVES

The Texas Coastal Zone comprises about 6 percent of the total area of the State, but about 34 percent of its economic resources are found adjacent to the 367 mi of Gulf of Mexico shoreline. This distribution results partly from the abundance of hydrocarbon and other mineral reserves, ground-water supplies, transportation facilities, fish and wildlife resources, and recreational opportunities in the area. Any coastal region is highly dynamic and is modified continually by daily processes of erosion and accretion, by the passage of storms, by natural biologic processes, and by the presence of man. Industrial, agricultural, and residential development continue to have an ever-increasing impact on the Texas coastal ecosystem. In order to evaluate the rate and direction of environmental change, in both unmodified and modified areas, periodic mapping is essential (McGowen and others, 1976b).

To help meet the needs of the State of Texas for current information on the dynamic coastal area, an investigation



of the application of Landsat imagery was conducted involving the visual interpretation of standard Landsat image products. The image-interpretation procedure that was developed is dependent only on optical enlargement of standard 1:1,000,000 7.3-inch, film-positive transparencies, combined with basic photointerpretation principles. The objective in applying this procedure and in perfecting the map format has been to support the capability of the State of Texas to monitor wetlands, coastal land cover and land

use, areas of shoreline change, and bay and estuarine systems of the Texas Coastal Zone. Although the image-interpretation techniques reported here are applicable to studies in other areas, the land use classification scheme has been designed specifically for the mapping of coastal features. Therefore, environmental geologic units, such as barren dredge spoil and dunes, are included, as are such coastal biologic assemblages as vegetated barrier flats and two distinct marsh types.

## BACKGROUND

### MAPPING TECHNIQUES FOR IMAGE INTERPRETATION

During literature review, emphasis was placed on locating research related to wetlands mapping and image interpretation of Landsat film products. Most techniques termed "conventional," as opposed to "computer aided," involve optical or electro-optical color-enhancement processes. Because acquisition of the special equipment needed to implement these techniques was not part of this investigation, developmental efforts were aimed at perfecting a relatively simple mapping technique.

### COASTAL ZONE APPLICATIONS OF REMOTE SENSING

Multiband photography used by Pestrone (1969) and color aerial photographs used by Grimes and Hubbard (1971) have documented the response of marshland vegetation on different film types. Wetland analyses using photography were also carried out by Anderson and Wobber (1973), Reimold and others (1973), and Klemas and others (1974). The use of Landsat data for mapping wetland vegetation has been described by R. R. Anderson and others (1973), Carter and Schubert (1974), and Bartlett and others (1975). The latter investigation, as well as that by R. R. Anderson and others (1975), includes analysis of Skylab orbital photography.

No comprehensive coastwide study of Texas marsh flora has been published. Differences in ecology between the well-documented Atlantic wetlands and the Gulf Coast

marshes contributed to the need for detailed ground studies of vegetation within this investigation. Such studies were carried out by the Texas Parks and Wildlife Department (Clements, 1976). Remote sensing studies (Erb, 1974, Weisblatt, 1976, and personal communications), analyses of vegetation in conjunction with geologic investigations (Andrews, 1970; McGowen and Brewton, 1975; Brown, coordinator, in progress), and dissertation research (Johnston, 1955) provided information on Texas marshes. For the southern Laguna Madre test site, where marshes are scarce and saline grasslands abundant, Fleetwood (1973) provided a valuable species list and summary of environments. For the middle and upper Texas coast, where marshes become more extensive as annual rainfall increases towards the northeast, a study of the Louisiana coastal region (Chabreck, 1972) was helpful in classifying field transect data.

The classification of land cover and land use other than wetlands was accomplished by adapting the categories of J. R. Anderson and others (1972, 1976) to the needs of this study. Specialized Level III units uniquely suited to the Coastal Zone, such as vegetated barrier flats, have been fitted within the framework provided by established classification systems.

Some of the standard Level II categories were entirely omitted. Water, for example, was classified on the basis of turbidity to emphasize flow patterns and suspended-sediment distribution rather than water-body type. Because most users of satellite data within Texas are already familiar with the distribution of reservoirs, canals, and estuaries, including such information was unnecessary.

## METHODS AND APPROACH

### UPDATING THE COASTAL ATLAS TO PROVIDE A REGIONAL BASE FOR THE TEXAS COAST

*The Environmental Geologic Atlas of the Texas Coastal Zone* series (Brown, coordinator, in progress) includes an environmental geology map published at a scale of 1:125,000 but originally mapped at a scale of 1:24,000. This map provides an excellent regional base which has been used to control the scale of enlargements of Landsat

images and to aid in evaluation of the test site mapping. To ensure that these maps reflect current conditions, the February 1975 aerial photographs taken for this investigation by NASA (Mission 300, 1:120,000 scale) were used to produce a transparent overlay showing recent changes. The area covered by the photographs approximately corresponds to the seaward half of each Environmental Geology sheet, or a coast-parallel strip 20 to 25 mi (32.2 to 40.2 km) wide.

Differences between the maps and the photographs were classified as either additions or deletions. Additions refer to boundary expansion of an existing area within the same category or to delineation and classification of a new area, all the boundaries of which are new. Deletions refer to areal contraction of an existing classified area. Most of the changes were considered additions. For example, the emplacement of new dredge spoil was considered addition of dredge spoil rather than deletion of bay bottom.

The updated overlays are intended to be used with the color prints of the Environmental Geology maps from the Coastal Atlas; the overlay line boundaries are derived from the same negatives as the original map (fig. 1). Categories in the explanation on the original map were numbered, making it easy to tag all changes with the appropriate new category on the overlay. Recent land use changes were also defined by comparison with the Current Land Use map of the Environmental Geologic Atlas, and the new areas were labeled according to the land cover - land use classification scheme adopted as part of this study.

Most changes detected using the Mission 300 photographs were minor revisions relating to realignment of channels, dumping of dredge spoil, erosion and deposition along shorelines, and changes in the configuration of tidal inlets. As expected, the man-induced changes relate to industrial, commercial, and residential development, whereas the natural changes occur where coastal geologic and biologic processes normally are most active. Natural changes include the effects of tidal and longshore currents, wind, and the colonization of new substrate by marsh vegetation. No field confirmation of these results was made, except coincidentally within areas of test site mapping. The overlays will remain available at the Bureau of Economic Geology in open-file format for use by all interested persons and State agencies.

## DATA ACQUISITION PACKAGE FOR IMAGE INTERPRETATION

The need to define a selected purchase package of Landsat imagery results from the wide variety of standard products available from the Earth Resources Observation System (EROS) Data Center. Table 1 lists the package suggested for use with the image-interpretation procedures developed during this investigation. Acquisition of the entire package is recommended only for scenes of primary interest that are entirely free of cloud cover and that exhibit individual bands of high quality (numerical rating of at least 8). Purchase of single black-and-white positive transparencies is recommended for scenes in which the data quality of individual MSS bands or the location of cloud cover requires further evaluation.

The following comments apply to the item-by-item listing (table 1):

1. *1:1,000,000 false-color transparency.*—This data format is excellent for discrimination within vegetated areas and is by far the most useful Landsat standard product. Comparison may easily be made with

color-infrared aerial photographs. Barren areas of moderate reflectance, industrial sites, and dredge spoil are readily distinguished from surrounding vegetation. Seasonal changes in wetland and range-land vegetation are easier to detect as differences in color tone than as differences in shades of gray.

2. *1:1,000,000 positive transparencies, bands 4 through 7.*—Together with the false-color composite, these are the primary products from which image interpretation by optical enlargement may be accomplished. Band 4 is of low utility because of the effects of atmospheric haze and humidity, but it may be useful in defining urban areas. Band 5 is affected less by these effects and may be used to delineate built-up areas, surface drainage patterns, roads and airports, and suspended-sediment patterns in water bodies. Bands 6 and 7 provide the best land-water boundary discrimination, including the details of coastal wetland drainage. The preparation of a map base showing land-water boundaries is facilitated by use of data from band 7.
3. *1:1,000,000 negative transparencies, bands 5 and 7.*—These products have been used to produce (1) paper (contact) prints for use in the field or group discussion and (2) film-positive enlargements for use in map preparation over the test site areas. River drainage seems somewhat easier to detect on the band 5 negative than on the positive.
4. *1:250,000 paper print, bands 5 and 7.*—The acquisition of these prints may be considered optional because they are not actually used in the map preparation process. However, the prints are useful for display and discussion and for quick reference to the imagery at a larger scale than that of the 7.3-inch transparencies.

Table 1. Suggested purchase package  
for each scene of Landsat imagery.

Item	Scale	Band	Cost
1. Color transparency	1:1,000,000	composite	\$ 15.00
2. Black-and-white print	1:250,000	5	20.00
		7	20.00
3. Black-and-white positive transparency	1:1,000,000	4	10.00
		5	10.00
		6	10.00
		7	10.00
4. Black-and-white negative transparency	1:1,000,000	5	10.00
		7	10.00
Cost if color master already available . . . . .			\$115.00
Additional cost of false-color composite master . . . . .			50.00
Cost if false-color composite master needed . . . . .			\$165.00



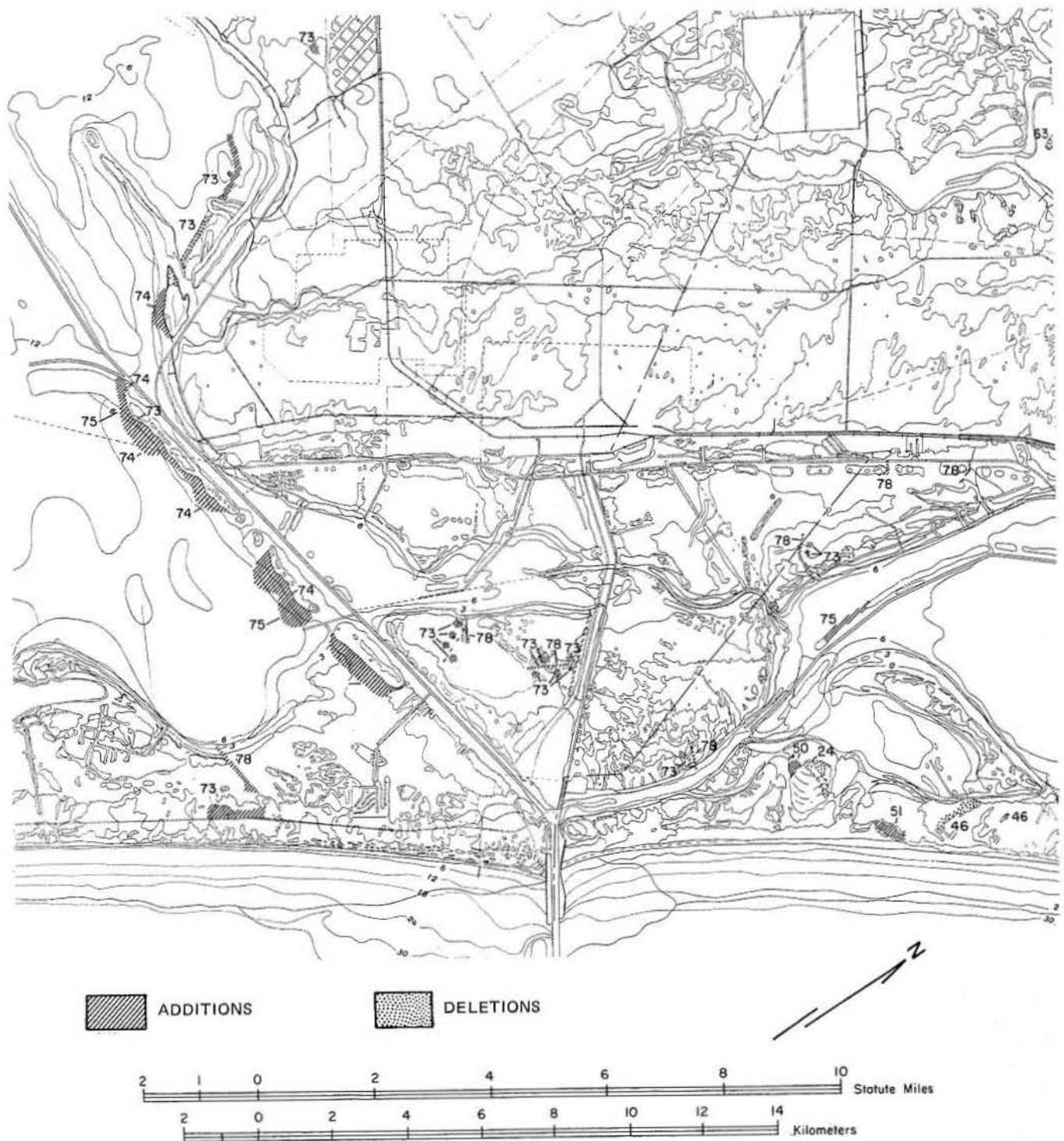


Figure 1. An example of the overlay updating the Environmental Geology map, published by the Bureau of Economic Geology, covering the Harbor Island area. The following categories are indicated: 24, wind-tidal flat; 46, stabilized blowout-dune complex; 50, washover distal fan; 51, fore-island blowout dunes; 63, bay and lagoon mud; 73, subaerial spoil; 74, subaerial reworked spoil; 75, subaqueous spoil; 78, dredged channel.

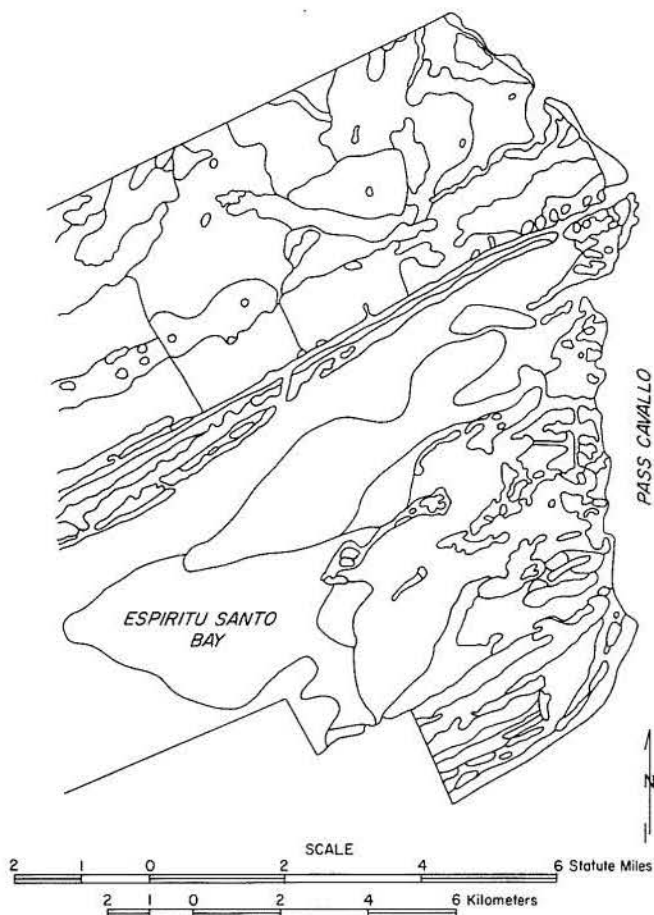


Figure 2. Image-interpretation line boundary map of part of test site 3, Pass Cavallo area.

### DEVELOPMENT OF IMAGE-INTERPRETATION TECHNIQUES

Direct image interpretation of standard Landsat products without optical or electro-optical color enhancement apparently has been attempted only on a minor scale. Literature on such procedures is limited. Initial development of mapping techniques in this investigation used imagery of the San Antonio - Espiritu Santo Bay area (test site 3) dated March 29, 1974 (1614-16261), and February 25, 1975 (2034-16200). The approaches that were considered included (1) mapping directly from 1:250,000 Landsat paper prints; (2) using the Bausch and Lomb Zoom Transfer Scope to enlarge 7.3-inch Landsat transparencies to a scale of 1:125,000, without a Landsat map base for the test site area; and (3) producing a 1:125,000 enlargement of band 7 data, for use as a base, followed by mapping from transparencies under the Zoom Transfer Scope.

#### The Optical-Interpretation Procedure

The 1:250,000 scale used for the Landsat print was considered too small to work with for site-specific studies.

Because an excellent coastwide map base is available in the form of 1:125,000 scale Environmental Geology maps (Brown, coordinator, in progress), this larger scale was given consideration as the project mapping scale. When it was found that the 1:1,000,000 Landsat transparencies could be optically enlarged 8 times without serious loss of image quality, the 1:125,000 mapping scale was adopted. A base of Landsat data across the test site was required, however, to avoid inaccuracies caused by shifts in field of view when using the Zoom Transfer Scope.

The map for each scene was initiated by making an enlarged positive transparency of the test site from the 1:1,000,000 band 7 negative. This enlargement was prepared by the Automation Division of the Texas Department of Highways and Public Transportation using either a Durst or a Laborator No. 184 enlarger. All land-water boundaries and other easily distinguishable features were transferred from the transparency to a transparent stable film. The map was then completed by projecting enlarged false-color composite and single-band transparencies onto the stable film, drawing line boundaries (fig. 2), and classifying each feature. The map units were hand colored according to the land cover - land use classification scheme developed during this investigation (maps in pocket).

### An Image-Analysis Schedule

The optical-interpretation procedure was integrated into a series of steps which was followed from initial review of each Landsat scene through final analysis of the resulting map (table 2). To use the classification scheme developed as part of this investigation, the interpreter must be familiar with the area to be mapped. This expectation is reasonable if Landsat data are to be used in monitoring critical coastal environments. The detailed Environmental Geologic Atlases of the coastal region (Brown, coordinator, in progress), in addition to standard topographic maps and aerial photographs, provided necessary supplemental data. A small aircraft was available for low-altitude observation and photography and was also used during initial study of each test site. Although supplemental data were available during mapping of the test sites, classification decisions made during the image-interpretation process were based solely on the Landsat data. Detailed study of supporting data relating to the classification of an area from Landsat imagery was not begun until after the entire test site was mapped (step 5, table 2). A description of mapping techniques and results of analysis (step 8, table 2) follows discussion of the individual test sites.

### DEVELOPMENT OF IMAGE-INTERPRETATION TECHNIQUES FOR CHANGE DETECTION

The types of change detection attempted using Landsat imagery during this investigation included (1) variations in areal extent of a category, (2) change in the classification of an area, and (3) temporal signature differences within a classified area. Examples of these types of change are, respectively, the addition of spoil material along the margins of dredged channels, change in classification



Table 2. Evaluation review schedule for image-interpretation analysis.

1. Review aerial photographs, Coastal Atlas maps, and published tide and weather data for test site and image date.
2. Take a preliminary field trip to become generally acquainted with test site (may include oblique aerial photography).
3. Complete line boundary map of test site area from image interpretation of Landsat.
4. Classify features delineated according to the project classification scheme.
5. Study supportive data in detail; review results; field check and select areas for biological verification.
6. Document results for the Landsat scene, especially problems and unique aspects of the imagery.
7. Hand-color image interpretation at 1:125,000 scale and produce overlays of selected quadrangles at 1:24,000 scale.
8. Perform accuracy analysis using randomly selected points.
9. Evaluate format and content of resulting Landsat map.
10. Evaluate image interpretation of this scene in conjunction with other scenes for the same test site.

because of leafing out of deciduous vegetation between a winter and summer scene, and temporal changes such as seasonal burning of coastal prairie grasslands. In the latter case, if the interpreter were aware of the burning practices, he would not alter his classification of a grassland area but would simply take notice of the sharp change in observed radiance.

Actual practice in delineating changes detectable with Landsat imagery indicated that (1) changes in areal extent of categories adjacent to water bodies could be detected by overlaying 1:125,000 line boundary maps, (2) category changes could be detected by using side-by-side comparison of classified maps, and (3) temporal changes resulting in radiance differences could be detected by overlaying positive and negative transparencies on a light table. These methods for detection of radiance differences were used with 1:125,000 scale enlargements of band 7 images covering test sites 3 and 4. Figure 3 shows that the sense of radiance change indicated for a light area depends on the selection of a positive or negative for the older or the newer scene, respectively. Changes which have been detected and mapped relate to burning of grasslands, status of agricultural fields, growth stage of wetland vegetation, and the degree of exposure of tidal flats. The specifics of these results are included in the discussion of test sites 3 and 4.

#### DEVELOPMENT OF A LAND COVER - LAND USE CLASSIFICATION SCHEME

In establishing a workable classification system for land cover and land use within the Texas Coastal Zone, the multilevel system of J. R. Anderson and others (1972, 1976) was modified to meet the needs of this investigation. These areas of emphasis were the monitoring of wetlands, other land uses, beaches and dunes, and bay systems. The resulting scheme (table 3) contains 23 secondary classes, 14 of which are specifically oriented toward uniquely coastal geologic processes and biologic assemblages. Categories in the standard system that are not applicable to the coastal environment were deleted, whereas wetlands were expanded from two to five categories, and water was subjectively classified on the basis of turbidity. The number codes assigned to each of the 23 subcategories are consistent with the U. S. Geological Survey system (J. R. Anderson and others, 1976). Most secondary categories

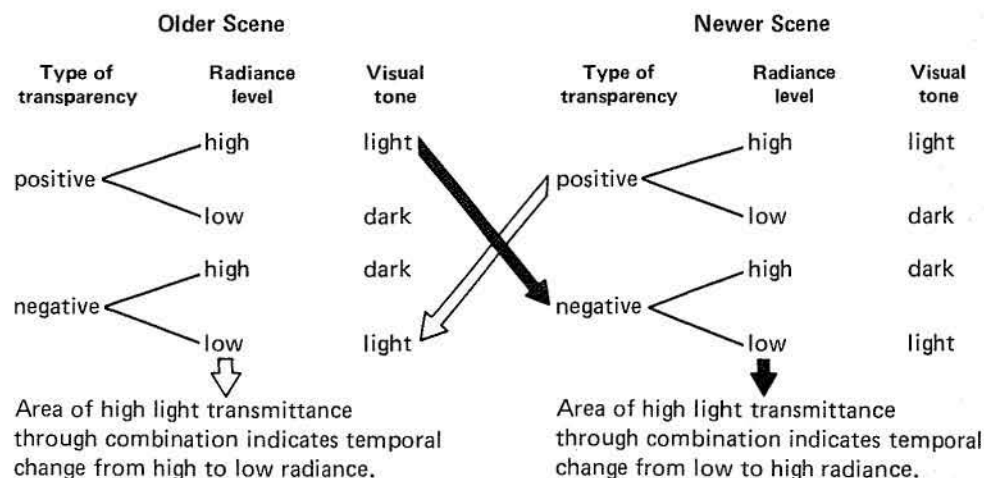


Figure 3. Schematic diagram of change-detection procedure based on observed radiance differences.

carry a three-digit code, indicating that they would be considered specialized units of regional interest, or Level III units, when placed in the context of the national system.

All wetland units, for example, are subunits of non-forested wetland, coded 62 in the standard system. Water was not classified at Level II because the designation of lakes, streams, estuaries, and so forth, is readily available to the intrastate user from supplementary information, whereas turbidity distribution is an indicator of surface-water circulation patterns.

Although wetlands may be defined on the basis of elevation references such as the mean high-tide mark (Clark, 1974), it would perhaps be more meaningful to define coastal wetlands as areas that are near sea level and adjacent to bay, lagoonal, or fluvial water bodies and that naturally contain plants tolerant of inundation, as by tidal or wind-tidal action. Swamps contain primarily woody vegetation in contrast to marshes, which are dominated by grasses and which are often mapped as fresh, brackish, or saline marsh associations, depending on species content. Erb (1974) found that only salt marshes could be mapped consistently from Landsat film data and that delineation of fresh and brackish marshes was only partly successful.

Table 3. Land cover and land use classification for use with unenhanced Landsat data in the Texas Coastal Zone (numbers refer to system in J. R. Anderson and others, 1976).

1. Urban or built-up land	(13)	Ui - Industrial
	(131)	Ue - Extractive—hydrocarbons
	(14)	Ut - Transportation
	(16)	U - Mixed urban
2. Agricultural land	(21)	A - Cropland
3. Grassland/rangeland	(31)	G - Range-pasture
	(311)	Gd - Vegetated dunes
	(312)	Gb - Vegetated barrier flat
	(32)	WO - Woodland or dense chaparral
4. Forest land	(43)	WO - Woodland or dense chaparral
5. Water	(501)	WA - Non-turbid
	(502)	WAs - Slightly turbid
	(503)	WAm - Moderately turbid
	(504)	WAt - Highly turbid/very shallow
6. Wetland	(621)	Wlm - Topographically low marsh
	(622)	Whm - Topographically high marsh
	(623)	Wtf - Tidal flat
	(624)	Wga - Sea grasses and algal flats
	(625)	Ws - Vegetated dredge spoil
7. Barren land	(72)	B - Beaches
	(731)	Bd - Dunes
	(732)	Bds - Barren dredge spoil
	(77)	Bu - Undifferentiated barren land

Study of the Texas coastal region indicates that the marshes could be divided into topographically high and low categories that appear to differ primarily in water content and in reflectivity of the vegetation on the Landsat false-color composite image. Computer classification of Landsat digital data for a test site near Galveston Bay (Erb, 1974) indicates a transition between the reflectivity of low, wet marsh groups and higher, drier zones, which in turn is related to the percentage of open water and soil-moisture variations rather than to the changes in vegetation type.

The Level I category of wetlands has been subdivided (table 3) into five units in order to extract as much information as possible from the Landsat data; each of these units is briefly described. The two marsh categories do not imply a particular assemblage of species regionwide; instead, field checking has shown that the same group of species generally occurs within a category throughout a test site. Local exceptions are found where river influx creates a fresh- to brackish-water environment or where tidal inlets admit water of full marine salinity.

Tidal flats are wetlands with sparse or no vegetation that occur on the bay margins of the barrier islands, adjacent to the marsh wetlands, and along the mainland margin. South Texas includes the greatest extent of tidal flats, as a result of the extremely shallow depth of Laguna Madre, the low-lying topography of the abandoned Arroyo Colorado delta, and the presence of shallow, generally barren depressions throughout the area that are connected to the lagoon. Algal flats and subaqueous grassflats also occur most widely in South Texas. The algal flats occur as a thick, sediment-binding mat on the surface of the extensive tidal flats. The largest sea-grass flats are found within the lagoon near Brazos Santiago Pass, where the circulation of Gulf waters helps maintain a conducive environment. Vegetated dredge spoil is classified as a distinct wetland mapping unit because of its composition and biologic assemblages. It is readily detectable on the Landsat imagery on the basis of form and position relative to the dredged channels. Its reflectance is similar to that of topographically high marsh, and field checking has indicated that many of the same plant species are found in both units. Because the presence of dredge spoil, either vegetated or barren, represents an important alteration of the coastal environment by man, the ability to detect this unit on repeated satellite imagery is significant for coastal zone management purposes.

The classification system shown in table 3 is strongly oriented toward image interpretation. With a background in coastal processes and familiarity with the Texas coastal environment, an interpreter can distinguish the secondary classes on the basis of radiance, texture, shape, and spatial position of an area in relation to other features seen on the Landsat imagery. It was recognized that the classes derived from digital processing would not precisely correlate with those delineated during the image-interpretation procedure. An example of such a disparity is the division of a tidal flat, during digital processing, into several classes on the basis of reflectance differences owing to varying moisture content. These classification dissimilarities were resolved by side-by-side comparison of visually interpreted and digital products, as well as by use of supplemental data.

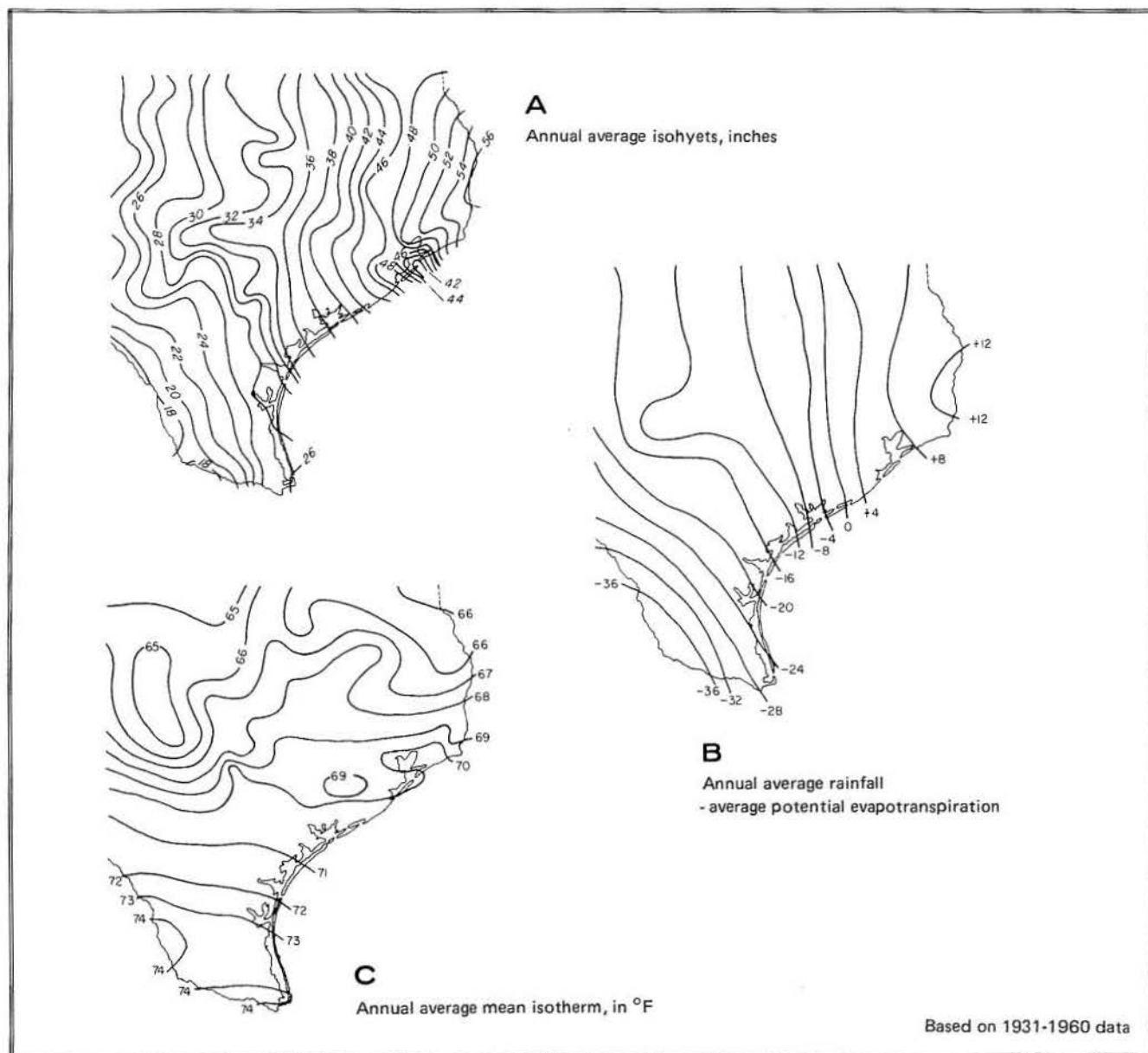


Figure 4. Precipitation and temperature data for the Texas Coastal Zone (from Fisher and others, 1972).



## RESULTS

### TEST SITE OVERVIEW

Climate along the Texas coast varies from humid at the Louisiana border to semiarid at the boundary with Mexico. The strong gradients of precipitation and temperature (fig. 4) result in contrasting land use, diverse biological assemblages, differences in environmental geology, and variations in active processes along the coast from north to south. To develop techniques for the application of Landsat imagery to wetland and land use mapping throughout this region, three test sites (2, 3, and 5, fig. 5) were chosen from differing climatic areas. Site 4 (fig. 5) was reserved for final testing of the mapping techniques and of the classification scheme developed during analysis of the other sites.

Dense coastal vegetation, absence of wind deflation of sandy areas, and the infrequent occurrence of hurricane-washover channels are indications of the importance of positive effective precipitation (excess of rainfall over evapotranspiration) on the northern Texas coast (Fisher and others, 1972). This importance is in contrast to the southern Texas coastal region where evapotranspiration exceeds rainfall, washover channels and dunes are abundant, and wind transport of sediment contributes to the formation of vast tidal flats on the landward side of the barrier islands.

Other factors which influence the physical environment of all test sites are wind and tidal range. The Texas coast is influenced by prevailing southeasterly winds from March through November and dominant northerly winds from December through February. The latter are associated with the passage of cold fronts, which are often followed by low temperatures, low humidity, and fair weather, during which excellent Landsat imagery can be obtained.

The tidal regime in the Gulf of Mexico is microtidal (range less than 2 m; Davies, 1964). Diurnal tidal ranges (U. S. Department of Commerce, 1975b) of 1.4 ft (0.42 m) and 1.7 ft (0.52 m) are given for Galveston Channel and Aransas Pass, respectively, and within the bays the periodic tide has a range of less than 0.5 ft (15 cm). With these low astronomical tides, wind stress becomes a relatively important influence on water levels. Northerly winter winds tend to lower water levels in the nearshore Gulf of Mexico, whereas the onshore component of the southeasterly

summer winds tends to raise water levels. These effects are evident on Landsat imagery, therefore wind direction and velocity summaries were prepared from published data (appendix A) as an aid in the interpretation of each scene. Actual records of water levels at the time of satellite passage were obtained from gauges located within the test site that are maintained by the Galveston District of the U. S. Army Corps of Engineers.

No phase of this investigation dealt directly with the physical results of hurricanes. Hurricanes, of course, have a tremendous impact on the Texas Coastal Zone, and the effects of such storms are felt an average of once every 2 to 3 years.

### ANALYSIS OF TEST SITE 2

#### Site Description

The Freeport - San Luis Pass test site is situated within a strandplain developed on a Holocene deltaic headland (McGowen and Scott, 1975). The Coastal Plain slopes gently gulfward at a rate of 2 to 3 ft per mi, and the relatively flat coastal prairies give way to marshes and bay systems toward the coastline (McGowen and others, 1976a). Dunes on Follets and western Galveston Islands are low and well vegetated. The regional excess of moisture beyond that evaporated or transpired by plants contributes to successful stabilization of the loose sand.

Topographically low saline marshes are present along the bay margins in the vicinity of San Luis Pass and contain abundant *Spartina alterniflora* (smooth cordgrass) and *Batis maritima* (maritime saltwort). Along the Gulf Intracoastal Waterway south of Freeport, saline to brackish marshes include these species and, at slightly greater elevation, *Distichlis spicata* (seashore saltgrass), *Salicornia* spp. (glasswort), and *Monanthochloe littoralis* (shoregrass). The upper elevations of the high marsh, subject to only occasional flooding by saltwater (Arp, 1975), include abundant *Spartina spartinae* (gulf cordgrass) and *Spartina patens* (marsh hay cordgrass). The high-marsh ecosystem grades laterally into coastal saltgrass prairie which is dominated by *Spartina spartinae*, but includes shrubs such as *Iva frutescens* (marsh elder) and *Baccharis halimifolia* (groundsel tree), as well as other grasses (Clements, 1976).



Figure 5. Project test site locations.

Urban development within this test site is centered around Freeport and the Brazosport shipping facilities. Major chemical and petroleum-production-related industries are concentrated here, along with numerous smaller industries serving the petrochemical complexes. Many dredged channels are associated with commercial activities in the area, and a series of hurricane-surge-protection dikes has been built. These structures have altered the natural distribution of flora in some areas. Very little cropland is

found within the test site; the coastal prairie grasslands are extensively grazed.

#### Mapping Results

Image interpretation of Landsat film transparencies readily reveals the complex active and abandoned natural drainage patterns, as well as dredged channels and the details of natural and jettied inlets within this coastal

## TEST SITE 2

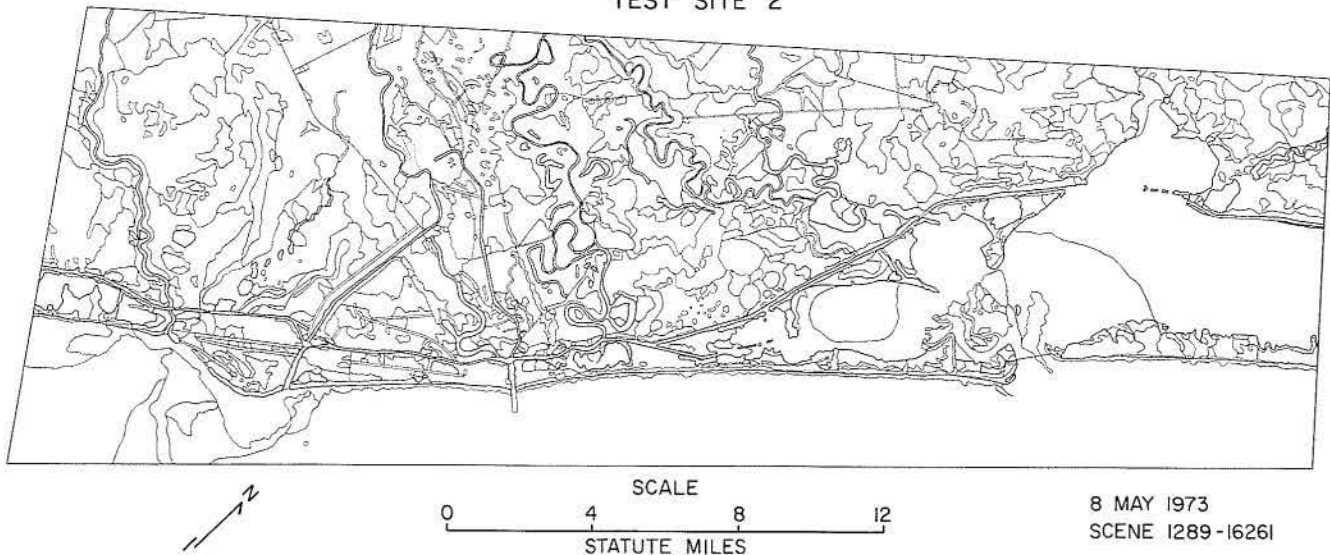


Figure 6. Unclassified line boundary map of the Freeport - San Luis Pass test site (map showing land cover - land use classes is included in pocket).

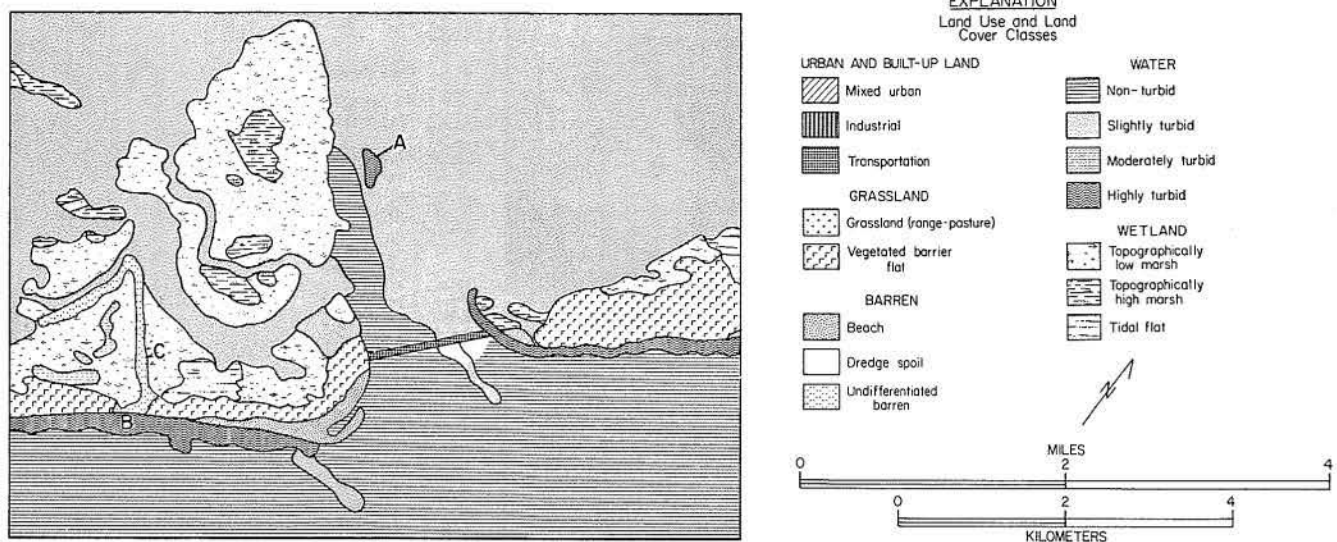


Figure 7. San Luis Pass area with classified land and water units delineated from Landsat scene 1289-16261, May 8, 1973 (lettered locations are explained in text).

segment (fig. 6). San Luis Pass (fig. 7), an unmodified tidal inlet, is spanned by a highway bridge that is detectable with Landsat data. Extensive topographically low marshes just inside the pass were correctly identified and contain an abundance of *Spartina alterniflora*. Islands of lesser water content and higher reflectance vegetation surrounded by the low marsh were classified as high marsh, a decision which appears valid after examination of 1:30,000 color-infrared aerial photographs.

However, some initial errors in classification also occurred; three examples are illustrated in figure 7. A barely emergent marshy island (A, fig. 7) was mapped as highly turbid or shallow water. Where beach width decreases to less than 80 m (B, fig. 7)—the size of one picture element

(pixel), or the minimum resolution element of the satellite detectors—the subaerial beach, breaking waves, and near-shore zone of turbid water appear as a zone of highly turbid or shallow water adjacent to the vegetated barrier flat. A strip of high-reflectance sand (C, fig. 7) is mapped as undifferentiated barren rather than dredge spoil because the adjacent channel, about 50 m wide, cannot be distinguished from the surrounding wet, low marsh.

Woodlands within the test site include *Quercus virginiana* (live oak), *Carya* spp. (hickory and pecan), and scattered *Celtis* spp. (hackberry) and were most easily detected where dense stands parallel creeks and rivers. The live oak seem to give an especially bright infrared response on the Landsat false-color composite. Brushland, where



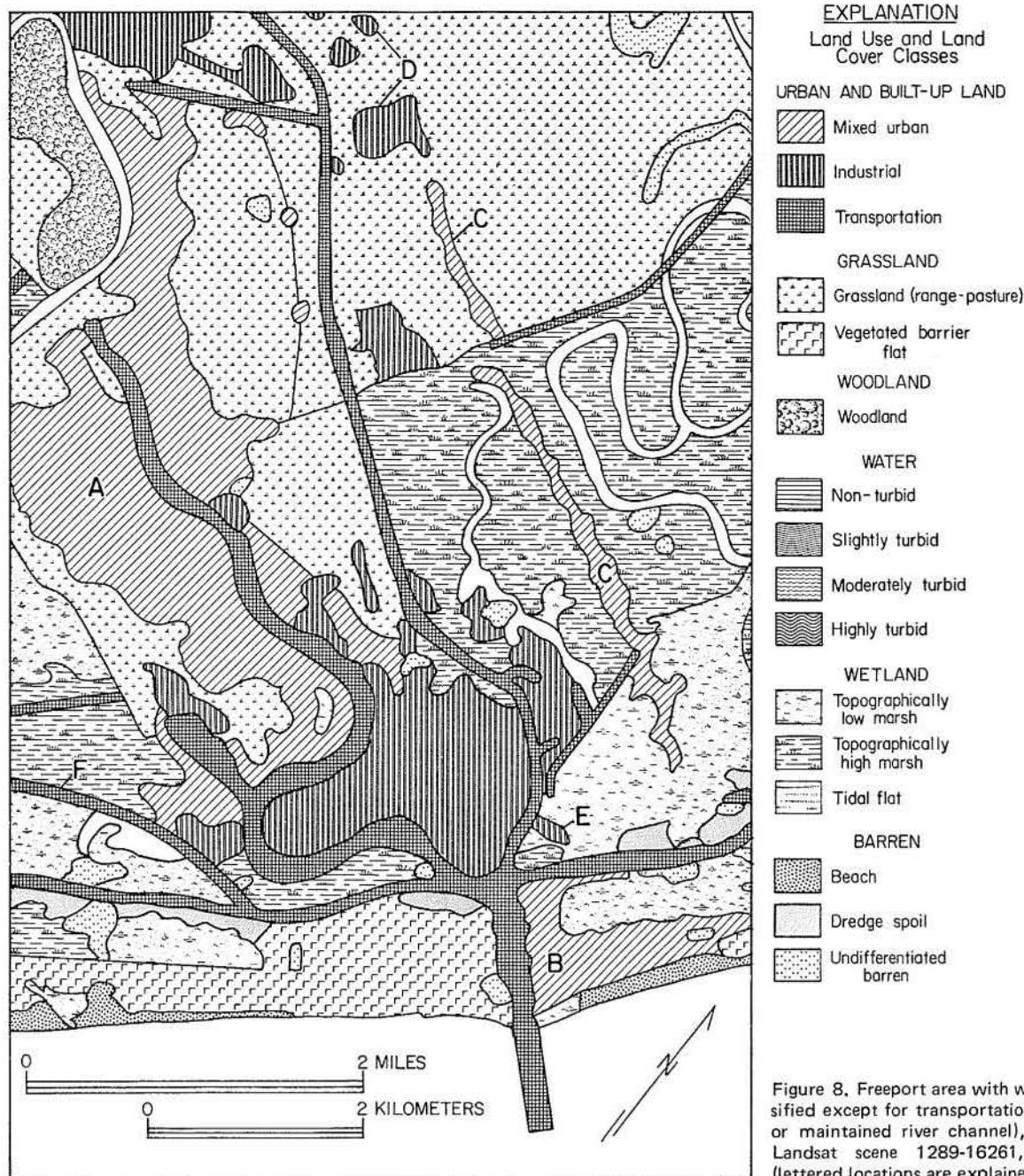


Figure 8. Freeport area with water units unclassified except for transportation (dredged canals or maintained river channel), delineated from Landsat scene 1289-16261, May 8, 1973 (lettered locations are explained in text).

cover was estimated from aerial photographs to be less than 15 percent, was not distinguishable from grassland. Where woodland graded laterally into brushland, difficulty was encountered in placing a correct boundary between these units.

The Freeport area (fig. 8) includes a major industrial-port complex almost 3 km in length and width, the urban areas of Freeport (A, fig. 8) and Surfside (B, fig. 8), and urban strip development (C, fig. 8) along State Route 332. This road leads northwest from Surfside but is not detectable where it crosses the low marshes landward of that city until the roadside development begins. At locality D (fig. 8), development becomes less continuous, but a

string of individual industrial sites provides a clue to the location of the highway. On Landsat false-color composite transparencies, industrial sites are recognizable by (1) the high-reflectance white to bluish-white tones caused by metal structures and by the use of shell and sand fill, (2) the presence of holding ponds for liquids, and (3) distinguishable roads or dredged channels which lead to the site. Use of the first criterion alone can be misleading; at E (fig. 8), a rectangular area covered by barren dredge spoil approximately 160 by 400 m in size was misinterpreted as an industrial location.

A detectable change in marsh type was mapped across a road (F, fig. 8) that, when checked in the field, was found

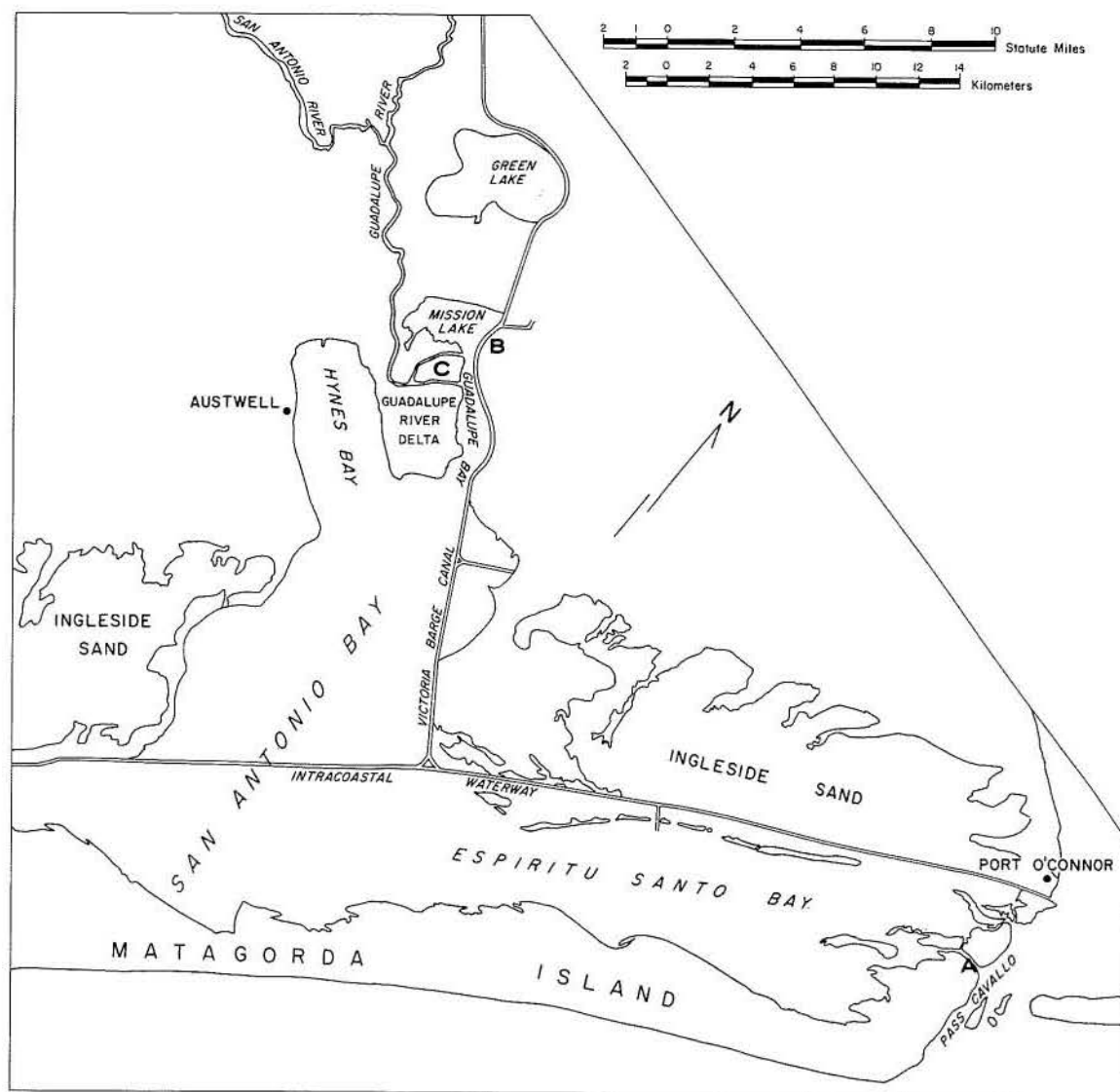


Figure 9. Geographic features in the vicinity of test site 3.

to follow the crest of a hurricane-surge protection dike at an elevation of 4.9 m (16 ft). Natural species zonation within saline marshes is related to gradual elevation changes, with less salt-tolerant species at greater elevations above mean sea level. In this example, the dike (F, fig. 8) separates saline marshes from brackish- to fresh-water marshes over an extremely short horizontal distance. *Spartina alterniflora* and *Batis maritima*, along with a relatively greater area of open water, are abundant seaward of the dike, whereas *Spartina spartinae*, *Distichlis spicata*, and some *Scirpus* spp. (bulrush) are found on the landward side. The false-color composite response of the brackish- to fresh-water marsh is dull red to blackish red, whereas the saline marsh is bluish black with faint reddish-black patches.

Clements (1976) concluded that topographically high marsh, or marsh which is inundated by the highest spring tides or by wind tides, is difficult to delineate owing to

gradational boundaries with coastal prairie and with other units. Within the Freeport - San Luis Pass test site, dredge spoil is colonized by high-marsh plant species. It can therefore be difficult to distinguish vegetated spoil from the natural marsh unless the characteristic shape of the spoil pile or its location adjacent to a channel is evident on the imagery.

Because only one scene was mapped in test site 2, no change-detection analysis was undertaken in the Freeport - San Luis Pass area.

### ANALYSIS OF TEST SITE 3

#### Site Description

Within the San Antonio - Espiritu Santo Bay test site (fig. 9), wetlands are found primarily adjacent to Pass Cavallo, along the mainland shoreline near the junction of

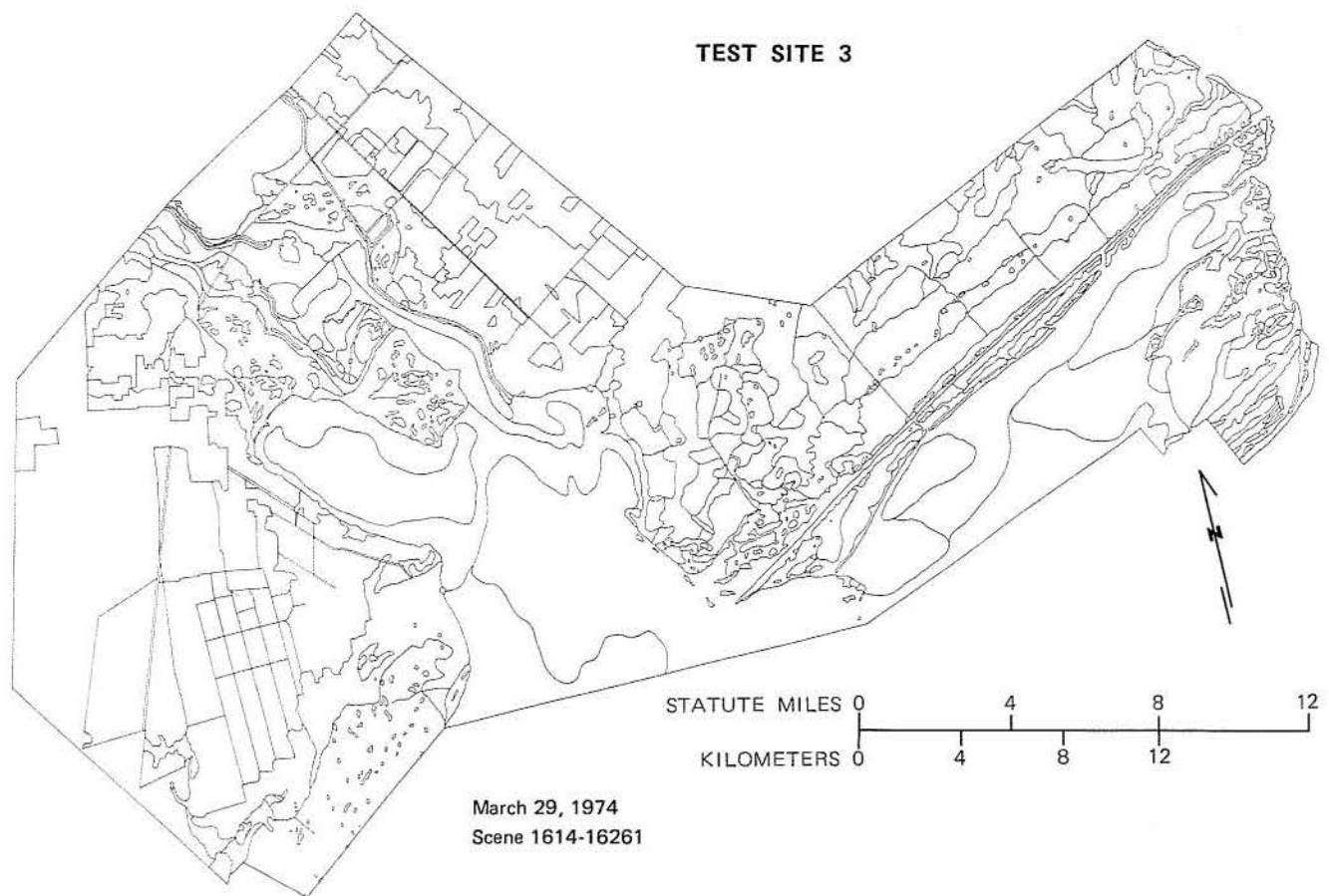


Figure 10. Unclassified line boundary map of test site 3 from March 29, 1974 imagery.

the two bays, and in the upper reaches of San Antonio Bay where approximately 12,800 acres (Clements, personal communication, 1976) of fresh to brackish marsh are located. Characteristic saline and brackish marsh plants are the same as those listed for test site 2, with the addition of *Borrchia frutescens* (sea oxeye), a shrubby plant found only in the topographically high marsh because it is not tolerant of prolonged saltwater inundation.

The flood-tidal delta marshes (A, fig. 9) of the Pass Cavallo area are the most extensive saline marshes within test site 3. The dominant species are *Spartina alterniflora*, *Batis maritima*, and *Salicornia* spp. in the low areas, and *Spartina patens* with bluestem and other grasses on the higher ground. Along the margins of upper San Antonio Bay (B, fig. 9) and on the delta of the Guadalupe River (C, fig. 9), brackish to fresh marshes include *Distichlis spicata*, *Spartina spartinae*, *Spartina patens*, *Phragmites communis* (reed), and *Juncus* spp. (rush).

The land adjoining the bays is rural, and communities (fig. 9) such as Austwell (population 272) and Port O'Connor (population 810) have a low density of develop-

ment with widely spaced buildings and wide intervening areas of grassland. Farming, ranching, and both sport and commercial fishing are the major sources of income in this region. Cropland in site 3 is concentrated over Pleistocene interdistributary mud with distributary silts and sands (McGowen and others, 1976b). Pleistocene deltaic sands, barrier strandplain sands, and sheet sands are not favorable for crops; therefore, such areas are used as range-pasture lands. The latter include the Ingleside sands southwest of Port O'Connor and south-southwest of Austwell (fig. 9), which appear mottled on Landsat imagery owing to accumulation of mud and organic material in isolated low depressions.

The marshes of the Guadalupe River delta (fig. 9) are developed on Modern and Holocene deltaic muds and sands and on associated levee and crevasse-splay deposits of mud, silt, and sand (McGowen and others 1976b). Grasslands with scattered shrubs are present on delta-plain muds and sands located inland of Hynes Bay and Mission Lake (fig. 9). The Guadalupe River and its distributaries are bordered by thin belts of woodland which include oak, hickory, pecan, and hackberry.



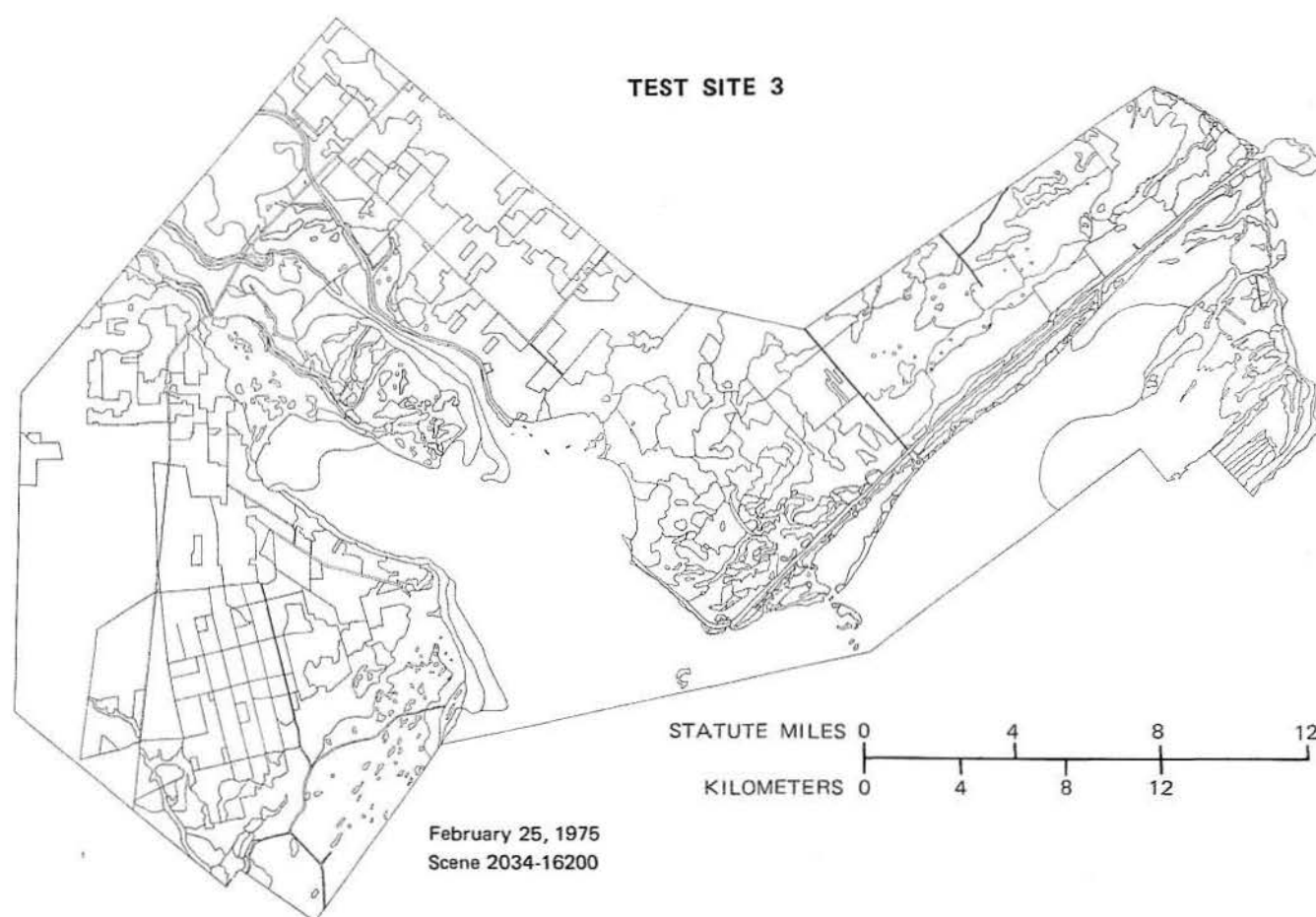


Figure 11. Unclassified line boundary map of San Antonio - Espiritu Santo Bays test site 3 from February 25, 1975 imagery (map showing land cover - land use classes is included in pocket).

### Mapping Results

The San Antonio - Espiritu Santo Bay test site was mapped using a March 29, 1974 Landsat-1 image (fig. 10) and a February 25, 1975 Landsat-2 image (fig. 11). The February scene is of better quality, enabling more accurate mapping of the topographically low marsh of the Pass Cavallo flood-tidal delta, and clearer discrimination of low-density development in Port O'Connor (A, fig. 12) from surrounding grasslands. The March 29, 1974 image proved more useful, however, in mapping the marshes at the head of San Antonio Bay. The 1-month difference in the times of these images apparently corresponds to a significant period of annual plant growth in these fresh- to brackish-water marshes (Clements, personal communication, 1976). This initial growth results in increased infrared reflectance, and therefore greater intensity and variation of the red tones in the false-color composite image. These color differences, along with the blue to black tones representing wet and/or barren substrate, are crucial to the discrimination of the floral zones.

The low Pass Cavallo marshes (fig. 12) gave a distinctive

greenish-blue to black Landsat signature, whereas the topographically high marsh areas appeared reddish black. Because of their proximity to a major tidal inlet, low-marsh species tolerant of full seawater salinities were expected, and this prediction was confirmed by sampling transects (table 4). A substantial difference in the area of wet, bare substrate and open water between the topographically high and low marshes supports the finding by Erb (1974) that water content may be an important factor in the delineation of marshes by means of satellite data. Ground observations confirm the existence of permanent tidal pools and patches of bare tidal flat within the Pass Cavallo marshes which range in area from several tens to several thousands of square meters.

Comparison of maps made from the March 29, 1974 and February 25, 1975 imagery suggests that Landsat data might be used to evaluate the extent of aperiodic inundation of marsh, tidal flat, and beach. Line boundary maps made from imagery taken on these dates and enlarged from 1:125,000 to 1:80,000 showed that 704.8 hectares (1,741 acres) of additional emergent area were evident on the February 1975 image (fig. 13). Tide-gauge data supplied by

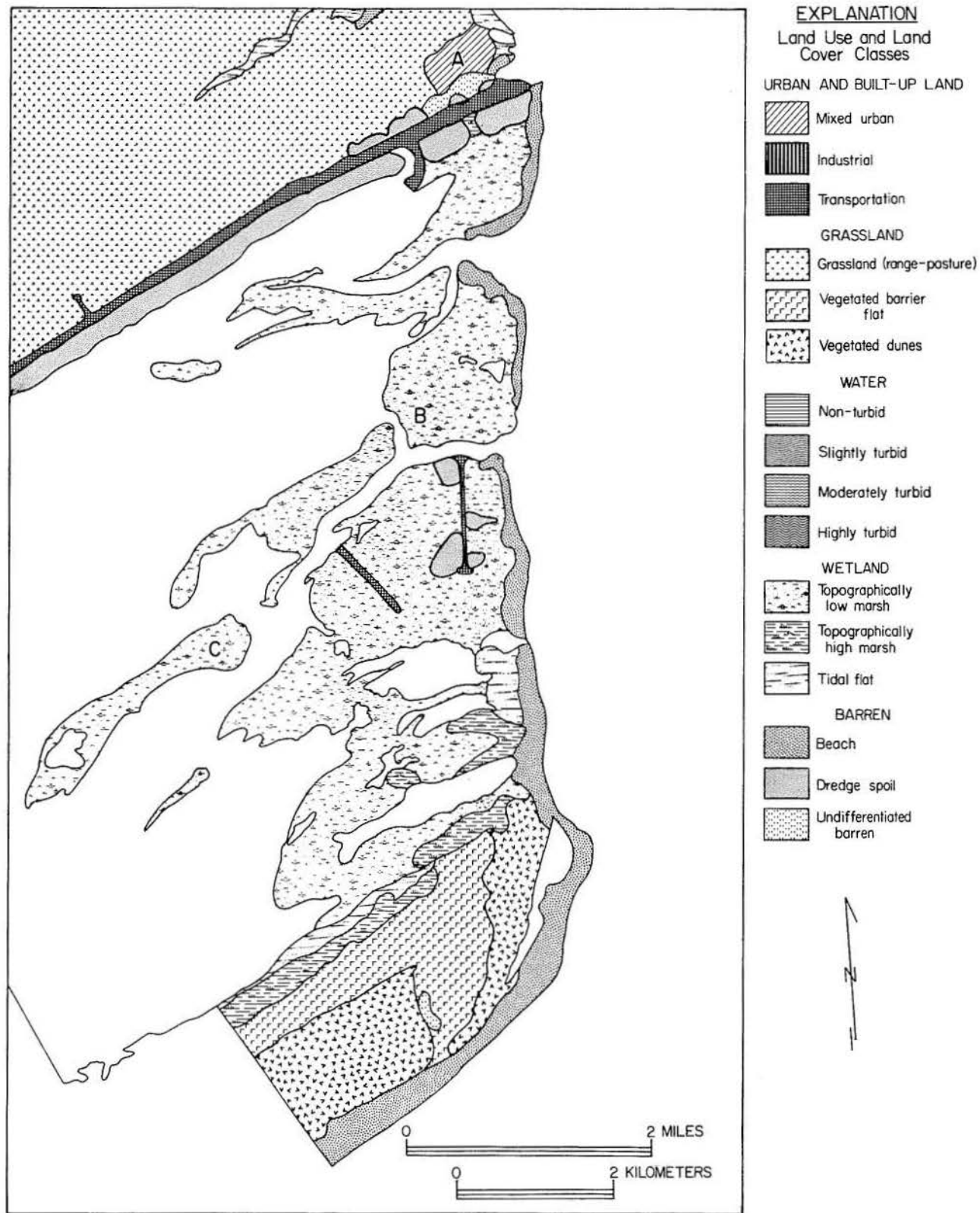


Figure 12. Pass Cavallo area with water units unclassified, except for transportation (dredged channels), and land units classified from Landsat scene 2034-16200, February 25, 1975 (lettered locations are explained in text).

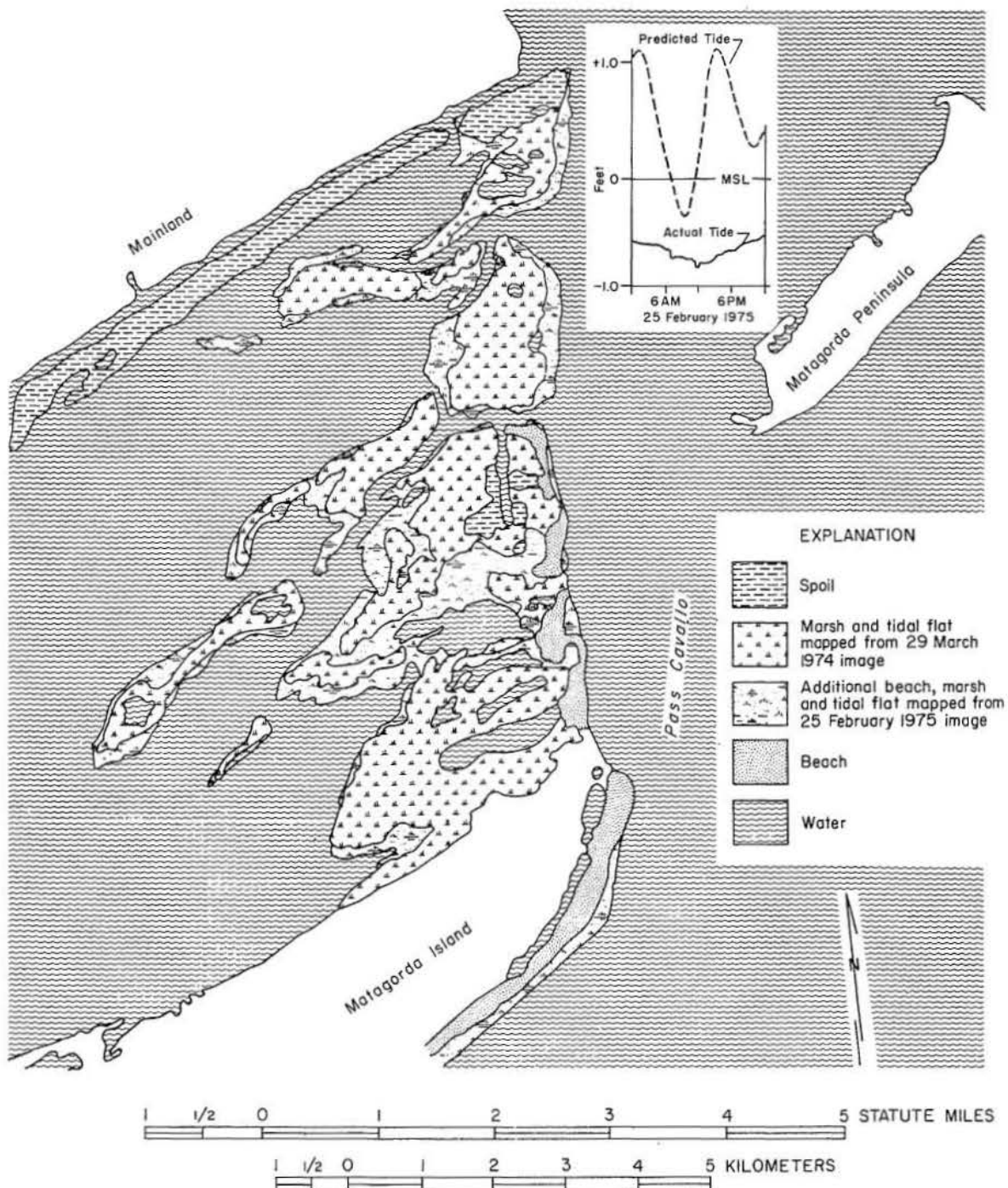


Figure 13. Map showing change in area of emergent marsh, tidal flat, and beach at Pass Cavallo owing to wind tide of February 25, 1975.



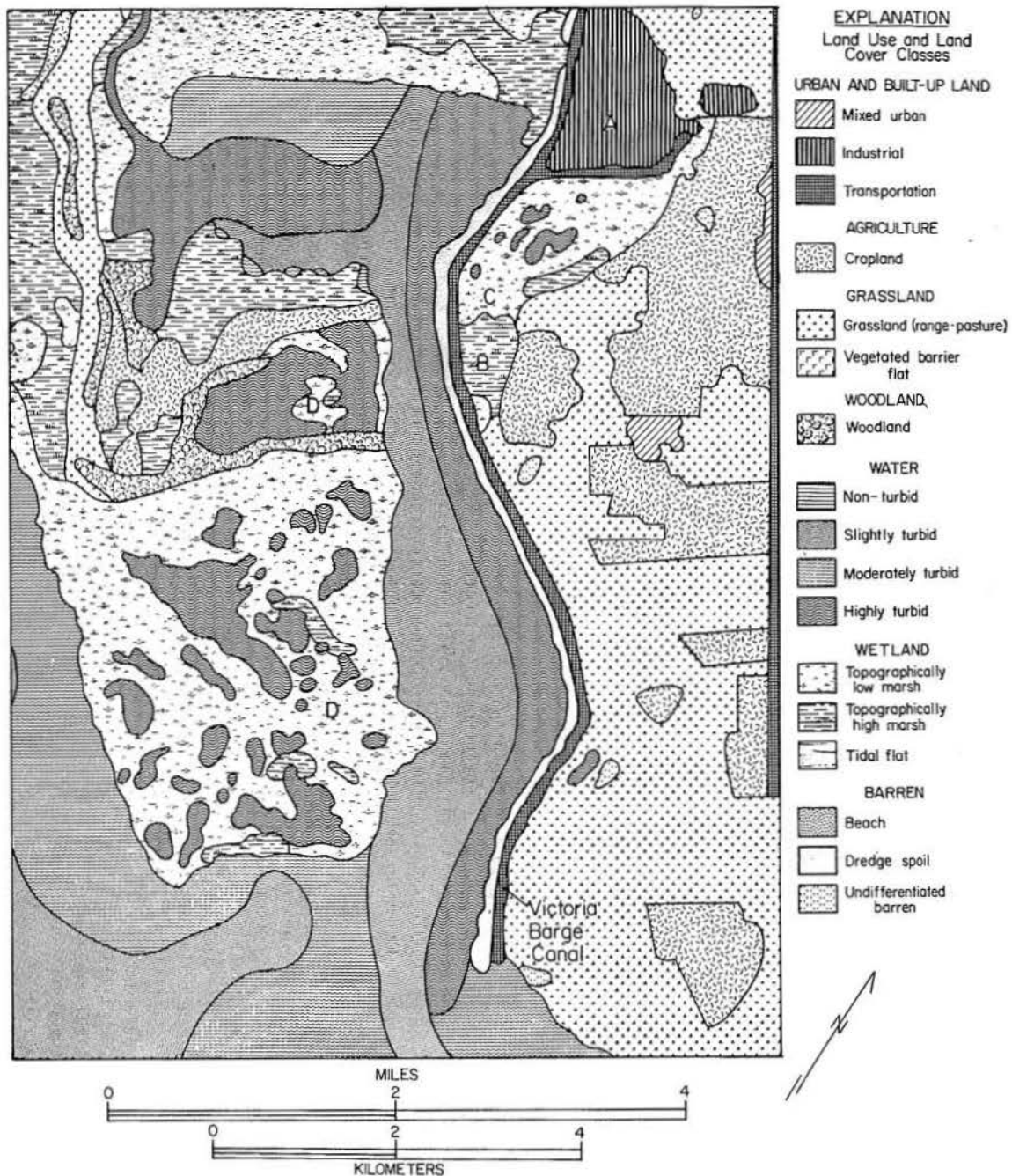


Figure 14. Guadalupe River delta area with classified land and water units, delineated from Landsat scene 1614-16261, March 29, 1974 (lettered locations are explained in text).

the Galveston District of the U. S. Army Corps of Engineers indicate (1) a 0.43 m (1.4 ft) lower water level for that date compared with March 29, 1974, and (2) a complete masking of the predicted astronomical tide (inset, fig. 13) by a wind tide resulting from strong northerly winds preceding the time of satellite passage (appendix A). The levels of both the upper bay and nearshore Gulf waters are lowered as a consequence of the offshore-directed wind

stress. These data illustrate the importance of obtaining time histories of wind and actual, rather than predicted, tidal elevations in evaluating water levels seen on Landsat imagery.

A stabilized dune complex with elevations of 2 to 6 m adjacent to Pass Cavallo and the negative effective precipitation (fig. 4) indicate that wind transport of sediment is relatively more important in this region than in test site 2.

Table 4. Vegetation transects in the low marshes at Pass Cavallo.

Location	Species	Relative cover, %	Average height, m
B, fig. 12	<i>Batis maritima</i>	37	0.28
	<i>Spartina alterniflora</i>	34	0.66
	<i>Avicennia germinans</i> (black mangrove)	9	
	Bare ground	20	
C, fig. 12	<i>Batis maritima</i>	39	0.40
	<i>Avicennia germinans</i>	16	
	<i>Spartina alterniflora</i>	9	
	<i>Salicornia</i> spp.	9	
	Bare ground and water	27	

The linear pattern of vegetated beach ridges evident on Matagorda Island near Pass Cavallo (figs. 10 and 11) was easily detected on Landsat imagery; the ridges are probably the best examples of vegetated dunes mapped within any of the test sites.

The Guadalupe River delta at the head of San Antonio Bay (fig. 14) includes fresh- to brackish-water marshes and fluvial woodlands. The distribution of turbidity within the bay reflects the influx of sediment-laden river water at the north end of the delta. A similar turbidity pattern is evident on high-altitude photographs (NASA Mission 300) taken 1 year after the Landsat imagery, suggesting that such semipermanent or seasonal flow patterns may be monitored with Landsat data. The river distributaries cannot be directly detected on Landsat images, however, because they are less than 40 m wide and they are masked by the fluvial woodlands along the riverbanks.

The influx of river water near the marshes at B and C (fig. 14) results in the presence of species that differ from those in the tidal-inlet marshes and those in the marshes near Freeport (F, fig. 8). Table 5 indicates that *Distichlis spicata*, which seems less tolerant of saltwater than *Spartina alterniflora* but more tolerant than *Spartina spartinae*, is more abundant in the area classified from Landsat as low marsh. *Spartina spartinae* is found primarily in areas of fresher water. These field results support the interpretation of the Landsat imagery. The topographically low marshes at D (fig. 14) are nearly as wet as the tidal-pass marshes (B, C, fig. 12) and have a similar Landsat signature, but they contain fresh- to brackish-water species such as *Polygonum punctatum* (smartweed) and *Phragmites australis* (common reed) (Benton and others, 1975). Thus, within a single test site, the species content of the low-marsh category (table 4 and table 5, location C) may vary greatly because of the

Table 5. Vegetation transects in the upper San Antonio Bay marshes.

Location	Species	Relative cover, %	Average height, m
B, fig. 14	<i>Spartina spartinae</i>	39	0.12
	<i>Distichlis spicata</i>	5	
	Bare ground	56	
C, fig. 14	<i>Distichlis spicata</i>	74	0.33
	<i>Rotala ramosior</i> (rotala)	18	0.55
	<i>Spartina patens</i>	4	
	<i>Spartina spartinae</i>	2	
	Bare ground	2	

effect of localized fresh- or salt-water influx; that variation is not readily discernible on Landsat imagery.

Cropland (fig. 14) is often recognizable by the regular boundaries of the fields and, when crops are not present, by the contrast of the low-reflectance muddy substrate with surrounding grasslands. The rangeland grasses show less infrared reflectance than do cultivated crops and therefore have a pale-red signature on the false-color composite in contrast to the vivid red of such crops as grain sorghum. The holding ponds (A, fig. 14) and a spur on the Victoria Barge Canal are evidence of the major industrial area located northeast of these ponds.

### Change Detection

The change-detection techniques outlined in figure 3 were first applied in test site 3, using band 7 transparencies enlarged to 1:125,000. The most distinct difference between the March 29, 1974 and February 25, 1975 scene was detected in the grasslands southwest of Port O'Connor, where tracts up to 1.5 mi<sup>2</sup> (3.8 km<sup>2</sup>) in area had been burned. Burning these grasslands removes dead culms and encourages the growth of young shoots, especially of *Spartina spartinae*, on which cattle thrive (Clements, personal communication, 1976). On the Landsat false-color composite, the blackish, burned areas contrast sharply with the infrared response of the grasslands; with repetitive Landsat imagery, acreage being managed by this technique can easily be estimated.

Vegetal differences were also noted in the wetlands of the delta plain north of the Guadalupe River delta because of the stage in the annual growth cycle of the vegetation. In the croplands, radiance differences evidently relate to whether or not fields are completely plowed under at the end of the growing season. Because water-level differences between these two scenes (fig. 13) resulted in substantially different shoreline configurations, land features were used to register the images during change-detection studies.

## TEST SITE 5

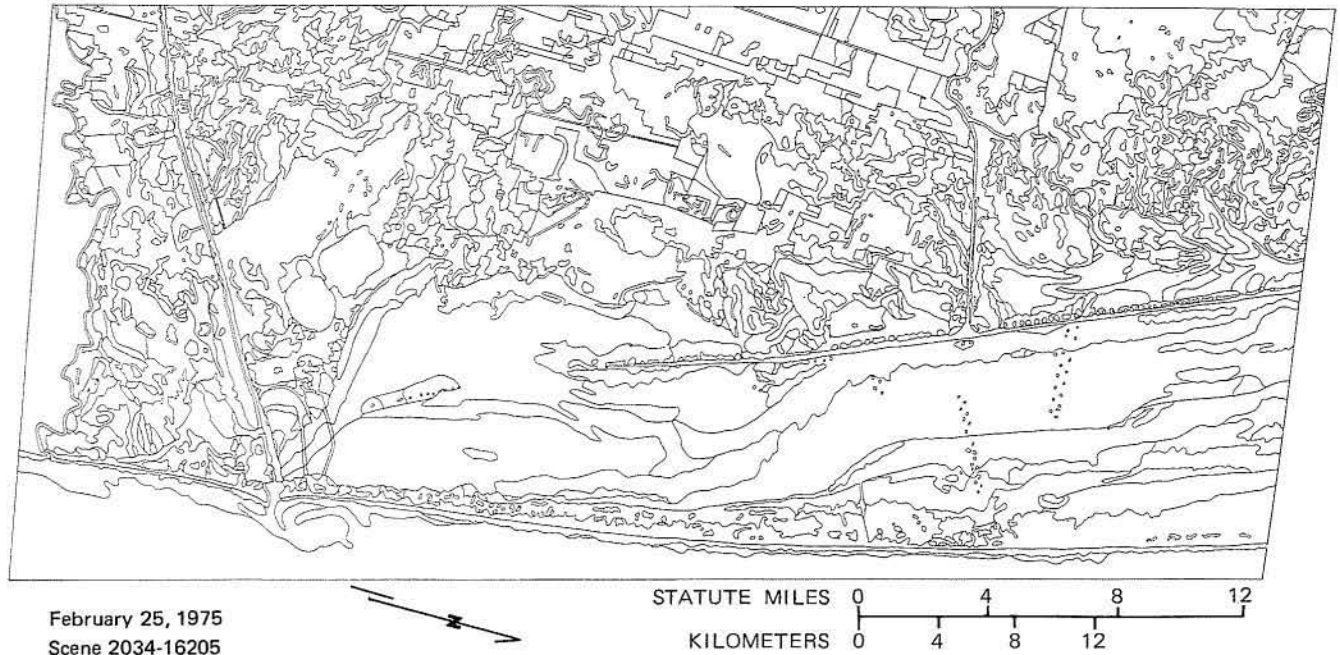


Figure 15. Unclassified line boundary map of the southern Padre Island - Laguna Madre test site (map showing land cover - land use classes is included in pocket).

## ANALYSIS OF TEST SITE 5

### Site Description

The southern Laguna Madre area test site (fig. 15) includes part of South Padre Island, the lagoon, and the saline and prairie grasslands of the adjacent mainland. The climate is semiarid with a normal annual rainfall of 26 inches; the pronounced deficit in precipitation leads to active aeolian transport of sediment and only sparse growth of barrier island vegetation. Species present on dunes and within scattered areas of vegetated barrier flat include *Uniola paniculata* (sea-oats), *Sporobolus virginicus* (sea-shore dropseed) and *Croton punctatus* (doveweed) (Sauer, 1967). Much of the barrier island consists of coalescing washover channels, washover fans, and blowouts. Broad tidal flats have been formed along the margin of Laguna Madre by wind transport of sediment derived from the overwash deposits (McGowen and Scott, 1975). Algal mats are present on parts of the wind-tide-dominated flats, and aquatic herbs such as *Halodule wrightii* (shoalgrass) and *Syringodium filiforme* (manateeegrass) grow submerged in the lagoon. Marshes similar to those found in test sites 2 and 3 are virtually absent.

West and southwest of the Arroyo Colorado (fig. 5), prairie grasslands are found inland from the wind-tidal sandflats which border Laguna Madre. These grasslands are characterized by flat topography developed over mud and sand substrate and are extensively cultivated (Brown and others, in progress). Crops of grain sorghum and cotton, as well as orchards, are common. Areas of chaparral-type

vegetation, containing *Prosopis glandulosa* (mesquite), *Pithecellobium flexicaule* (Texas ebony), and other poorly formed trees occur southwest of Arroyo Colorado and were mapped from Landsat imagery.

The saline grasslands, located from south of the Arroyo Colorado to the Brownsville Ship Channel and the Rio Grande, are developed on mud substrates and include *Salicornia* spp., *Batis maritima*, *Monanthochloe littoralis*, and *Borrchia frutescens* at slightly greater elevations; in less saline soils, *Spartina spartinae* is found (Johnston, 1955). The grassland association dominated by *Spartina spartinae* (gulf cordgrass) is locally known as "sacahuistal." Note that some of the same plant species which form marshes on the northern Texas coast form grasslands on poorly drained, saline soils under the semiarid conditions of this southernmost test site. Some fresh-water marsh is found in oxbows and abandoned channel courses, known locally as "resacas," and the low reflectance of mud infilling and standing water within these units characterize them on Landsat scenes.

### Mapping Results

Test site 5 shows a complex of environments which is especially evident across the inactive Modern-Holocene deltaic plains (Brown and others, in progress) between the Rio Grande and the Brownsville Ship Channel and north of the Arroyo Colorado mouth (see fig. 5 for locations). The latter area is a complex of channels, tidal flats, subaqueous grassflats, algal mats, and undifferentiated barren substrate.



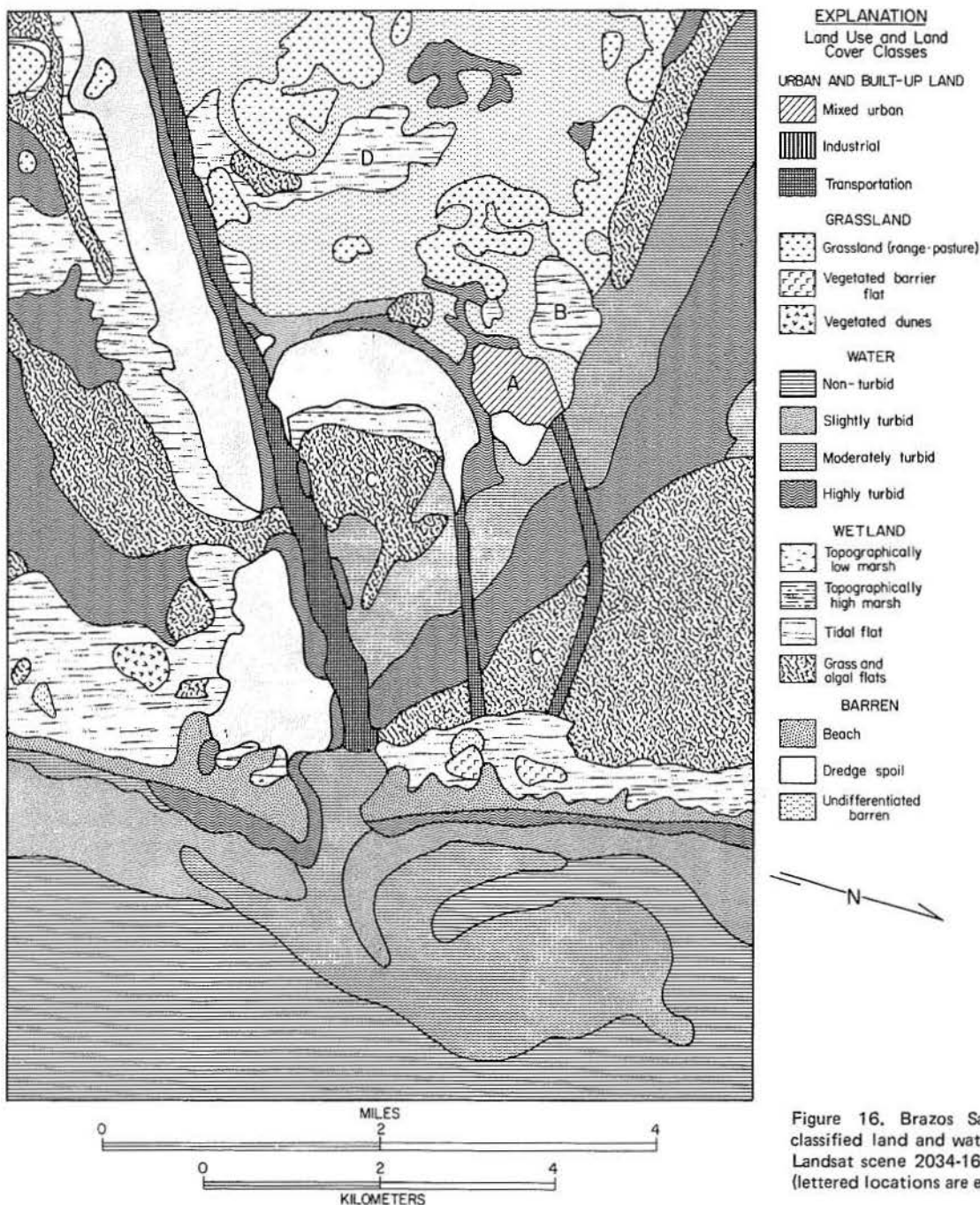


Figure 16. Brazos Santiago Pass area with classified land and water units delineated from Landsat scene 2034-16205, February 25, 1975 (lettered locations are explained in text).

Small isolated areas ( $0.2$  to  $0.09 \text{ km}^2$ ) have been mapped as topographically low marsh within this complex of environments, but they total no more than  $1.1 \text{ km}^2$  and may not represent true marsh; rather, these areas may be clumps of halophytic vegetation set within the upper reaches of highly saline wind-tidal flats that are rarely flooded by lagoonal waters.

The city of Port Isabel (A, fig. 16) is detectable with Landsat imagery, as are the two causeways leading across Laguna Madre to South Padre Island. The lawns and trees of the city, interspersed with paved roads and urban structures, give a pebbly, dull red-and-white pattern on the

false-color composite which, especially when seen with transportation features, helps in identifying urban complexes. Urban development on Padre Island, however, is not detectable because (1) many streets are simply cleared areas of loose sand or shell, (2) lawns and planted trees characteristic of developed areas are not present, and (3) structures immediately adjacent to the beach and within the foredune area are masked by the high reflectance of the barren sands. These residential and commercial areas therefore have nearly the same reflectance as the surrounding natural environment of barrier-flat vegetation, tidal flat, and bare sand.



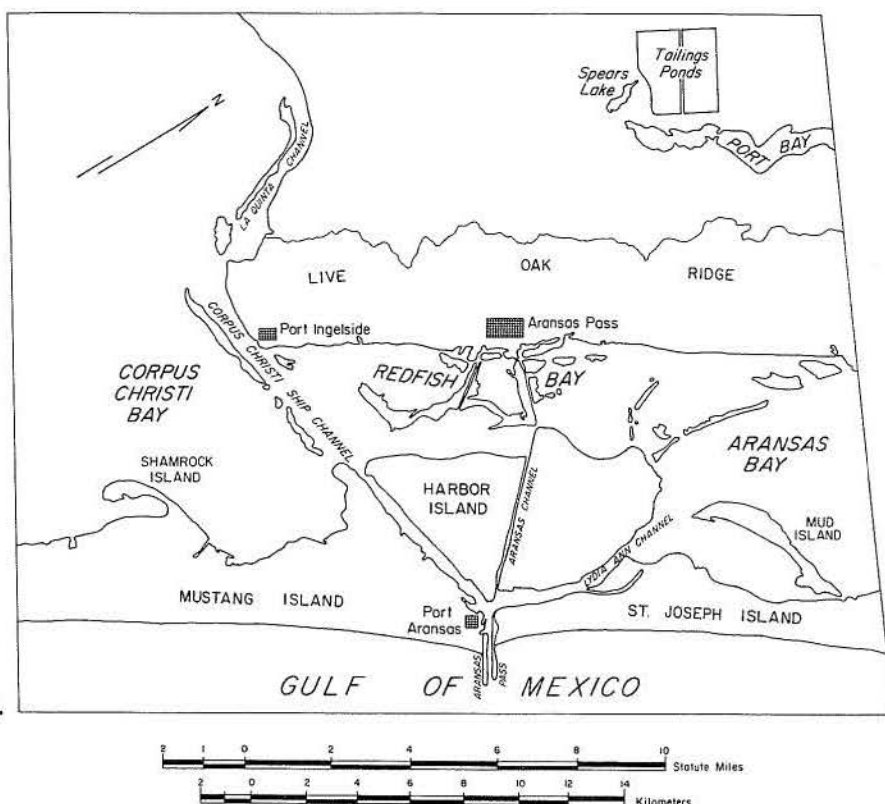


Figure 17. Geographic features in test site 4.

Difficulty was also encountered in mapping residential development along the margins of Laguna Madre. A housing development consisting of dredged channels and spoil fill was mapped as tidal flat (B, fig. 16) because both environments appear simply as wet sandy substrate on Landsat imagery. The channels range from 30 to 45 m wide and could not be differentiated from the surrounding high-reflectance barren spoil.

Within the Brazos Santiago Pass area are subaqueous grassflats (C, fig. 16) and barren sandflats (D, fig. 16), which are occasionally flooded (Brown and others, in progress), and vegetated clay-sand dune ridges, which were mapped on the basis of their orientation and linearity. Note that the moderately turbid water issuing from the tidal pass turns northward (fig. 16) because the nearshore circulation was under the influence of 12- to 16-knot winds from the south (U. S. Department of Commerce, 1975a) at the time of satellite passage.

No change detection was undertaken for this test site because mapping from only one scene was completed.

#### ANALYSIS OF TEST SITE 4

##### Site Description

The Harbor Island test site (fig. 17) includes segments of two barrier islands and, at Harbor Island, a complex of marshland, tidal flat, emergent sandflats, and dredge spoil. Areas of shallow water, including Redfish Bay, the bay sides of the barrier islands, and areas within Harbor Island, support dense submergent stands of sea grasses such as

*Ruppia maritima* (widgeongrass) and *Halodule wrightii* (shoalgrass). Extensive low marshes are found on Harbor Island; these include *Spartina alterniflora*, *Batis maritima*, and *Avicennia germinans* (black mangrove). *Spartina alterniflora* is abundant throughout the area along the submergent to barely emergent margins of natural and man-made land. These marshes are interspersed with shallow ponds and bare to slightly vegetated tidal flats; locally they grade laterally into higher marsh margins that may contain *Spartina patens*, *Distichlis spicata*, *Spartina spartinae*, *Monanthochloe littoralis*, and *Borreria frutescens*. Vegetated dredge spoil supports the latter species, as well as grasses and shrubs typical of the Coastal Plain and the vegetated flats of the barrier islands.

On the mainland, a live oak (*Quercus virginiana*) woodland is developed on Pleistocene barrier-strandplain sands at elevations up to 20 to 25 ft (6.1 to 7.6 m) (Live Oak Ridge, fig. 17). Vines, such as *Smilax* spp. and *Ibervillea lindheimeri*, occur in the woodland undergrowth which, with the sometimes scrubby growth of the oak, can form an impenetrable thicket. As in test site 3, shallow ponds occur in depressions within the barrier-strandplain sands and are seen as black specks on the Landsat false-color composite. Rooted submergent vegetation (*Myriophyllum* spp.) is found within these ponds and a blue-green algal mat occurs around the margins (Clements, personal communication, 1976). The bottoms of several ponds checked in the field had a 1-inch-thick coating of organic muck, contributing to the low-reflectance signature of these features.

# TEST SITE 4



Figure 18. Unclassified line boundary map of the Harbor Island test site, February 25, 1975 (map showing land cover - land use classes is included in pocket).

Between Live Oak Ridge and Port Bay (fig. 17), brushland was detected on summer imagery but not on the winter scenes. *Prosopis glandulosa* provides 80-percent canopy cover (Clements, 1976) in this area, with cactus, *Spartina spartinae*, and various herbs and grasses also occurring. Grasslands west of Live Oak Ridge are dominated by *Cynodon dactylon* (Bermuda grass) and are developed on locally mud-veneered sheet sands (Brown and others, 1976) and used for grazing. Pleistocene intertributary muds, southwest of Spears Lake and the industrial tailings ponds (fig. 17), support a cropland producing grain sorghum almost exclusively.

A large volume of shipping, both deep-water and intercoastal, moves through the inlet of Aransas Pass and the adjacent ship channels (fig. 17). Transportation of crude oil, production of petrochemicals and carbon black,

and commercial fishing are major activities in the area. Channel maintenance results in the need to dispose of substantial amounts of dredge spoil. Dredging and filling is also occurring along the bay margins of Mustang Island because of residential development.

## Mapping Results

Landsat scenes dating from February 25, 1975 (fig. 18), July 10, 1975 (fig. 19), and February 2, 1976 (fig. 20), have been mapped and fully classified. A fourth scene (1146-16320) (fig. 21), dating from December 16, 1972, was completed as a line boundary map, and the seaward half of the test site area was classified. Results were unsatisfactory, however, as described in the following section. Special emphasis was placed on change detection

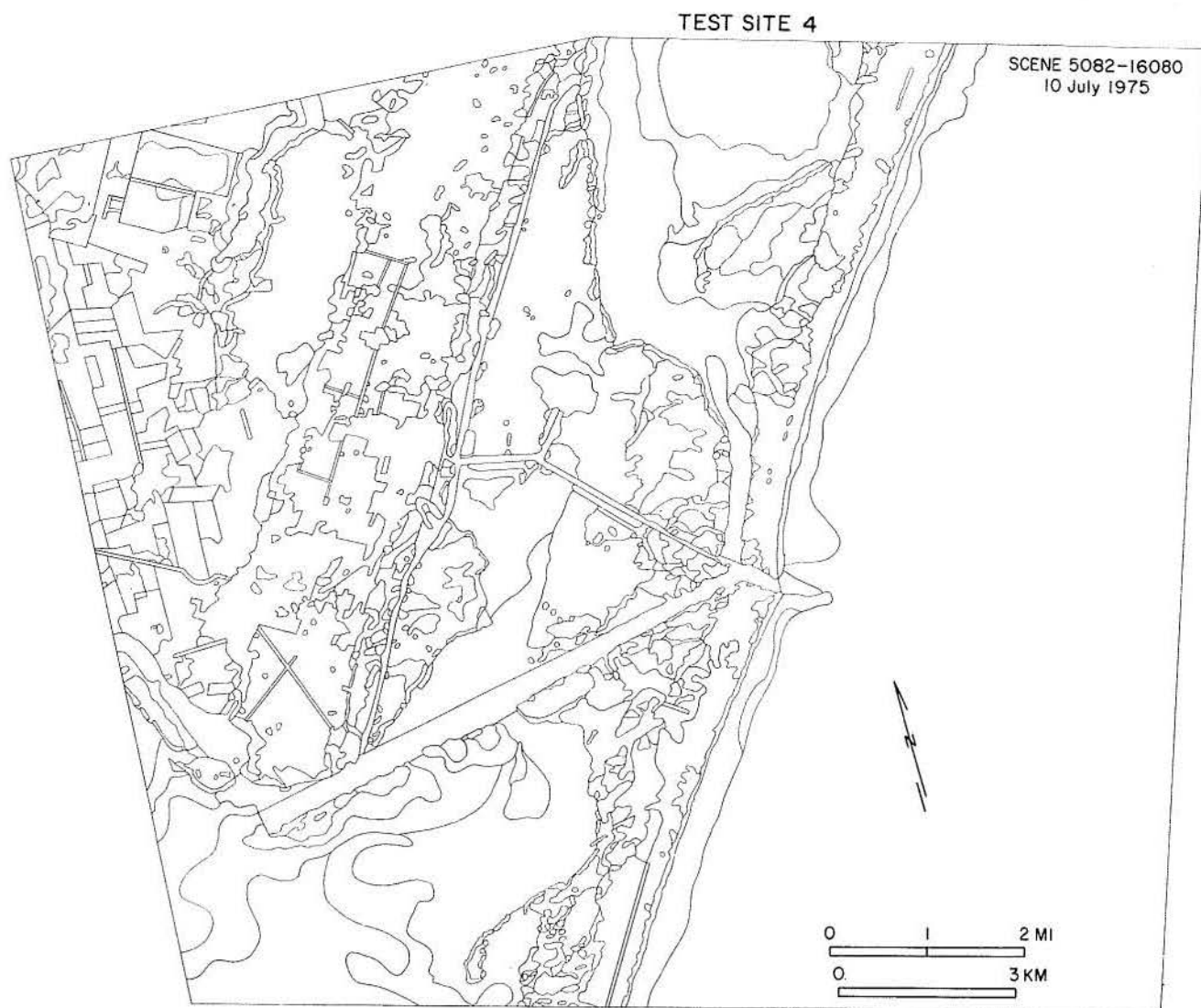


Figure 19. Unclassified line boundary map of the Harbor Island test site, July 10, 1975 (map showing land cover - land use classes is included in pocket).

and the mapping of dredge spoil within test site 4.

The wetlands of Harbor Island represent the only area studied during this investigation within which a single marsh species could be uniquely identified. Between Aransas and Lydia Ann Channels, dense stands of black mangrove are evident because of their high infrared reflectance. These areas appear deep red on the Landsat false-color composite: the signature is enhanced by reflectance from leaves 4 to 8 cm long and greatly resembles the response of live oak. Black mangrove is an evergreen (Jones, 1975); hence it has a consistent Landsat signature throughout the year. Other areas of the Harbor Island marshes have a blue to blue-black signature where *Spartina alterniflora* and *Batis maritima* are dominant, tending to light blue when lower tide levels expose more bare substrate.

Difficulty was sometimes encountered in placing the

boundary between sea grass and algal flats, tidal flats, and low marsh as a result of the intermixing of these units in the natural environment (fig. 22). Many narrow strips of marsh were not detected or were included in the tidal-flat category owing to the dominant signature of the wet substrate or of ponded water. Bay-margin sand and shell berms, which would be classified as beaches, are difficult to distinguish from adjoining tidal flats and areas of shallow water. Along the northeast margin of Redfish Bay, the high-radiance subaerial sand and shell accumulations are less than 80 m wide in many areas. Their light-blue signature resembles that of the wide areas of tidal flat behind Mustang Island or on Harbor Island.

On the barrier islands, the areas mapped as beach include sandflats with wind-shadow dunes and washover channels, all of which have high reflectance and therefore indistin-

# TEST SITE 4

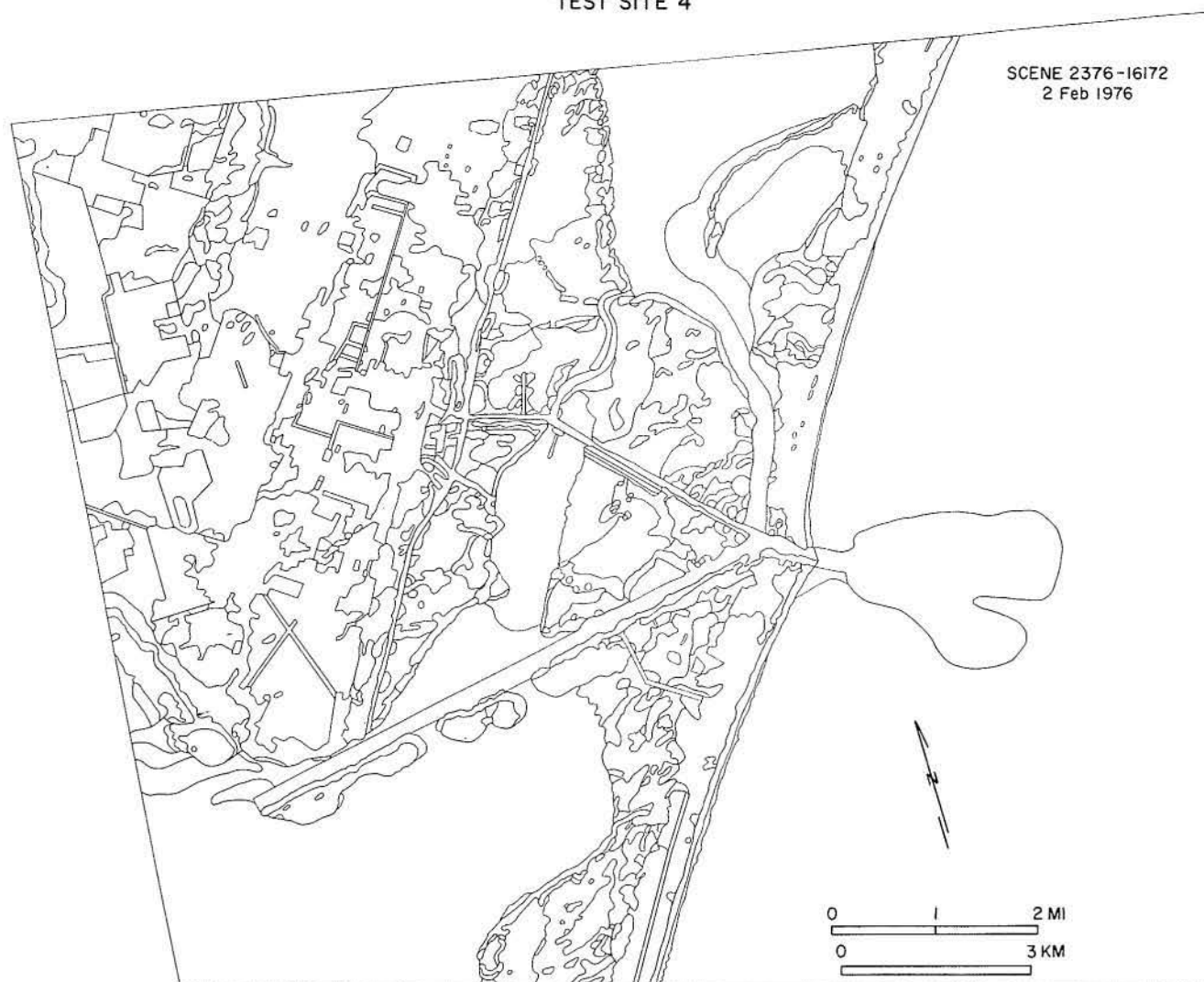


Figure 20. Unclassified line boundary map of the Harbor Island test site, February 2, 1976.

guishable mutual boundaries. Vegetated dunes behind the beach are not readily separated from the adjoining vegetated barrier flat, but were differentiated adjacent to the town of Port Aransas owing to the more highly textured appearance of the dune area (fig. 22). Small (less than 275 by 375 m) areas of barren dunes have been mapped on Mustang Island where they occur as blowout complexes extending from the beach into the vegetated barrier flat.

The built-up area of Port Aransas (fig. 17) is difficult to recognize compared with the mainland urban areas of Aransas Pass and Ingleside. As in site 5, where development on Padre Island was not discernible on the Landsat imagery, a characteristic urban signature is not developed unless the natural barrier-island vegetation is largely displaced and the density of structures reaches some critical level. The setting of the mainland urban areas, such as Aransas Pass, within a

live oak woodland enhances their detectability because the imagery shows both a radiance difference and a textural contrast between areas.

The exact boundaries of each mainland urban area show some variation when maps produced from successive scenes are compared. These differences are attributed to operator judgment in the placing of unit boundary lines. Atmospheric and sun-angle variations among images, differences in image processing, and variations in image quality affect the interpreter's decisions. Differences in the seasonal growth stage of the natural vegetation (other than the live oak) may also be a factor in delineating the urban areas, especially along transitional margins where the density of development is low.

Landward of Live Oak Ridge (fig. 17) is an area of mixed grass-and-brush rangeland. On the February 25, 1975



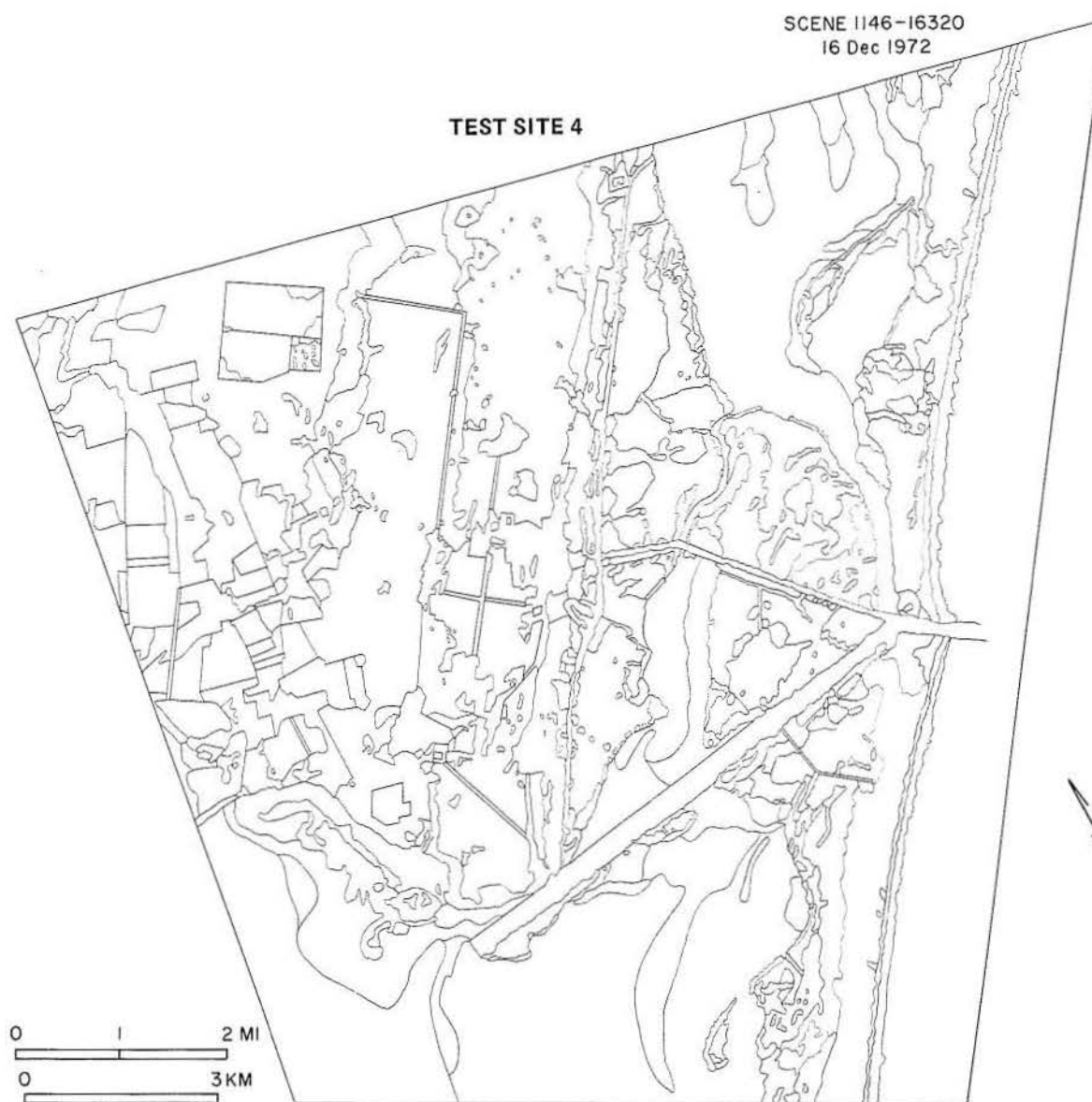


Figure 21. Unclassified line boundary map of the Harbor Island test site, December 16, 1972.

and February 2, 1976 scenes, the entire area was mapped as grassland, whereas on the July 10, 1975 scene, as detailed in the site description, the area adjacent to Port Bay was classified as brushland. This difference would be expected where brushy vegetation is deciduous. The tonal and textural variation within the brushland unit is substantial, and field checking has shown that both fairly open and very dense brush growth occur there. These results suggest that Landsat coverage during both the winter and the growing season is required to identify deciduous brushland and entirely deciduous woodland.

Expected seasonal differences were distinguished in the cropland on the northwest margin of the test site. Winter scenes show barren fields that consist of a muddy substrate and are defined by linear field boundaries. The false-color composite of the summer scene shows signatures varying from bright red through pale red to bluish gray over the cropland. Field checking in July 1976 indicated that sorghum fields were in various stages of development from just before full ripening through postharvest stubble and plowed ground, thereby adding variation to the cropland tonal response.

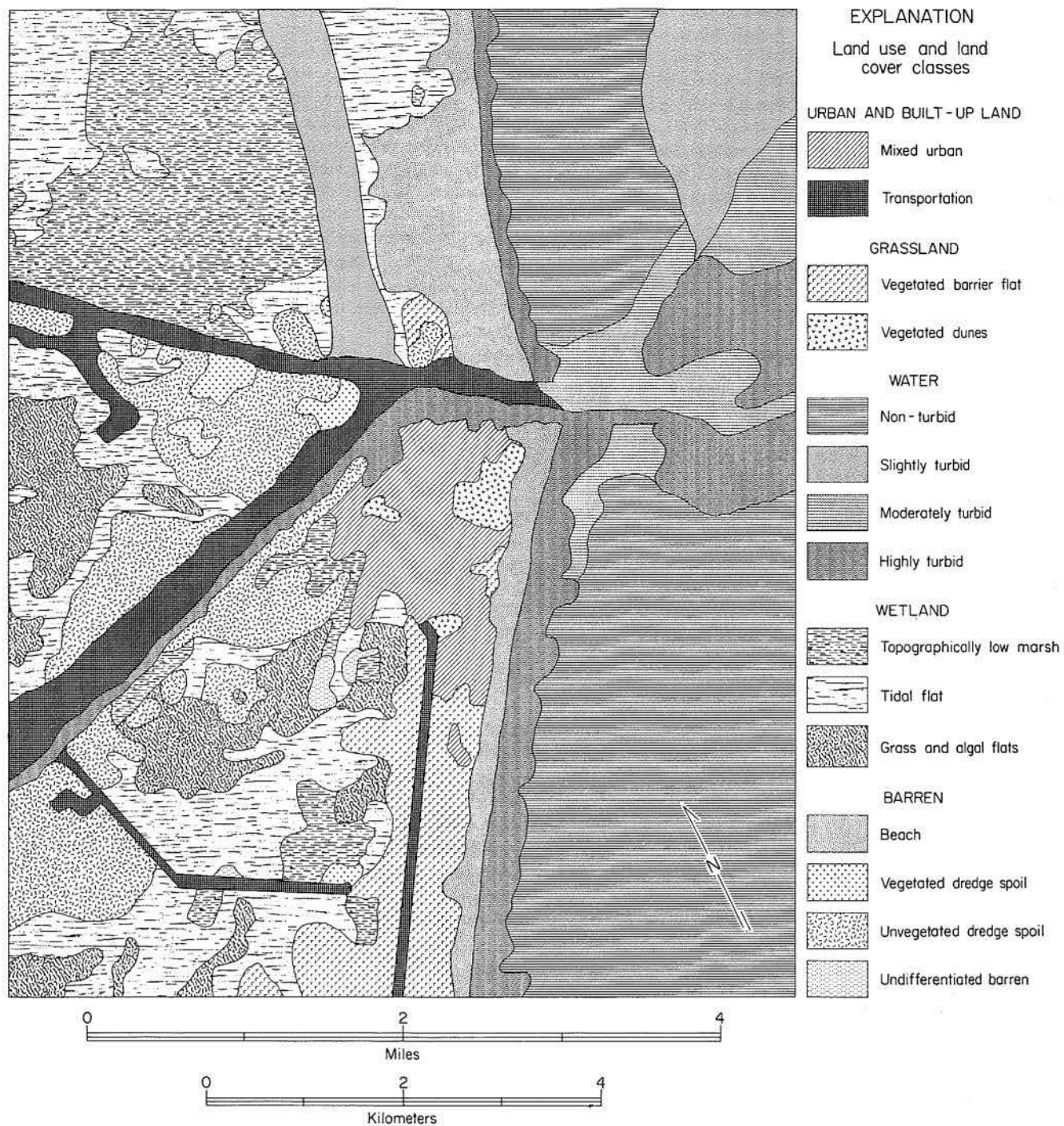


Figure 22. Aransas Pass area with classified land and water units delineated from Landsat scene 2034-16202, February 25, 1975.

### Dredge-Spoil Detection

Because of the importance of dredging as a factor in the coastal environment, a special study of dredge-spoil additions within the Harbor Island test site was undertaken. The extent of barren subaerial spoil was mapped from Landsat imagery for 10 dates (table 6) during the period January 21, 1973, to February 2, 1976. Band 5 images were used to locate spoil deposited on areas already subaerially exposed, whereas band 7 data were used to delineate spoil dumped into water bodies to create spoil islands. The high-contrast band 7 images did not provide enough detail for the subaerial sites, hence the use of band 5 images supplemented by use of the false-color composite image when available.

Figure 23 provides a summary of all spoil added in test site 4, as detected from the Landsat images; two distinct periods of spoil addition were noted along with areas which remained unchanged. Most of the spoil was added to the channel-margin spoil islands and the East Flats area between June 14, 1973, and March 29, 1974, and between September 7, 1974, and October 17, 1975 (fig. 24). A large amount of spoil was also deposited on Harbor Island between June 14, 1973, and March 19, 1974, and was evident on the band 7 image from the latter date. Within specific areas on Harbor and Mustang Islands, no spoil was added over the January 21, 1973 to February 2, 1976 time period. Results indicate, therefore, that image interpretation of Landsat transparencies can be used to monitor dredge-spoil placement, a capability which is enhanced by the high reflectance of the spoil material.

### Change Detection

Radiance changes within test site 4, as affected by time, were studied by overlaying band 7 positive and negative 1:125,000 scale transparencies for different dates (fig. 3). Two grades of change were distinguished: distinct and less distinct. The difference between these changes was qualitative. If the area was difficult to outline and/or lighter than the surrounding area, it was considered less distinct (fig. 25). Changes considered questionable, and therefore not mapped, included margins of Port Bay and of a tailings pond. It is doubtful that either one changed size; the change in radiance was probably a result of the poor fit of

the two images. Other changes were judged questionable because no clear physical boundary or difference in vegetation between the area of changed radiance and its surroundings could be found on color-infrared aerial photographs of the area at a scale of 1:30,000.

Comparison of February 25, 1975 (scene 2034-16202) and February 2, 1976 (scene 2376-16172) images with a July 10, 1975 image (scene 5082-16080) revealed that radiance changes were not simple mimics of boundaries between cropland and rangeland areas, although some areas were well defined by turnrows and other field boundaries. In February scenes, some areas of cropland were found with radiance levels that ranged from the levels equal to rangeland (relatively high) to low and intermediate levels. Generally, the lowest levels in croplands were interpreted as barren, possibly wet, muddy fields, whereas the highest radiance levels were interpreted as fields with crops present. Intermediate levels were interpreted as drier substrate or younger crops.

The July 10, 1975 image showed a broad range of radiance levels. Most areas had well-defined boundaries. One area which was not outlined by obvious field boundaries corresponded to a natural drainage pattern within the fields. This was discovered upon examination of color-infrared aerial photographs at a scale of 1:120,000.

Field checking at the test site area from July 17 to July 29, 1976, showed variation in the annual cycle of crop conditions as the cause of the broad range of radiance levels. Grain sorghum and grasses covered most of the cropland. The grain sorghum fields were in various stages from preharvest ripeness to postharvest stubble and plowed ground. Undergrowth of weeds in the furrows between rows of sorghum was seen in some fields. Some fields were overgrown with weeds, the sorghum not harvested. All these conditions would result in different radiance levels on Landsat Imagery.

Variations in radiance levels in areas cleared of trees and along margins of water bodies and marshes were also easily detected. The reason for radiance changes where trees have been removed and undergrowth exposed is clear. Radiance changes along the margins of water bodies and marshes are probably caused by changes in water levels in these areas. In spoil areas, tidal flats, and the interior of marshes, radiance changes generally were not observed.

Aerial photographs at scales of 1:30,000 and 1:120,000 (NASA Missions 300 and 325) were used to evaluate the changes detected on the imagery. The smaller scale photographs were used primarily because they provided adequate detail for the confirmation of radiance changes, and difficulty was encountered in locating on the larger scale photographs the corresponding area on the 1:125,000 scale Landsat enlargement. Too much time was expended trying to adjust distances from one scale to the other.

Initial interpretations of Landsat radiance changes were usually confirmed by the aerial photographs. The photographs were most useful for clarification of low-radiance natural drainage patterns within croplands that did not follow field boundaries.

The fact that the Landsat enlargements were not all precisely registered to the same map scale resulted in

Table 6. Landsat images used in dredge-spoil study.

Date	Image Identification No.	Band
January 21, 1973	1182-16315	5, 7
June 14, 1973	1326-16315	7
March 29, 1974	1614-16263	7
August 2, 1974	1740-16225	7
September 7, 1974	1776-16212	7
February 25, 1975	2034-16202	5, 7
March 24, 1975	1974-16135	7
July 10, 1975	5082-16080	5, 7
October 17, 1975	2268-16184	7
February 2, 1976	2376-16172	5, 7

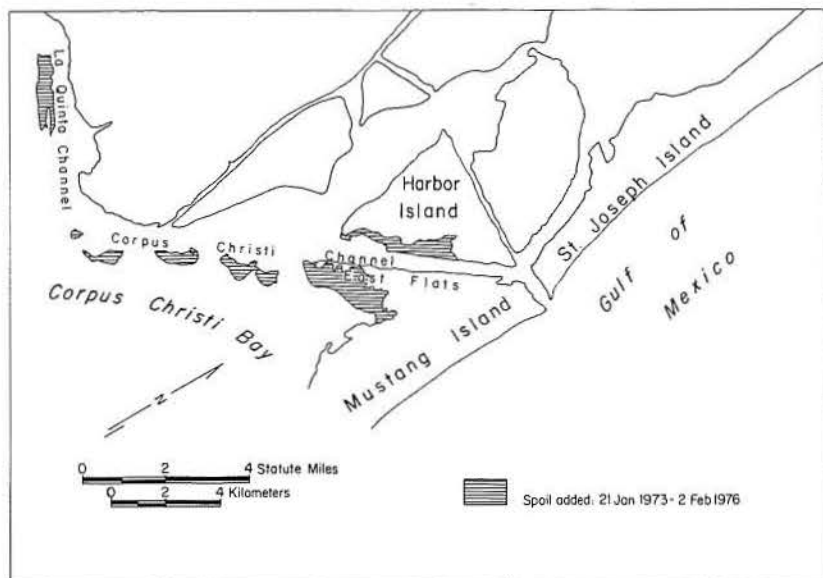


Figure 23. Summary of recent dredge-spoil additions along channels in the Harbor Island test site.

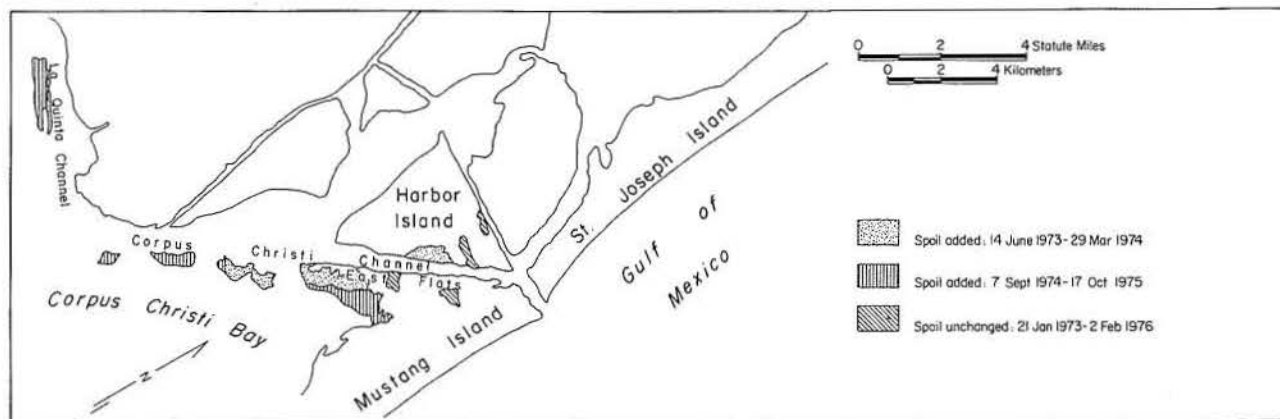


Figure 24. Sequence of dredge-spoil additions in the Harbor Island area.

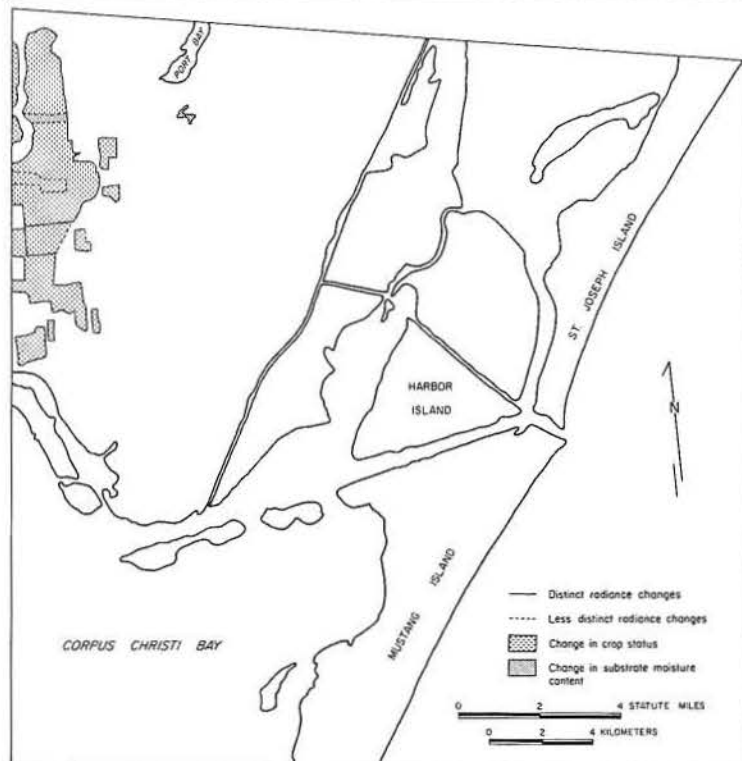


Figure 25. Radiance changes detected between February and July scenes in the Harbor Island test site.



variations in fit among images. These small differences in image scale were compensated for by adjusting the transparencies as each area of the test site was examined. If an investigation of radiance changes were desired at a larger scale than that of fig. 25 (for example, identification of specific cropland acreage), the investigator who did not have the necessary aerial photographs would have difficulty.

## DISCUSSION OF TEST SITE RESULTS

Forested wetlands, such as the swamps within the Trinity River delta vicinity, were not included in the test site areas, and fresh-water marshes were sampled only on a limited basis. In spite of the exclusion of these areas from extensive sampling, the selected test sites have provided an adequate sample of the climatically controlled variation in natural environments that is found along the Texas coast. More widespread use of the classification scheme (table 3) to include bay-head areas would require the addition of a swampland category.

The difficult task of differentiating wetland species or species groups was avoided during this study in favor of delineating wetlands primarily on the basis of observable water content and exposed bare substrate, as reflected by the general level of infrared response. The categories of topographically high and topographically low marsh therefore vary in species content even within a limited area, such as test site 3. To go beyond these designations is not within the capability of the optical-mapping techniques employed during this investigation. An exception to this limited capability is the potential to locate dense stands of *Avicennia germinans* (black mangrove) in test site 4.

Although the delineation of low marsh areas was readily agreed upon by a group of observers in the field, the delineation of high marsh was controversial. The coastal prairie grasslands of Texas are generally developed on low, poorly drained, heavy clay soils and are dominated by *Spartina spartinae* (Clements, 1976). These grasslands lie adjacent to the coastal bay and marsh systems and intergrade with the high marshes, resulting in indistinct floral zonation within this zone. Although the topographically high marsh is difficult to differentiate, retention of that category seems warranted, especially on the upper coast north of test site 3. Botanical evidence supports this conclusion (Clements, 1976) because *Distichlis spicata*, *Monanthochloe littoralis*, *Sporobolus virginicus*, and *Borrichia frutescens* occur at greater elevations than low-marsh species such as *Spartina alterniflora* and *Batis maritima* but generally not within the coastal saltgrass prairie. Field investigations indicate that the inner boundary between high marsh and the coastal prairie is more difficult to map accurately than is the boundary between high marsh and low marsh. Certainly the low (0.42 m) astronomical tidal range on the Texas Gulf Coast is less of a causal factor in marsh zonation than the 1.5- to 2.0-m tidal range off southeastern United States.

Although submerged grasses and algal mats are not wetlands according to common definitions (Clark, 1974), these units most logically fit within the Level I wetland

category (table 3). Submersed within Redfish and Aransas Bays and Laguna Madre, *Thalassia testudinum* (turtlegrass), *Syringodium filiforme* (manateeegrass), *Halodule wrightii* (shoalgrass), and *Ruppia maritima* (widgeongrass) form an important part of the bay ecosystem and an excellent substrate for the growth of epiphytic algae (Edwards, 1976). Algal mats develop on inundated wind-tidal flats, leaving a black organic residue when desiccated by subaerial exposure. Sea grasses are best detected when water levels have been lowered because of strong offshore-directed winds.

Submerged grasses can be easily differentiated from algal mats over known open-bay areas, but optical differentiation using Landsat data becomes more difficult along the shallow bay margins. Sea grass and algal mats therefore have been combined into a single class with the understanding that the largest sea-grass beds could be delineated from supplementary information available to users of natural resource data in Texas.

No moderate-density urban areas, such as Galveston or Corpus Christi, were included in any of the test sites. With the exception of Freeport, all urban areas mapped were of relatively low density. Wide spacing of structures and a great percentage of natural vegetation make less intensely developed urban areas difficult to map by Landsat-image interpretation. The outermost margins of towns such as Port Aransas (fig. 17) merge with surrounding woodlands or grasslands, and detectability depends on image quality and favorable atmospheric conditions during satellite passage. Roads vary in detectability, depending on reflectivity contrast of the road material with surrounding areas and on characteristics of each image. Mapping of oil fields (category 131, table 3) was limited to the detection of the field at Hoskins Mound, a shallow salt dome. The circular pattern of barren well sites and access roads and the holding ponds associated with hydrocarbon production are readily recognized on Landsat imagery.

Woodlands and vegetated dredge spoil can be detected with optical enlargement of Landsat standard products. The Coastal Plain of the Atlantic and Gulf states is the habitat of live oak (*Quercus virginiana*) (Haislet, 1963), the ever-green characteristic of which aids in the mapping of woodlands. The signature of this tree remains consistent throughout the year; even a few live oaks within a deciduous forest aid in the mapping of woodlands on winter scenes. Live oak is found along watercourses, hence a high-infrared-reflectance signature on a winter image can be indicative of a fluvial woodland containing *Quercus virginiana*.

Mapping of vegetated dredge spoil depends on shape and position of this land cover unit. Upland, dune, and barrier-flat grasses are found on spoil mounds and result in a Landsat signature which contrasts sharply with surrounding marshlands. Position parallel to dredge channels and an oblong to circular shape are keys to recognition of vegetated spoil. Because these characteristics can be used by the human interpreter but not by digital-recognition routines, the inclusion of this unit in a land cover - land use system (table 3) requires visual interpretation of imagery to use the present classification scheme.

## EVALUATION OF MAP PRODUCTS

### PROCEDURES

To evaluate the classification accuracy of Landsat-based test site mapping, a comparison was made with aerial photographs. A stratified random sample (Berry and Baker, 1968; Wood, 1955) of points within the land area of each map was obtained by using a random-number table and a 1-by 1-inch grid with 1/10-inch subdivisions. This grid corresponds to a 2- by 2-mi (3.2 by 3.2 km) spacing at the map scale for the major divisions. Two points were randomly selected from within the 4 mi<sup>2</sup> (10.24 km<sup>2</sup>) area represented by each block.

Aircraft photographs (NASA Missions 300 and 325), dating from February and October 1975, supplemented by the *Environmental Geologic Atlas of the Texas Coastal Zone* series (Brown, coordinator, in progress), were used to interpret land cover and land use for the selected locations. Each location was considered to represent a circle 3 pixels (0.24 km) in diameter on the ground. The network of points was selected for each map by placing a transparent print of the line boundary map on the point grid and transferring all locations. For those points falling near boundaries, that part of the circle which extended into another unit was ignored.

The analysis was performed by an interpreter who had not been involved in classification of the Landsat data. Both color and color-infrared films were used, as were facilities for stereoscopic viewing.

### RESULTS

The accuracy determinations for each scene are included in appendix B. Table 7 summarizes the results, by category, for all seven maps completed during this investigation. Because the amount of information included on the aerial photographs and the published maps exceeds that of the Landsat imagery, these data were considered valid sources of ground data. Points that could not be classified according to land cover - land use after examination of 1:30,000 aerial photographs were termed questionable. No

field checking of these locations was attempted; therefore, this analysis represents only a comparison of Landsat imagery with medium-altitude photographs. An analysis of unit boundaries or total unit areas was not made; hence these results differ from the comparisons of photographs and Landsat imagery made by Fitzpatrick (1975).

Taking all scenes together (table 7), a mean level of 87.4-percent accuracy was achieved for the 806 points checked based on the assumption that one-half of the questionable points could later be determined correct by study of additional information. This compares favorably with the 85-percent minimum level of interpretation accuracy suggested by J. R. Anderson (1976) as a criterion for evaluating land cover and land use classification systems. Results of evaluating the first scene mapped for each of the four test sites (table 8) yield an accuracy of 90.0 percent, indicating that a learning effect was not taking place as a test site was mapped repetitively.

Among the categories (table 7) with the lowest accuracy were undifferentiated barren land (Bu, 64.9 percent) and tidal flats (Wtf, 74.6 percent). Within test site 4, one-third of the undifferentiated barren areas termed incorrect and questionable could be identified as urban areas on the photographs. Industrial areas, dredge spoil, and other barren categories, when lacking distinguishing characteristics, were placed in the undifferentiated barren category; hence the low accuracy was not entirely unexpected. High reflectance common to many of these types of land use contributes to this confusion. Accuracy of tidal-flat identification was influenced by gradational boundaries with submergent sea grass and areas of algal mat; differentiation of these environments can be difficult, especially at higher water levels.

Categories with large samples and for which excellent results were achieved were cropland (93.1-percent accurate) and grassland/rangeland (92.2-percent accurate). Wetlands other than tidal flats were delineated at accuracies exceeding 80 percent; the 85.0-percent value for topographically low marsh is a reasonable result considering the species diversity present and the occasionally indistinct marsh boundaries.

Table 7. Results of accuracy analysis by stratified random sampling; all images for all test sites.

Land Cover - Land Use Classification	Points Inspected			Accuracy (%), assuming		
	Number Correct	Number Incorrect	Number Questionable	All the Questionables Correct	All the Questionables Incorrect	Half the Questionables Correct
U	15	2	3	90.0	75.0	82.5
Ui	10	1	1	91.7	83.3	87.5
Ut	20	0	0	100.0	100.0	100.0
A	95	7	0	93.1	93.1	93.1
G	287	23	3	92.7	91.7	92.2
Gd	4	0	0	100.0	100.0	100.0
Gb	21	2	0	91.3	91.3	91.3
WO	3	0	2	100.0	60.0	80.0
WO	37	2	9	95.8	77.1	86.4
Wlm	44	7	2	87.0	83.0	85.0
Whm	23	5	1	82.8	79.3	81.1
Wtf	34	9	8	82.4	66.7	74.6
Wga	50	1	1	98.1	96.2	97.2
Ws	7	0	0	100.0	100.0	100.0
B	11	2	2	86.7	73.3	80.0
Bds	13	1	1	93.3	86.7	90.0
Bu	23	12	2	67.6	62.2	64.9
<b>Subtotals</b>	<b>697</b>	<b>74</b>	<b>35</b>	<b>91.3</b>	<b>83.5</b>	<b>87.4 Mean</b>
<b>Total</b>	<b>806</b>					

Table 8. Results of accuracy analysis by stratified random sampling;  
first images mapped for all test sites.

Land Cover - Land Use Classification	Points Inspected			Accuracy (%), assuming		
	Number Correct	Number Incorrect	Number Questionable	All the Questionables Correct	All the Questionables Incorrect	Half the Questionables Correct
U	7	2	1	80.0	70.0	75.0
Ui	5	0	1	100.0	83.0	92.0
Ut	11	0	0	100.0	100.0	100.0
A	55	2	0	96.5	96.5	96.5
G	179	17	3	91.5	89.9	90.7
Gd	3	0	0	100.0	100.0	100.0
Gb	12	0	0	100.0	100.0	100.0
WO	1	0	0	100.0	100.0	100.0
WO	16	0	6	100.0	72.7	86.4
Wlm	35	2	1	94.7	92.1	93.4
Whm	18	3	1	86.4	81.8	89.1
Wtf	24	4	2	86.7	80.0	83.3
Wga	26	0	0	100.0	100.0	100.0
Ws	5	0	0	100.0	100.0	100.0
B	8	2	0	80.0	80.0	80.0
Bds	6	1	1	87.6	75.0	81.3
Bu	19	9	2	70.0	63.3	66.7
<b>Subtotal</b>	<b>430</b>	<b>42</b>	<b>18</b>	<b>92.5</b>	<b>87.3</b>	<b>90.0 Mean</b>
<b>Total</b>	<b>490</b>					

## CONCLUSIONS

Results of interpreting Landsat images of the Texas coast indicate that a substantial degree of success can be achieved in mapping 23 specialized categories of land cover and land use (table 3). Landsat transparencies can be optically enlarged up to 8 times without serious loss of image quality to produce maps at a scale of 1:125,000. An understanding of coastal geologic processes and biologic assemblages is essential to visual interpretation because it enables the human interpreter to use much more than just reflectance in delineating coastal features. The shape of an object, its internal texture, and its characteristic position regarding adjoining environmental units often supersede reflectance as the basis for making classification decisions. Perhaps, because Landsat data originate in a digital format and are readily processed by machine, these aspects of imagery interpretation have received less attention than they certainly warrant.

Reflectance alone, seen as the color tones of the false-color composite or the gray tones of a single-band image, is not the absolute property for identifying each type of land cover and land use. The growth phase of the vegetation, recent weather conditions, atmospheric conditions at the time of image acquisition, and tide level are factors which must be taken into account in interpreting reflectance in a Landsat scene of the coastal region. Furthermore, seasonal change in sun angle, photographic processing of the image, and functioning of the satellite sensors and recorders can introduce additional variation in color tone and intensity. The interpreter using standard Landsat products therefore must rely on familiarity with the coastal environment to compensate for the limit of resolution of about 80 m and the 1:1,000,000 scale of the imagery.

Information concerning the location of urban and built-up areas in a particular study site is readily available from published maps and aerial photographs. Because small urban areas which have a low density of development and therefore lack reflectivity contrast with the naturally surrounding area may be totally missed, the use of auxiliary information in making some Level II and Level III classification decisions is essential. Indeed, J. R. Anderson and others (1972) define the second classification level to include the use of topographic maps as an additional data

source. The techniques outlined in this paper can be easily and inexpensively adapted for use with existing map data. In this manner, the user can take advantage of Landsat's unique vantage point, its repeated coverage, and the low direct-purchase cost for data concerning a large area.

Change detection can be accomplished during optical-image interpretation by combining transparencies (fig. 3). This technique is easy to use, and registration of the images is not a problem because a good local fit can be achieved over small areas of interest. Changes in rangeland and cropland and in wetlands resulting from water-level differences closely correlated with ground data. Changes in low-density urban areas and the detectability of roads varied with image characteristics and the subjective decisions of the image interpreter. These urban categories, therefore, could not be handled reliably during optical-change detection.

The delineation of land use and land cover in any area involves a detailed initial inventory using all available types of information followed by monitoring to ensure that the data remain indicative of current conditions. This monitoring is especially important in coastal regions in which the development of natural resources and the sometimes catastrophic natural processes can induce rapid change. It is in the monitoring function that the procedures outlined here for use with the Landsat data can play an important role. Such changes as channel dredging, placement of spoil, conversion of rangeland to cropland, filling of wetlands for other uses, and migration of large (up to several kilometers wide) active dune complexes can, depending on the scale of the change, be readily detected and mapped. The synoptic coverage of the bays and nearshore areas provides data on turbidity distribution, and therefore circulation patterns, which are not often obtained repetitively by aerial photography because of cost constraints. The results obtained during this investigation are indicative of the need to maintain the availability of standard Landsat image products. The mapping technique using simple optical enlargement of Landsat imagery and a multilevel classification system are the means of incorporating current regional information, which might not be available from other sources at a comparable cost, into a valuable body of information concerning coastal resources.

## ACKNOWLEDGMENTS

Funds for this research were provided by the General Land Office of Texas through Contract NAS5-20986 with the National Aeronautics and Space Administration. Peggy Harwood coordinated the project for the General Land Office. Robert W. Baumgardner, Jr., served as project research assistant. Additional assistance was provided by Sam Shannon. E. G. Wermund, Jr., W. A. White, and L. F.

Brown, Jr., critically reviewed the manuscript. Final maps were prepared by Claudia Farmer. Discussions with W. Hupp and S. McCulloch of the Texas Department of Water Resources, J. A. Schell, formerly of the Texas A & M University Remote Sensing Center, and R. K. Holz of the Geography Department, The University of Texas at Austin, were of benefit to the author during this project.



## REFERENCES

- Anderson, J. R., Hardy, E. E., and Roach, J. T., 1972, A land use classification system for use with remote sensor data: U. S. Geol. Survey Circ. 671, 16 p.
- Anderson, J. R., Hardy, E. E., Roach, J. T., and Witmer, R. E., 1976, A land use and land cover classification system for use with remote sensor data: U. S. Geol. Survey Prof. Paper 964, 18 p.
- Anderson, R. R., Alsied, L., and Carter, V., 1975, Applicability of Skylab orbital photography to coastal wetland mapping: Proc. American Soc. Photogrammetry, 41st Ann. Mtg., p. 371-377.
- Anderson, R. R., Carter, V. P., and McGinness, J. W., 1973, Applications of ERTS data to coastal wetland ecology with special reference to plant community mapping and typing and impact of man, *in* Freden and others, eds., Third Earth Resources Technology Satellite Symposium, v. 2: Washington, D. C., NASA, p. 1225-1242.
- Anderson, R. R., and Wobber, F. J., 1973, Wetlands mapping in New Jersey: Photogramm. Eng., v. 39, p. 353-358.
- Andrews, P. B., 1970, Facies and genesis of a hurricane-washover fan, St. Joseph Island, central Texas Coast: Univ. Texas, Austin, Bur. Econ. Geology Rept. Inv. 67, 147 p.
- Arp, G. K., 1975, The rationale for attempting to define salt marsh mosquito breeding areas in Galveston County by remote sensing the associated vegetation, *in* Smistad and others, coordinators, NASA Earth Resources Survey Symposium: Houston, Lyndon B. Johnson Space Center, NASA TM X-58168, p. 289-299.
- Bartlett, D., Klemas, V., and Rogers, R., 1975, Investigations of coastal land use and vegetation with ERTS-1 and Skylab EREP: Proc. American Soc. Photogrammetry, 41st Ann. Mtg., p. 378-389.
- Benton, R. A., Jr., Hatch, S. L., Kirk, W. L., and Newnam, R. M., 1975, Monitoring of Texas coastal wetlands with aerial photography, Phase I—Feasibility study: College Station, Texas A & M Univ.
- Berry, B. J., and Baker, A. M., 1968, Geographic sampling, *in* Berry, B. J. and Marble, D. F., eds., Spatial analysis—A reader in statistical geography: Englewood Cliffs, N. J., Prentice Hall, p. 91-100.
- Brown, L. F., Jr., project coordinator, in progress, Environmental geologic atlas of the Texas Coastal Zone: seven volumes, Univ. Texas, Austin, Bur. Econ. Geology.
- Brown, L. F., Jr., Brewton, J. L., Evans, T. J., McGowen, J. H., Groat, C. G., and Fisher, W. L., in progress, Environmental geologic atlas of the Texas Coastal Zone—Brownsville - Harlingen area: Univ. Texas, Austin, Bur. Econ. Geology.
- Brown, L. F., Jr., Brewton, J. L., McGowen, J. H., Evans, T. J., Fisher, W. L., and Groat, C. G., 1976, Environmental geologic atlas of the Texas Coastal Zone—Corpus Christi area: Univ. Texas, Austin, Bur. Econ. Geology, 123 p.
- Carter, V., and Schubert, J., 1974, Coastal wetlands analysis from ERTS MSS digital data and field spectral measurements: Ann Arbor, Michigan, Proc. Ninth Internat. Symposium on Remote Sensing of Environment, p. 1241-1260.
- Chabreck, R. H., 1972, Vegetation, water and soil characteristics of the Louisiana coastal region: Baton Rouge, Louisiana State Univ., Agr. Expt. Sta. Bull. 664, 31 p.
- Clark, J., 1974, Coastal Ecosystems: Washington, D. C., The Conservation Foundation, 178 p.
- Clements, G., 1976, Landsat field investigation summary: Austin, Texas Parks and Wildlife Dept. unpub. report to the General Land Office of Texas, 7 p. and attachments.
- Davies, J. L., 1964, A morphogenic approach to world shorelines: Zeitschr. Geomorphologie, v. 8, p. 127-142.
- Edwards, P., 1976, An illustrated guide to the seaweeds and sea grasses in the vicinity of Port Aransas, Texas: Austin, Univ. Texas Press, 128 p.
- Erb, R. B., 1974, The ERTS-1 investigation, V. II - ERTS-1 Coastal/estuarine analysis: Houston, Lyndon B. Johnson Space Center, JSC-08457, 284 p.
- Fisher, W. L., McGowen, J. H., Brown, L. F., Jr., and Groat, C. G., 1972, Environmental geologic atlas of the Texas Coastal Zone—Galveston - Houston area. Univ. Texas, Austin, Bur. Econ. Geology, 91 p.
- Fitzpatrick, K., 1975, Cost accuracy and consistency comparisons of land use maps made from high-altitude aircraft photography and ERTS imagery: Reston, Va., Final report, v. 6, CARETS project, Goddard Space Flight Center, Greenbelt, Md., and U. S. Geol. Survey, 61 p.
- Fleetwood, R. J., 1973, Plants of Laguna Atascosa National Wildlife Refuge, Cameron County, Texas: Harlingen, Tx., U. S. Dept. Interior, Fish and Wildlife Service, Bur. Sport Fisheries and Wildlife, 48 p.
- Freden, S. C., Mercanti, E. P., and Becker, M. A., eds., 1973a, Symposium on significant results obtained from the Earth Resources Technology Satellite-1, v. I, Technical presentations, Sections A and B: Washington, D. C., Goddard Space Flight Center, NASA SP-327, 1730 p.
- \_\_\_\_\_, 1973b, Third Earth Resources Technology Satellite-1 Symposium, V. I, Technical Presentations, Sections A and B: Washington, D. C., Goddard Space Flight Center, NASA SP-351, 1974 p.
- Grimes, B. H., and Hubbard, J. C. E., 1971, A comparison of film type and the importance of season for the interpretation of coastal marshland vegetation: Photogramm. Rec., v. 7, p. 213-222.
- Haislet, J. A., 1963, Forest trees of Texas: College Station, Texas A & M Univ. Texas Forest Service Bull. no. 20, 156 p.
- Johnston, M. C., 1955, Vegetation of the eolian plain and associated coastal features of southern Texas: Univ. Texas, Ph.D. dissert. (unpub.).
- Jones, F. B., 1975, Flora of the Texas Coastal Bend: Sinton, Tx., Welder Wildlife Found., 262 p.
- Klemas, V., Daiber, F. C., Bartlett, D., Crichton, O. W., and Fornes, A. O., 1974, Inventory of Delaware's wetlands: Photogramm. Eng., v. 40, p. 433-439.
- McGowen, J. H., and Brewton, J. L., 1975, Historical changes and related coastal processes, Gulf and mainland shorelines, Matagorda Bay area, Texas: Univ. Texas, Austin, Bur. Econ. Geology, 72 p.

- McGowen, J. H., Brown, L. F., Jr., Evans, T. J., Fisher, W. L., and Groat, C. G., 1976a, Environmental geologic atlas of the Texas Coastal Zone—Bay City - Freeport area: Univ. Texas, Austin, Bur. Econ. Geology, 98 p.
- McGowen, J. H., Proctor, C. V., Jr., Brown, L. F., Jr., Evans, T. J., Fisher, W. L., and Groat, C. G., 1976b, Environmental geologic atlas of the Texas Coastal Zone—Port Lavaca area: Univ. Texas, Austin, Bur. Econ. Geology, 107 p.
- McGowen, J. H., and Scott, A. J., 1975, Hurricanes as geologic agents on the Texas coast, *in* Cronin, L. E., ed., Estuarine research, V. II: New York, Academic Press, p. 23-46.
- Pestrong, R., 1969, Multiband photos of a tidal marsh: Photogramm. Eng., v. 35, p. 453-470.
- Price, W. A., 1975, Physical environmental dynamics of tidewater zone, Texas, and human interferences in the Corpus Christi area: Port Aransas, Tx., Coastal Science Workshop, unpub. notes, Sept. 25-27, 1975.
- Reimold, R. J., Gallagher, J. L., and Thompson, D. E., 1973, Remote sensing of tidal marsh: Photogramm. Eng., v. 39, p. 477-488.
- Sauer, J., 1967, Geographic reconnaissance of seashore vegetation along the Mexican Gulf coast: Baton Rouge, Louisiana State Univ. Coastal Studies Institute Tech. Rept. 56, 59 p.
- Short, N. M., Lowman, P. D., Jr., Freden, S. C., and Finch, W. A., Jr., 1976, Mission to Earth: Landsat views the world: Washington, D. C., National Aeronautics and Space Administration, NASA SP-360, 459 p.
- Smistad, O., Zeitler, E. O., and Richard, D., coordinators, 1975, NASA Earth Resources Survey Symposium, V. IA through ID: Houston, Lyndon B. Johnson Space Center, NASA TM X-58168, 2685 p.
- U. S. Department of Commerce, 1975a, Local climatological data: Brownsville, Texas: Asheville, N. C., National Climatic Center.
- \_\_\_\_\_, 1975b, Tide tables, 1976: Washington, D. C., Natl. Oceanic and Atmospheric Adm., Natl. Ocean Survey, 290 p.
- Weisblatt, E., 1976, Satellite inventories of coastal zone environments, (abs.), *in* Symposium on Research Techniques in Coastal Environments: Baton Rouge, Louisiana State Univ., March 18-19, 1976, p. 42.
- Williams, R. S., Jr., and Carter, W. D., eds., 1976, ERTS-1—A new window on our planet: U. S. Geol. Survey Prof. Paper 929, 362 p.
- Wood, W. F., 1955, Use of stratified random samples in a land use study: Annals Assoc. American Geographers, v. 45, p. 350-367.

## APPENDIX A

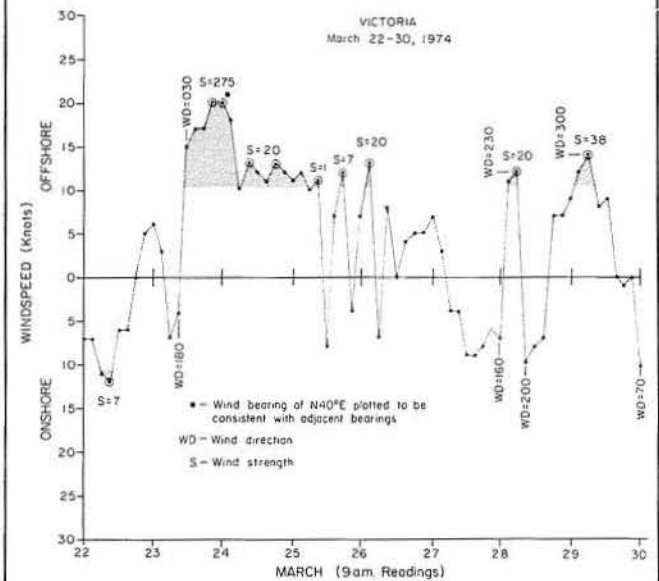
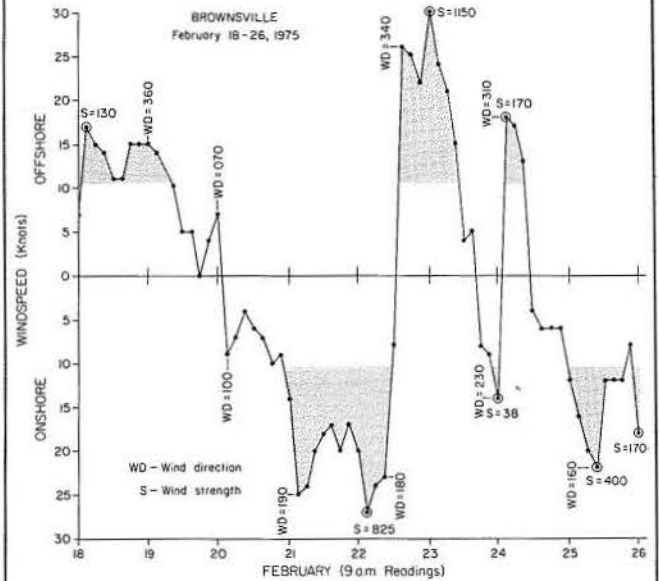
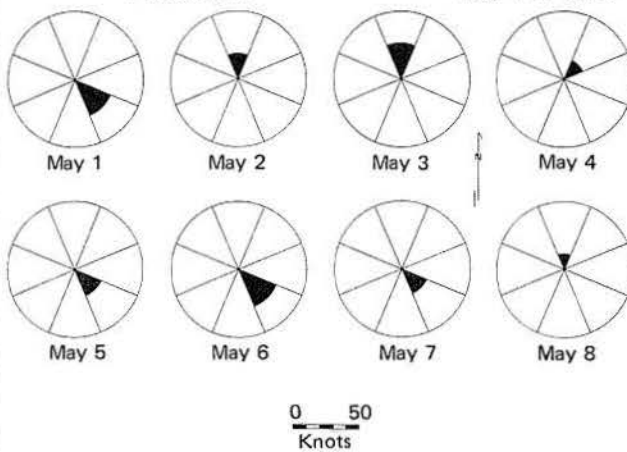
### WIND VELOCITY AND DIRECTION TIME HISTORIES AT THE TIME OF EACH LANDSAT IMAGE ANALYZED

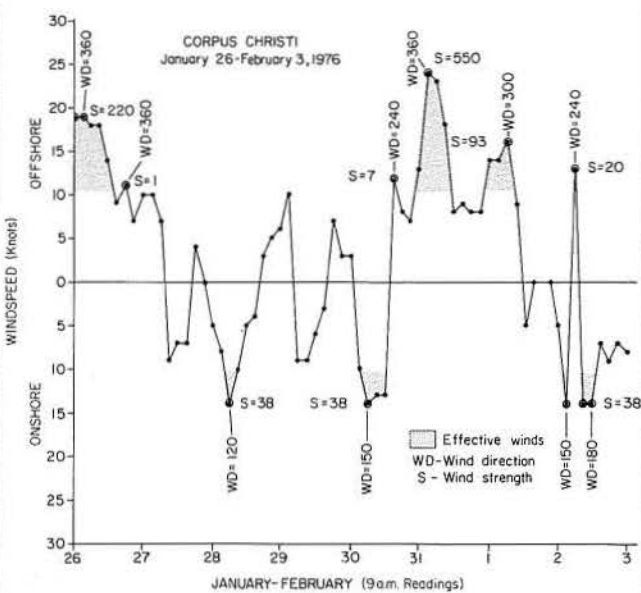
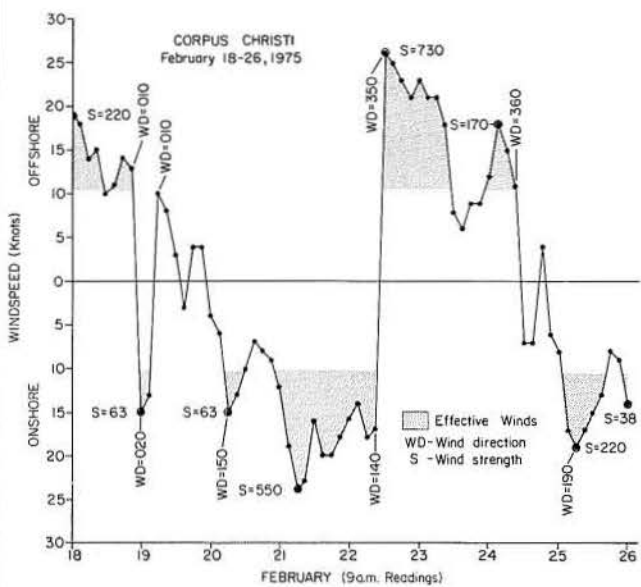
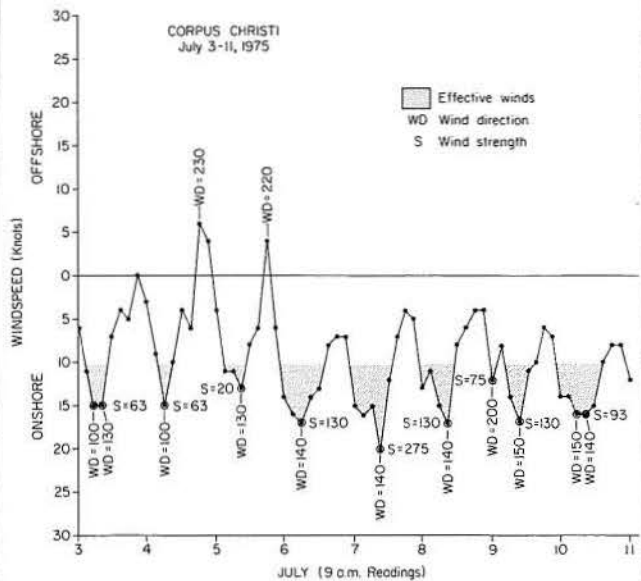
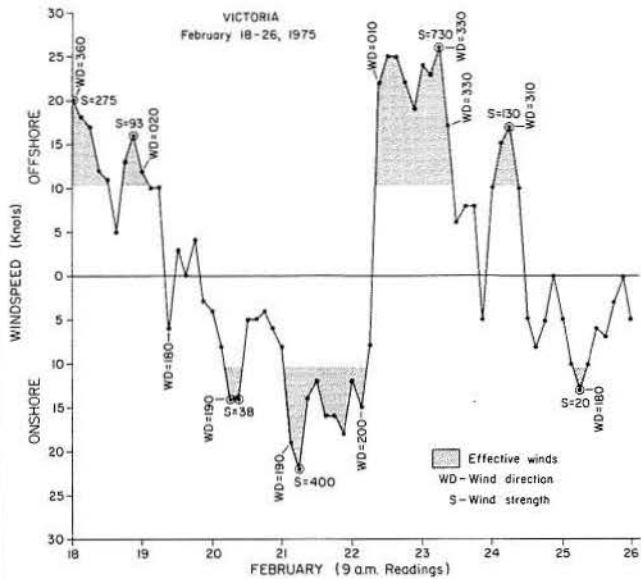
Effective winds are those over 12 mph (10.4 knots).

Wind strength is defined by  $S=(V-v)^2d$  where  $V$  is observed velocity,  $v=12$  mph,  $d$  is duration in hours (Price, 1975).

#### WINDSPEED AND DIRECTION Fastest mile

Galveston, Texas  
May 1-8, 1973







## APPENDIX B

### ACCURACY EVALUATION FOR EACH SCENE MAPPED, BY LAND COVER - LAND USE CATEGORY

The percent-correct value for each category is based on the assumption that one-half of the questionable points would ultimately be considered correct if additional data became available.

Analysis of Test Site 2  
Landsat Scene 1289-16261, May 8, 1973

Classification	Number of Points Checked			Total	Percent Correct
	Correct	Incorrect	Questionable		
U	3	0	0	3	100
Ui	1	0	0	1	100
Ut	4	0	0	4	100
Ue	--	--	--	--	--
A	0	1	0	1	0
G	42	10	3	55	80.0
Gd	--	--	--	--	--
Gb	8	0	0	8	100
WOb	1	0	0	1	100
WO	4	0	3	7	85.7
Wlm	21	2	0	23	91.3
Whm	14	1	0	15	93.3
Wtf	1	0	0	1	100
Wga	--	--	--	--	--
Ws	3	0	0	3	100
B	1	0	0	1	100
Bd	--	--	--	--	--
Bds	--	--	--	--	--
Bu	--	--	--	--	--
Total	103	14	6	123	86.2

Percent correct assuming one-half of questionables are correct 86.2  
Percent correct assuming all of questionables are correct 88.6  
Percent correct assuming all of questionables are incorrect 83.7

Analysis of Test Site 3  
Landsat Scene 1614-16261, March 29, 1974

Classification	Number of Points Checked			Total	Percent Correct
	Correct	Incorrect	Questionable		
U	--	--	--	--	--
Ui	1	0	0	1	100
Ut	--	--	--	--	--
Ue	--	--	--	--	--
A	36	0	0	36	100
G	81	6	0	87	93.1
Gd	2	0	0	2	100
Gb	--	--	--	--	--
WOb	--	--	--	--	--
WO	0	0	1	1	100
Wlm	11	0	0	11	100
Whm	4	2	0	6	66.7
Wtf	--	--	--	--	--
Wga	--	--	--	--	--
Ws	2	0	0	2	100
B	2	0	0	2	100
Bd	--	--	--	--	--
Bds	3	0	0	3	100
Bu	--	--	--	--	--
Total	142	8	1	151	94.7

Percent correct assuming one-half of questionables are correct 94.7  
Percent correct assuming all of questionables are correct 94.7  
Percent correct assuming all of questionables are incorrect 94.0

Analysis of Test Site 3  
Landsat Scene 2034-16200, February 25, 1975

Classification	Number of Points Checked			Total	Percent Correct
	Correct	Incorrect	Questionable		
U	--	--	--	--	--
Ui	1	0	0	1	100
Ut	1	0	0	1	100
Ue	--	--	--	--	--
A	32	1	--	33	97.0
G	88	5	--	93	94.6
Gd	--	--	--	--	--
Gb	--	--	--	--	--
WOb	--	--	--	--	--
WO	--	--	--	--	--
Wlm	7	4	0	11	63.6
Whm	5	2	0	7	71.4
Wtf	2	0	0	2	100
Wga	--	--	--	--	--
Ws	1	0	0	1	100
B	1	0	0	1	100
Bd	--	--	--	--	--
Bds	--	--	--	--	--
Bu	1	1	0	2	50.0
Total	139	13	0	152	91.5

Percent correct assuming one-half of questionables are correct 91.5  
Percent correct assuming all of questionables are correct 91.5  
Percent correct assuming all of questionables are incorrect 91.5

Analysis of Test Site 4  
Landsat Scene 2034-16202, February 25, 1975

Classification	Number of Points Checked				Percent Correct
	Correct	Incorrect	Questionable	Total	
U	4	2	1	7	71.4
Ui	3	0	1	4	100
Ut	6	0	0	6	100
Ue	--	--	--	--	--
A	3	0	0	3	100
G	14	0	0	14	100
Gd	--	--	--	--	--
Gb	4	0	0	4	100
WOb	--	--	--	--	--
WO	12	0	2	14	92.9
Wlm	3	0	1	4	100
Whm	0	0	1	1	100
Wtf	8	3	2	13	69.2
Wga	13	0	0	13	100
Ws	--	--	--	--	--
B	1	0	0	1	100
Bd	--	--	--	--	--
Bds	2	1	1	4	75.0
Bu	1	2	2	5	40.0
Total	74	8	11	93	86.0

Percent correct assuming one-half of questionables are correct 86.0  
Percent correct assuming all of questionables are correct 91.4  
Percent correct assuming all of questionables are incorrect 79.6

Analysis of Test Site 4  
Landsat Scene 2376-16172, February 2, 1976

Classification	Number of Points Checked				Percent Correct
	Correct	Incorrect	Questionable	Total	
U	3	0	1	4	100
Ui	2	1	0	3	66.7
Ut	5	0	0	5	100
Ue	--	--	--	--	--
A	4	1	0	5	80.0
G	12	0	0	12	100
Gd	1	0	0	1	100
Gb	5	0	0	5	100
WOb	--	--	--	--	--
WO	8	1	1	10	90
Wlm	0	0	1	1	100
Whm	--	--	--	--	--
Wtf	5	5	6	16	50.0
Wga	8	0	0	8	100
Ws	--	--	--	--	--
B	1	0	1	2	100
Bd	--	--	--	--	--
Bds	4	0	0	4	100
Bu	1	1	0	2	50.0
Total	59	9	10	78	82.1

Percent correct assuming one-half of questionables are correct 82.1  
Percent correct assuming all of questionables are correct 88.5  
Percent correct assuming all of questionables are incorrect 75.6

Analysis of Test Site 4  
Landsat Scene 5082-16080, July 10, 1975

Classification	Number of Points Checked				Percent Correct
	Correct	Incorrect	Questionable	Total	
U	5	0	1	6	100
Ui	2	0	0	2	100
Ut	3	0	0	3	100
Ue	--	--	--	--	--
A	4	3	0	7	57.1
G	8	1	0	9	88.9
Gd	--	--	--	--	--
Gb	4	2	0	6	66.7
WOb	2	0	2	4	75.0
WO	13	1	2	16	87.5
Wlm	2	1	0	3	66.7
Whm	--	--	--	--	--
Wtf	3	0	0	3	100
Wga	16	1	1	18	94.4
Ws	1	0	0	1	100
B	1	0	1	2	100
Bd	--	--	--	--	--
Bds	3	0	0	3	100
Bu	2	1	0	3	66.7
Total	69	10	7	86	84.9

Percent correct assuming one-half of questionables are correct 84.9  
Percent correct assuming all of questionables are correct 88.4  
Percent correct assuming all of questionables are incorrect 80.2

Analysis of Test Site 5  
Landsat Scene 2034-16205, February 25, 1975

Classification	Number of Points Checked				Percent Correct
	Correct	Incorrect	Questionable	Total	
U	--	--	--	--	--
Ui	--	--	--	--	--
Ut	1	0	0	1	100
Ue	--	--	--	--	--
A	16	1	0	17	94.1
G	42	1	0	43	97.6
Gd	1	0	0	1	100
Gb	--	--	--	--	--
WOb	--	--	--	--	--
WO	--	--	--	--	--
Wlm	--	--	--	--	--
Whm	--	--	--	--	--
Wtf	15	1	0	16	93.8
Wga	13	0	0	13	100
Ws	--	--	--	--	--
B	4	2	0	6	66.7
Bd	--	--	--	--	--
Bds	1	0	0	1	100
Bu	18	7	0	25	72.0
Total	111	12	0	123	90.2

Percent correct assuming one-half of questionables are correct 90.2  
Percent correct assuming all of questionables are correct 90.2  
Percent correct assuming all of questionables are incorrect 90.2



## Part 2

---

# A Guide to Visual Interpretation of Texas Coastal Features from Landsat Imagery





## ABSTRACT

The multispectral scanning devices carried onboard the Landsat satellites provide images in multiple spectral bands that may be used for the mapping of Earth resources. Optically enlarging Landsat standard image products 8 times, from a scale of 1:1,000,000 to a scale of 1:125,000, provides a simple but effective means of delineating land cover and land use. Classification of land cover and land use mapped within selected test sites along the Texas coast was accomplished by modifying published classification schemes to emphasize the monitoring of wetlands, land use, beaches and dunes, and bay systems. Seven primary categories of land cover and land use include 23 secondary categories. Wetlands, a major category, was divided into topographically high marshes, topographically low marshes,

tidal flat, sea grass and algal flats, and vegetated spoil.

The Landsat false-color composite image resembles a color-infrared aerial photograph and is the most useful product for direct image interpretation. The color tones associated with each land cover - land use class and the shape, position, and texture of these coastal features are keys to their delineation. With a knowledge of coastal geologic processes and of biologic assemblages, the interpreter can partly compensate for the limited resolution and the original small scale of the Landsat imagery. Within the context of remote sensing technology available today, the methods described are relatively simple, yet they allow the user to take full advantage of the repetitive coverage, synoptic view, and relatively low direct-purchase cost of Landsat imagery.

## INTRODUCTION

With the launch of Landsat-1 (originally Earth Resources Technology Satellite (ERTS-1) in July 1972, Landsat-2 in January 1975, and Landsat-3 in March 1978, satellite imagery became routinely available for use in mapping and interpreting Earth resources. Each satellite carries two sensor systems, a return beam vidicon or television system and a multispectral scanner (MSS) system. Analysis of MSS images has yielded tremendous amounts of information on agricultural and forest resources, land cover and land use,

mineral resources, Earth structure and landforms, water resources, and the marine environment. The objectives of part 2 of this publication are (1) to provide a brief introduction to the Landsat satellite system and its standard MSS output products, (2) to describe a simple technique of optical interpretation and mapping using Landsat transparencies, and (3) to describe the tonal and textural characteristics of land cover and land use observed on Landsat imagery of the Texas coastal region.

## SATELLITE SYSTEM CHARACTERISTICS

The multispectral scanning device aboard Landsat uses an oscillating mirror which continuously scans perpendicular to the spacecraft's track and covers an area 115 mi (185 km) wide (National Aeronautics and Space Administration, 1976). Detectors within the MSS are sensitive to electromagnetic radiation reflected from the Earth in multiple spectral bands (table 9). Data from the detectors are coded in a digital format and either tape recorded for later retrieval or transmitted directly back to Earth. At National Aeronautics and Space Administration (NASA) facilities, the continuous strip of imagery is transformed into framed and annotated images, each covering approximately 13,225 mi<sup>2</sup> (34,225 km<sup>2</sup>).

Table 9. Spectral bands of Landsat multispectral scanner (MSS) products.

MSS Band	Spectral Region individual black-and-white image	Wavelength $\mu$
4	visible green	0.5 to 0.6
5	visible red	0.6 to 0.7
6	infrared	0.7 to 0.8
7	infrared	0.8 to 1.1
8	thermal infrared*	10.4 to 12.6

\* Landsat-3 only

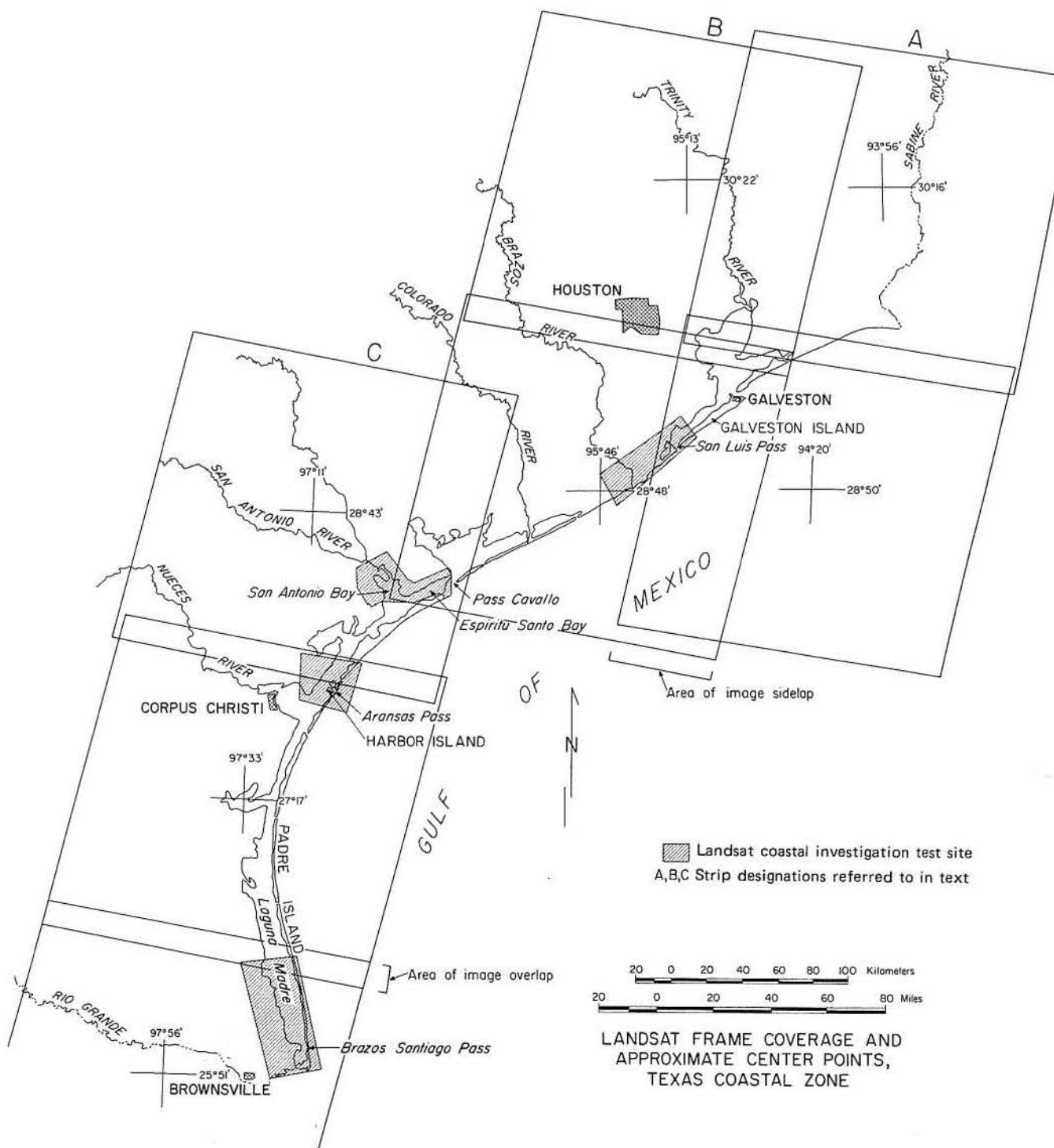


Figure 26. Locations of Landsat investigation test sites and positions of imagery covering the Texas coastal region.

The orbital path of the satellite carries it from north-northeast to south-southwest across the United States, and each image has a 10-percent overlap along the path of spacecraft travel (fig. 26). Sidelap between adjacent images varies with latitude and is approximately 20 percent over the Texas coast (fig. 26). Each satellite follows the same path every 18 days and obtains repetitive imagery over nearly identical areas on Earth at approximately the same local time. For the frames covering the Texas coastal region (fig. 26), image times are usually between 10:08 a. m. and 10:30 a. m., Central Standard Time. The repetitive image centers are maintained to within 23 mi (37 km) (National Aeronautics and Space Administration, 1976).

Each satellite's scheduled path is such that adjacent tracks are covered at 1-day intervals. For example, track A (fig. 26), if scheduled for the first day of a given month, would be followed by track B on the second day and track C on the third day; track A would be covered again on the nineteenth day of the month. Originally Landsat-2 was timed so that it lagged behind Landsat-1 with a delay of 9 days to provide coverage of a given ground point every 9 days. Orbital drift had altered this timing such that coverage was obtained at 6- and 12-day intervals. Electronic malfunctions have now (April 1978) made Landsat-1 largely inoperable. Landsat-3 (launched in March 1978) follows Landsat-2 coverage of a given ground point every 9 days.

### STANDARD LANDSAT DATA PRODUCTS

Landsat data originate as a series of digital values of Earth reflectance recorded on magnetic tape. Copies of such data tapes are available to users who have the capability to handle and classify the data using computer systems. Hard copies of processed data can then be produced with various types of computer-controlled printing devices. Further discussion of computer processing is beyond the scope and purpose of this publication; however, it should be remembered that Landsat standard products originate from numerical data generated by an electronic scanner aboard the satellite and reconstituted to form an image by a recording device. This recording device creates a "working master" from which Landsat standard products can then be produced in quantity with common photographic materials. The process of obtaining the data within the satellite, however, is completely electronic and does not involve the conventional use of camera and film.

Standard Landsat image products are available as black-and-white reproductions of single bands and as false-color composite images. The formats of these products are summarized in table 10. The false-color composite resembles a color-infrared aerial photograph and is produced by exposing the band 4, 5, and 7 images through filters on color film. The spectral regions of green, red, and infrared radiation, corresponding to each of these three spectral

Table 10. Formats of standard Landsat MSS image products available from the Earth Resources Observation Systems (EROS) Data Center, Sioux Falls, South Dakota.

Black-and-White Single Band		
Size, inches	Scale	Format
2.2	1:3,369,000	film, positive or negative
7.3	1:1,000,000	film, positive or negative, or positive paper print
14.6	1:500,000	paper print
29.2	1:250,000	paper print
False-Color Composite		
7.3	1:1,000,000	film positive
7.3	1:1,000,000	paper print
14.6	1:500,000	paper print
29.2	1:250,000	paper print

bands, produce blue, green, and red tones, respectively, in the resulting false-color composite. Vegetation appears in tones of red depending on the level of infrared reflectance of the plant material (brighter reds indicating greater reflectance); water varies from dark to light blue with increasing turbidity or decreasing depth; and barren areas appear white to dark gray, depending on the proportion of sand to mud in the substrate. The false-color composite is the most useful standard product for Earth resource analysis, especially land cover - land use mapping, because it can be interpreted in the same manner as conventional color-infrared aerial photographs.



## THE LANDSAT COASTAL PROJECT

To help meet the needs of the State of Texas for current information on the rapidly changing and developing coastal area, an investigation into the application of standard Landsat image products was undertaken by the Bureau of Economic Geology. Four test sites (fig. 26) were mapped at a scale of 1:125,000 using an image-interpretation procedure that involved optical enlargement of standard 7.3-inch 1:1,000,000 scale film-positive transparencies. The objective in applying this procedure, developing a land cover - land use classification scheme and perfecting the map product format, was to assist the General Land Office of Texas in its capability to monitor wetlands, coastal land cover and land use, beach and dune areas, and the bay and estuarine systems. The land cover - land use classification scheme has been specifically de-

signed for mapping coastal features. Included are environmental geologic units, such as barren dredge spoil and dunes, and such coastal biologic assemblages as vegetated barrier flats and two distinct marsh types.

During test-site mapping, features were identified on Landsat images primarily from the interpreter's knowledge of coastal geologic environments and biologic assemblages. More general principles of aerial photographic interpretation, such as those relating to urban and agricultural land use patterns (Avery, 1968), were also employed. Although the image-interpretation procedure reported here would be applicable in other areas, the land cover - land use classification scheme has been specifically designed for use in coastal regions.

## COASTAL ZONE APPLICATIONS OF LANDSAT IMAGERY

Appendix C is an annotated bibliography of published applications of Landsat imagery and aerial photographs in coastal regions. Aerial photographs are included because the interpretation of Landsat standard products, especially the false-color composite, is similar to the evaluation and mapping of wetlands using conventional films. Skylab S190A multispectral camera and S190B earth terrain camera photographs have also been used by some investigators (Klemas and others, 1974; R. R. Anderson and others, 1975a and 1975b) in wetlands delineation. Skylab data were collected from manned orbital spacecraft at a lower altitude than Landsat and hence have better resolution, but coverage is less complete than that of Landsat, and periods of data collection are limited to Skylab missions.

Direct visual interpretation of Landsat images for the purpose of coastal wetland mapping has been investigated by R. R. Anderson and others (1973; 1973b), R. R. Anderson and others (1975a), and Bartlett and others (1975). These authors, as well as Klemas and others (1974), Carter and Schubert (1974), Erb (1974), Weisblatt (1975, 1976), and additional authors listed in appendix C, have also mapped coastal areas using computer-assisted data processing or other enhancement techniques. Emphasis was placed on marshland mapping during these studies because of the key role which marshlands play as nurseries and centers of productivity in coastal ecosystems (Clark, 1974). However, because adjacent land use and land cover can significantly influence wetlands, mapping of all environments within a given area is a requirement in the management of coastal resources. To apply Landsat data to the study of coastal regions, a general classification scheme for coastal land and water and a mapping technique are required.

### CLASSIFICATION MODIFICATION AND DEVELOPMENT

To develop a land cover - land use classification scheme for use with Landsat imagery of the Texas coastal region,

the U. S. Geological Survey system (J. R. Anderson and others, 1976) was modified to meet the needs of the General Land Office of Texas. These needs relate to the role of the General Land Office as the custodian of coastal public lands in Texas. The U. S. Geological Survey system (table 11) provides an adaptable, multilevel scheme to which the user may add or remove categories to fit individual requirements. The adopted classification system shown in table 3 (see p. 9) was developed. The numbering system for each category correlates with the national system in that the first and second digits designate similar level I and level II categories in table 11. A three-digit code indicates the addition of a level III unit which was generated during Landsat coastal mapping in Texas.

A zero at level II, such as in the water categories (table 3), indicates that the level II categories of the national system were not delineated. Water was not classified at level II because the designation of streams, lakes, estuaries, and so forth is readily available to the intrastate user from supplementary information, whereas turbidity distribution is an indicator of surface-water circulation patterns.

Of the 23 secondary classes (table 3), 14 were specifically oriented toward unique coastal geologic processes and biologic assemblages. Nonforested wetland, for example (coded 62 in the standard system, table 11), was expanded into five units in order to extract as much information as possible from the Landsat imagery. The secondary classes were distinguished not only on the basis of radiance, but also texture, shape, and spatial position of an area in relation to other features seen on the Landsat imagery (Finley, 1976). A basic background in coastal processes and some familiarity with the Texas coastal environment are essential to the mapping procedure and can be gained through study of the *Environmental Geologic Atlas of the Texas Coastal Zone* series (Brown, coordinator, in progress) and U. S. Geological Survey 7.5-minute quadrangle maps. The classification scheme was prepared specifically for use with the image-interpretation mapping procedure presented

Table 11. U. S. Geological Survey land use and land cover classification with remote sensor data (J. R. Anderson and others, 1976).

Level I		Level II
1. Urban or built-up land	(11)	Residential
	(12)	Commercial and services
	(13)	Industrial
	(14)	Transportation, communications and utilities
	(15)	Industrial and commercial complexes
	(16)	Mixed urban or built-up land
	(17)	Other urban or built-up land
2. Agricultural land	(21)	Cropland and pasture
	(22)	Orchards, groves, vineyards, nurseries, and ornamental horticultural areas
	(23)	Confined feeding operations
3. Rangeland	(24)	Other agricultural land
	(31)	Herbaceous rangeland
	(32)	Shrub and brush rangeland
4. Forest land	(33)	Mixed rangeland
	(41)	Deciduous forest land
	(42)	Evergreen forest land
5. Water	(43)	Mixed forest land
	(51)	Streams and canals
	(52)	Lakes
6. Wetland	(53)	Reservoirs
	(54)	Bays and estuaries
	(61)	Forested wetland
7. Barren land	(62)	Nonforested wetland
	(71)	Dry salt flats
	(72)	Beaches
8. Tundra	(73)	Sandy areas other than beaches
	(74)	Bare exposed rock
	(75)	Strip mines, quarries, and gravel pits
9. Perennial snow or ice	(76)	Transitional areas
	(77)	Mixed barren land
	(81)	Shrub and brush tundra
	(82)	Herbaceous tundra
	(83)	Bare ground tundra
	(84)	Wet tundra
	(85)	Mixed tundra
	(91)	Perennial snowfields
	(92)	Glaciers

here, and would not be entirely suitable for computer-aided digital-processing techniques.

### MAPPING TECHNIQUES

Direct image interpretation of standard Landsat products has apparently been attempted only on a minor scale, and literature on such procedures is very limited (appendix C). R. R. Anderson and others (1973b) used a Bausch and Lomb Zoom Transfer Scope to enlarge Landsat transparencies and map wetland areas approximately 5 by 9 mi (8 by 15 km). Resulting maps were at a scale of 1:250,000. A Bessler enlarger (R. R. Anderson and others, 1975b) has been used as well for image interpretation, however none of the areas mapped approached the sizes of the test sites (380 to 780 mi<sup>2</sup> or 984 to 2020 km<sup>2</sup>) studied on the Texas coast (Finley, 1976).

Since an excellent coastwide map base was available in the form of 1:125,000 scale environmental geology maps (Brown, coordinator, in preparation), this mapping scale

was adopted when it was found that the 1:1,000,000-scale Landsat transparencies could be optically enlarged 8 times without serious loss of image quality. The mapping process involved four steps. First, the portion of the 1:1,000,000 scale band 7 negative covering the test site was enlarged 8 times to produce a film-positive transparency. This process was accomplished by the Automation Division of the Texas Department of Highways and Public Transportation using either a Durst or Laborator No. 184 enlarger. Product scale was controlled by matching land-water boundaries to 1:125,000 scale environmental geology maps from the *Environmental Geologic Atlas of the Texas Coastal Zone* series. Second, water boundaries, cropland boundaries, and other easily discernible features were transferred from the photographic enlargement to a transparent overlay. Third, the overlay was used as a map base onto which enlarged, 1:1,000,000 Landsat transparencies were projected using the Zoom Transfer Scope. The boundaries of all features of interest were filled in by using the features mapped from the photographic enlargement to match scales between the enlarged image and the overlay map. Finally, the hand-drawn map was scribed, a print was produced, and each unit was classified according to land cover and land use. The Zoom Transfer Scope was again used to enlarge Landsat transparencies and project them onto the line-boundary map as classification decisions were made. Note that the enlarged base transparency of band 7 Landsat data, which cover the entire test site, was required to avoid inaccuracies caused by shifts in field of view when using the Zoom Transfer Scope. Finally, the maps were hand colored according to the land cover - land use classification scheme (table 3).

### RECOGNITION OF LAND COVER - LAND USE CLASSES

The primary constraint in the interpretation of Landsat image products is their limited resolution. The smallest unit of reflectance from Earth that the satellite detectors can discriminate comes from a square area 259 ft on a side (79 by 79 m) (National Aeronautics and Space Administration, 1976). This unit is called a picture element (pixel) and has a digital value in each of the bands of the MSS. The thermal infrared band on Landsat-3 can resolve only an area 788 ft (240 m) on a side. Owing to physical characteristics of the scanning process, adjacent pixels overlap making the "effective" area sampled 184 by 259 ft (56 by 79 m) in size (National Aeronautics and Space Administration, 1976) for bands 4 through 7. These dimensions correspond to an area of 1.1 acres, which is usually cited as the minimum size of ground unit which can be detected on Landsat MSS data. More than 7 million of these units make up each Landsat image, and when optically viewing a 1:1,000,000 scale image that is 7.3 inches on a side, the interpreter can deal only with large groups of pixels in making classification decisions.

In specific instances, small areas with a great reflectance contrast with surrounding units can be detected on standard Landsat image products. Very high reflectances associated with areas of barren, sandy dredge spoil or shell fill, for example, tend to dominate a pixel, although they



Figure 27. Locations of Landsat false-color composite segments shown in plate 1.

might be much less than an acre in size. Unpaved shell roads less than 30 ft (9 m) wide show up clearly against the low reflectance of cleared fields developed on dark-gray muddy soils. The orientation of linear features such as roads and narrow dredged canals (<160 ft wide) is also a factor in their detection. When these features lie parallel to the scan lines of the imagery, they become difficult to distinguish from the scan lines themselves.

Bulk-processed Landsat images, the type most readily available and most commonly used, show substantial variation in color tone of the same area when seen repetitively on false-color composite images. Such variation may result from natural and human-induced changes, seasonal changes in vegetation, and water-level differences, which are of primary interest to the interpreter, or may also result from atmospheric haze, differences in sun angle and azimuth, and the color-film-processing procedures. To help avoid errors caused by the latter factors, the shape of an object, its internal texture, and its characteristic position regarding adjoining environmental units may supersede color tone as the basis for making classification decisions.

If the interpreter has reviewed available map data over the area of interest before using Landsat imagery, the following descriptions and examples of land cover - land use categories should aid in their delineation. Examples of Landsat imagery (fig. 27) have been chosen from the vicinity of test sites previously mapped (fig. 26) and are reproduced on plate 1 (A through F). All color tones refer to those seen on the false-color composite image.

## URBAN AND BUILT-UP LAND

### Industrial

Major industrial sites, such as refineries and petrochemical plants (pl. 1A-1), smelting operations, drilling platform construction sites, and port facilities (pl. 1A-2) are often recognizable by (1) the high-reflectance white to bluish-white tones resulting from metal structures, areas of concrete, and associated shell and sand fill, (2) the presence of holding ponds for liquids, and (3) distinguishable roads or dredged channels. Use of the first criterion alone can be misleading because high-reflectance barren areas, such as dredge spoil, may be misinterpreted as industrial locations. Supplemental map data can be used to avoid such errors.

### Extractive—Hydrocarbons

Sites of oil and gas production generally cannot be distinguished on Landsat imagery; however, production around salt domes is an exception: High Island Dome and Hoskins Mound (fig. 28) are readily detected. The land surface at Hoskins Mound has been disturbed by sulfur mining which may increase its detectability on Landsat imagery. At Hoskins Mound a circular pattern of high-reflectance barren areas (white on the false-color composite) are indicative of access roads, well sites, and sulfur-storage areas. A large holding pond is detectable adjacent to the circular feature, suggesting some type of industrial or extractive facility.

## Transportation

Both roads and dredged channels were placed in this category, although other users may wish to classify channels in the level I category of water while retaining turbidity designations for other types of water bodies. The detectability of roads varies greatly, depending on width of the right-of-way, reflectivity contrast with surrounding environments, degree of development along the road, and image quality. Interstate highways and other four-lane roads with distinct medians and shoulders and parallel strip development can be detected with the greatest consistency. Route 288 between Angleton and Freeport (pl. 1A-3) is an example of such a major road. In contrast, Route 332, which extends northwest from Surfside (pl. 1B-1), is not detectable where it crosses the low marshes landward of that city until roadside development begins. The pattern of patchy, high-reflectance areas originates from commercial and small industrial sites (pl. 1B-2). Many local roads and city streets were simply classified from Landsat data as mixed urban when they could not be separated from surrounding environments.

Channels, such as the Intracoastal Waterway (pl. 1C-1), can be recognized on the basis of form and position and the presence of dredged material in linear or circular patterns. The deepest parts of the dredged channel appear medium to dark blue; the shallower areas are lighter blue; and the wet or barely subaqueous spoil-pile margins appear very light blue (pl. 1F-1). Narrow channels became very difficult to map when they precisely paralleled the east-west scan lines of the MSS image.

### Mixed Urban

High-density urban areas, such as downtown Houston, appear in medium-blue tones. The red tones caused by the infrared reflectance of vegetation are completely absent in highly built-up areas. Less dense urban areas, such as Freeport (pl. 1A-4) and Port Isabel (pl. 1D-1) give a pebbly, dull reddish-pink-and-white pattern because the lawns and trees of the city are interspersed with paved roads and urban structures. When these characteristics are seen in conjunction with transportation features, urban complexes can be readily identified.

Urban development on Padre Island (pl. 1D-2), however, was not detectable because (1) many streets are simply cleared areas of loose sand and shell, (2) lawns and planted trees characteristic of developed areas are not extensive, and (3) structures immediately adjacent to the beach and within the foredune area are masked by the high reflectance of the barren sands. Port O'Connor (pl. 1C-2) represents another type of urban area that is difficult to detect because structures are well dispersed within the natural grassland vegetation.

## AGRICULTURAL LAND

### Cropland

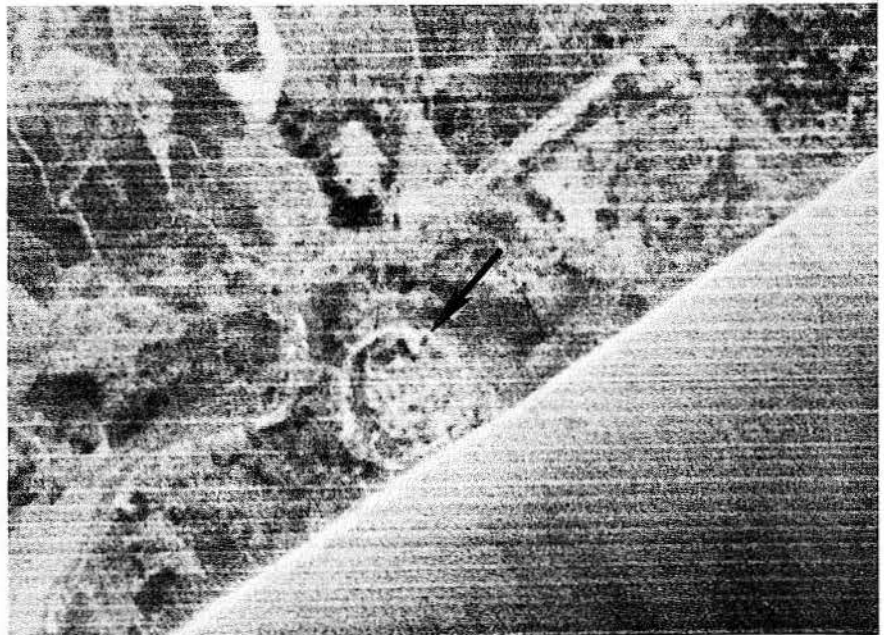
Cropland is best distinguished by the regular geometric boundaries created by turnrows and fencelines. Winter



Figure 28A



Figure 28B



Hydrocarbon production facilities at Hoskins Mound (A) and High Island (B) salt domes are revealed by circular features on Landsat band 5 imagery (length of area covered by photographs is approximately 13.5 mi). Photograph A is from Landsat scene 1289-16261, May 8, 1973; photograph B is from Landsat scene 1576-16152, February 19, 1974.

images of barren fields show gray to black tones where substrates are muddy (pl. 1F-2), becoming light gray to white with increasing sand content. When crops are present, the geometric shape of each field is more difficult to detect. The greater infrared reflectance of crops (deep, intense red tone) (pl. 1A-5) compared with a background of unimproved grassland (slightly pink or faded red) facilitates boundary delineation between these two land use categories. Broad-leaf trees also produce an intense red coloration on Landsat false-color composites, hence area shape and location must be considered when mapping croplands. Imagery from different seasons would be a further aid in cropland identification. Cropland that has been left uncultivated for

one or more seasons begins to resemble grassland; even as noncrop species invade the field; however, the regularity of the field boundaries remains detectable on Landsat imagery.

## GRASSLAND/RANGELAND

### Range-Pasture

Because cattle raising is ubiquitous in Texas and because most coastal grasslands have some potential as pastureland, this category was removed from the level I agricultural category of the national classification (table 11) and

## Plate 1

Annotated segments of Landsat false-color composite images.  
See figure 27, p. 50, for an index to segment locations.

**A. Freeport area**

May 8, 1973

Scene No. 1289-16261

**B. Freeport area**

February 2, 1976

Scene No. 2375-16112

**C. Matagorda Island - Espiritu Santo Bay area**

February 25, 1975

Scene No. 2034-16200

**D. South Padre Island area**

February 25, 1975

Scene No. 2034-16205

**E. Kenedy County inland dune area**

February 25, 1975

Scene No. 2034-16202

**F. Harbor Island - Corpus Christi Bay area**

February 25, 1975

Scene No. 2034-16202



# Plate 1

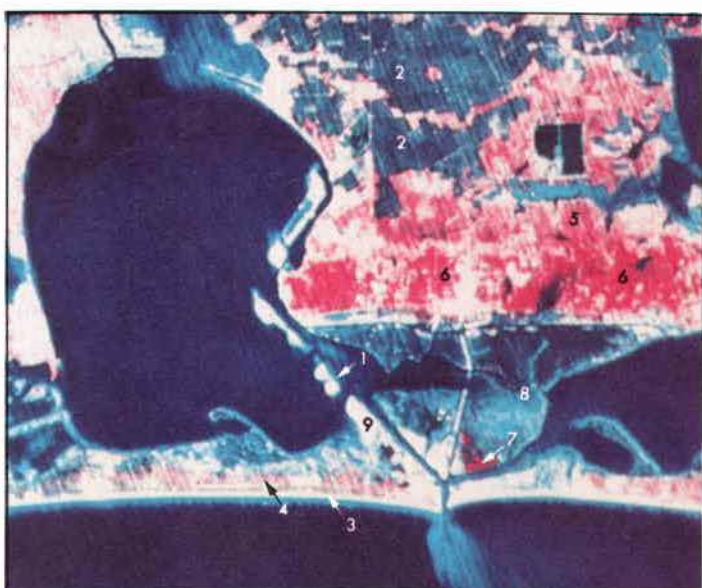
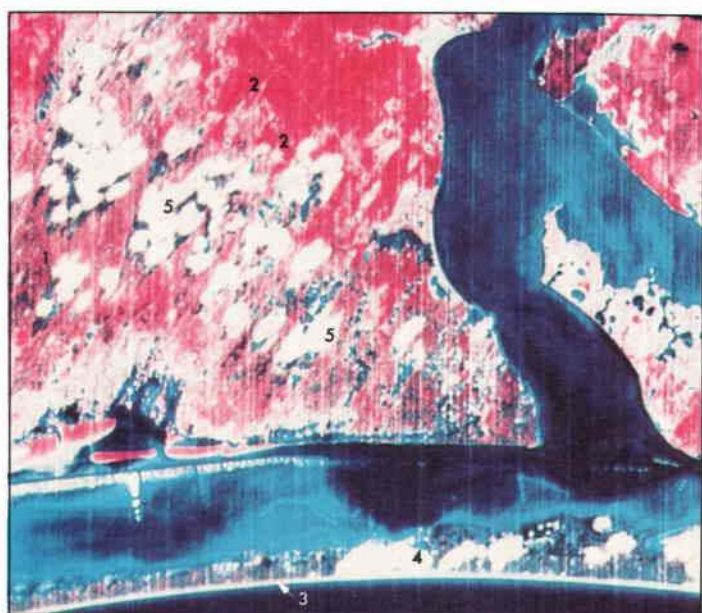
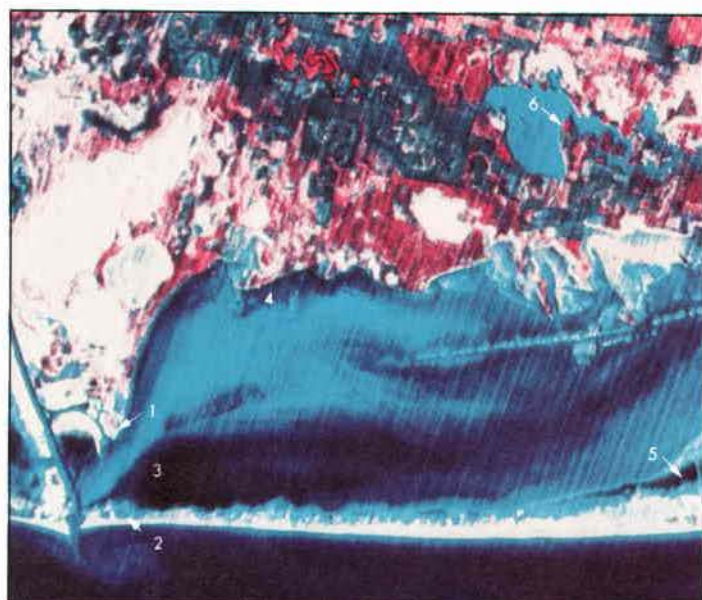
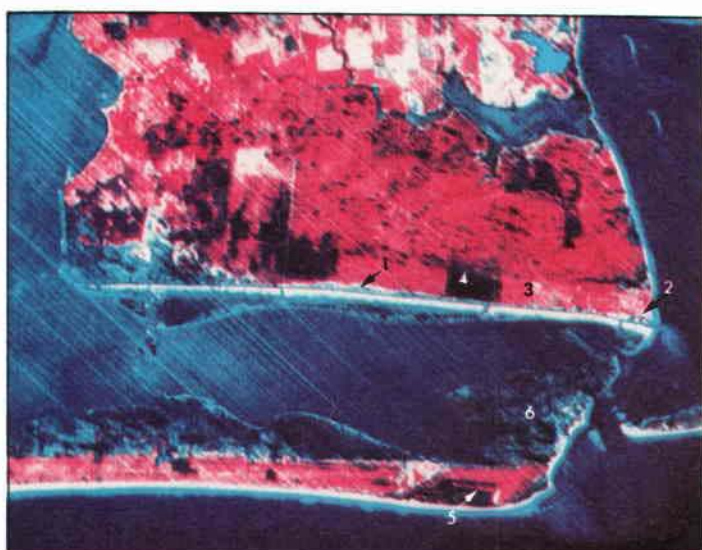
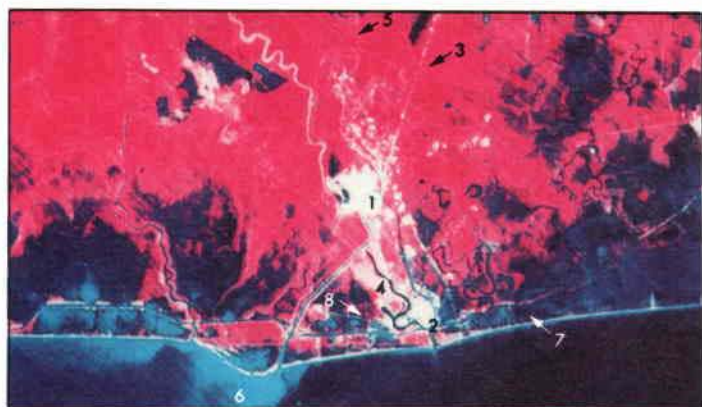
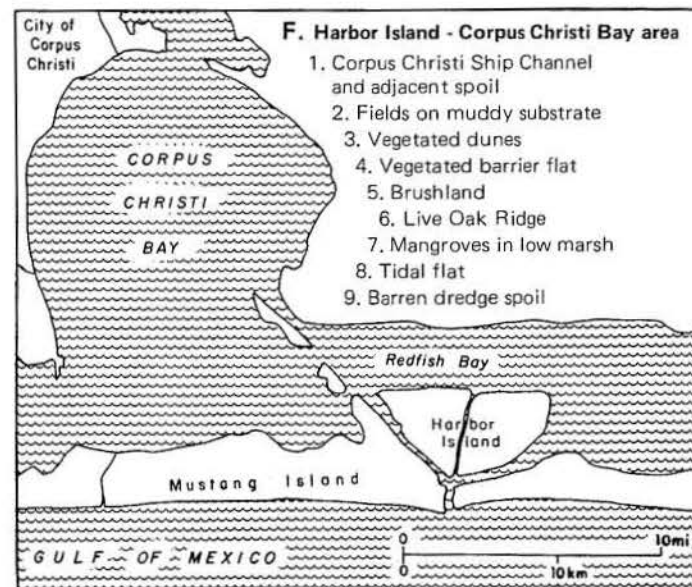
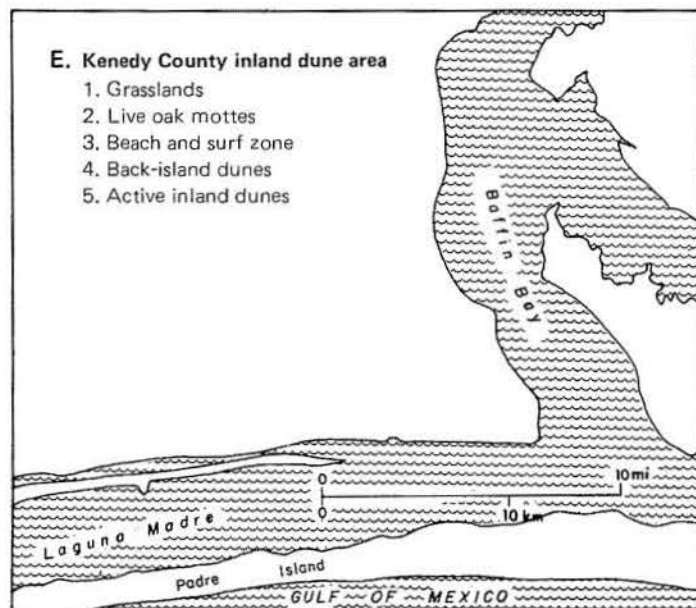
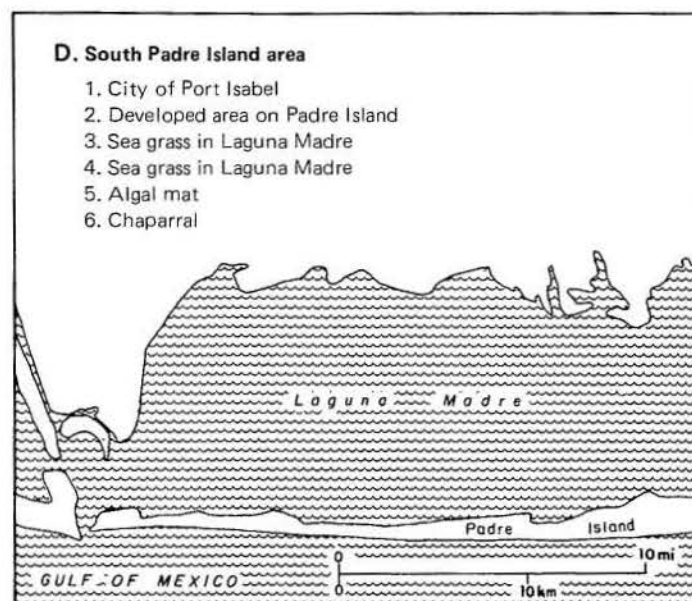
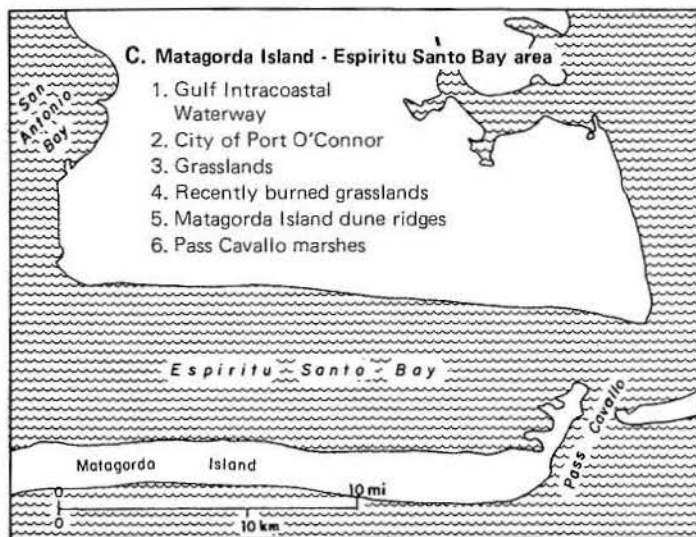
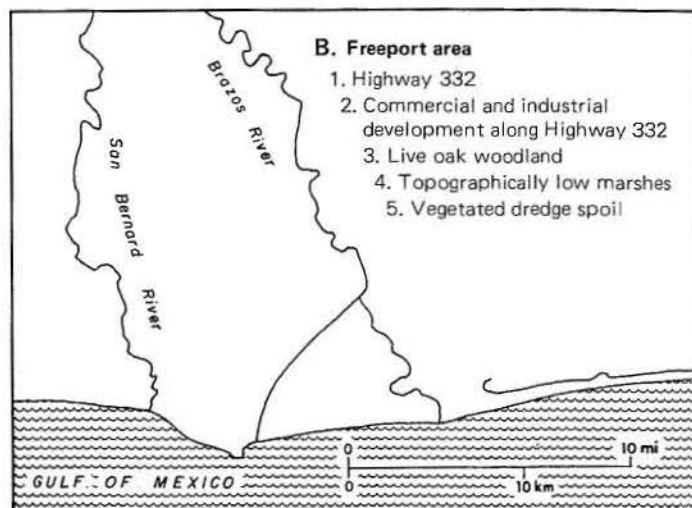
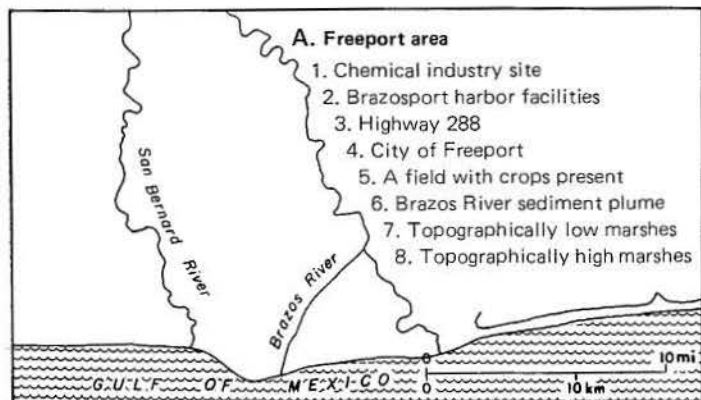




# Plate 1 Explanation







included here. All grasslands other than those which could be delineated as vegetated dunes or vegetated barrier flats were designated as range pasture. Tonal characteristics of range-pasture grasslands are quite variable, from brownish reds (pl. 1E-1) to medium reds and reddish pinks (pl. 1C-3). These color variations depend on the infrared reflectance of the grasses, which, in turn, is related to growth, overall plant vigor, and the mixture of plant species within a given area. Substantial tonal variation in coastal grasslands occurs on the saline soils of South Texas where halophytic plant species atypical of most coastal grasslands are found in areas being grazed.

In areas where *Spartina spartinae* occurs in the coastal prairie grasslands, burning removes dead culms and encourages the young growth on which cattle thrive. Burned areas may resemble idle croplands (pl. 1C-4) on winter imagery; a comparison of summer and winter scenes would resolve such confusion.

#### Vegetated Dunes

Vegetated dunes are covered with coastal grasses, many of which are the same species that occur within range-pasture grasslands and on the vegetated barrier flats. The variation in color tone is similar, therefore, to that of range-pasture grasslands; the best distinguishing feature of vegetated dunes is the linear pattern of the dune ridges, as observed on Matagorda Island (pl. 1C-5) and on Brazos Island and Mesa del Gavilan near the mouth of the Rio Grande. Dune areas on Mustang Island appear slightly more brownish to grayish red than the surrounding vegetated areas (pl. 1F-3), but without a distinctive linear pattern vegetated dunes are extremely difficult to delineate from Landsat imagery.

#### Vegetated Barrier Flat

Between the beach and the tidal flats on the bay sides of barrier islands, such as Mustang Island, there are areas of slightly hummocky topography that lack ridges and low swales (McGowen and others, 1976; Brown and others, 1976) and are termed barrier flats. These areas have a tonal response similar to that of range-pasture grasslands (pl. 1F-4) and contain many of the same plant species. Vegetated dunes that lack a linear pattern would fall within this category during the image-interpretation process.

#### Brushland

Brushland was the most difficult land cover unit to distinguish by Landsat mapping in the Texas coastal region. An area of stunted mesquite (*Prosopis glandulosa*) brushland, where the mesquite was estimated to provide 80-percent canopy cover (Clements, 1976), registered a muddy reddish brown on winter imagery (pl. 1F-5) and a slightly brighter grayish red on summer imagery. Although comparison of summer and winter images may help identify brushland, field observations, either on the ground or from low-altitude aircraft, are needed to locate and adequately map brushlands. In general, the level of brushland infrared

reflectance, and hence intensity of red tones in the false-color composite image, would be intermediate between deciduous woodland and grassland on summer imagery.

### FOREST LAND

#### Woodland or Dense Chaparral

All examples of woodland in this publication pertain to deciduous woodland only, except in the sense that live oak (*Quercus virginiana*) represents a broadleaf evergreen (Jones, 1975). Reflectance in the infrared wavelengths is high for healthy broadleaf trees, hence the most intense red coloration on Landsat imagery, other than that of croplands, is usually produced by woodlands. Examples include the live oak woodlands occurring in clumps in Kenedy County (pl. 1E-2) and covering the Pleistocene barrier-strandplain sands (Brown and others, 1976) of San Patricio County (pl. 1F-6). Woodlands along watercourses, termed fluvial woodlands (McGowen and others, 1976), include deciduous species such as *Carya* spp. (pecan and hickory), *Ulmus* spp. (elm), *Celtis* spp. (hackberry) and *Liquidambar styraciflua* (sweetgum). Summer imagery is best for mapping these woodlands, but winter imagery may be used where the woodland signature is detectable throughout the year because of the presence of live oak (pl. 1B-3).

The dense growth of shrubby, diminutive trees found, for example, in Cameron County, Texas, (Brown and others, in preparation) has been termed chaparral. Species found within this unit include *Prosopis glandulosa* (mesquite), *Celtis spinosa* (spiny hackberry), and *Acacia farnesiana* (huisache) (Clements, 1976). Chaparral resembles woodland on Landsat imagery (pl. 1D-6), with a more intense red tone than adjacent grasslands have. When chaparral occurs in small patches, it is likely to be overlooked in mapping.

### WATER

Water varies from a dark-navy-blue tone where the concentration of suspended matter is low, to a baby-blue or turquoise color where relatively greater amounts of suspended matter are present. These differences can be subjectively interpreted from false-color composite images and can be described as nonturbid, slightly turbid, moderately turbid, or highly turbid on the basis of color. It should be noted that very shallow water over tidal flats or the reworked margins of spoil piles may also appear very light blue because of bottom reflectance rather than the turbidity of the water column.

Areal delineation of water masses based on apparent turbidity permits the tracing of surface-water circulation patterns in that the reflectance detected by the satellite sensors comes primarily from the upper meter of the water column. River discharge into the Gulf, such as the mud-laden waters of the Brazos (pl. 1A-6), the expansion of turbid tidal-inlet effluent, the distribution of river waters within bay systems, and the alongshore movement of turbid coastal waters can all be traced with Landsat imagery.

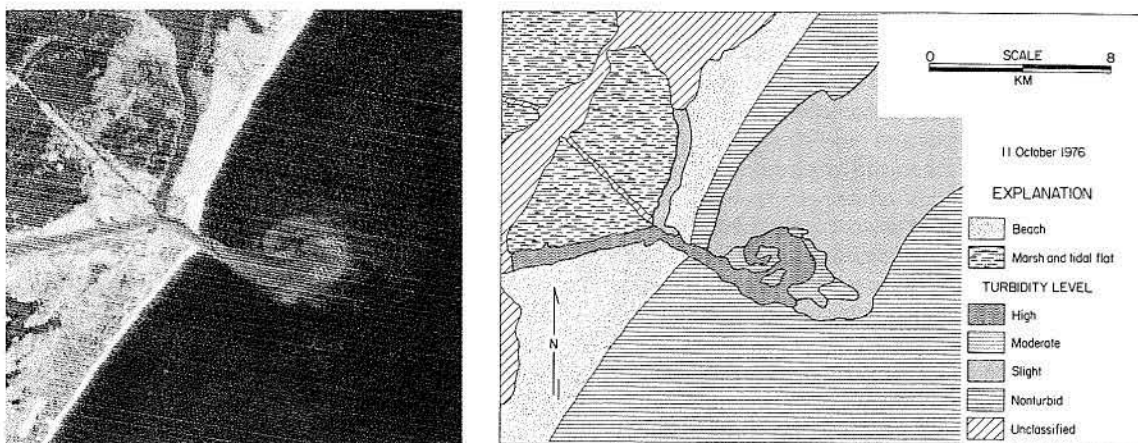


Figure 29. Band 5 imagery and interpretation of turbidity plume, Aransas Pass, Texas, October 11, 1976, Landsat scene no. 2628-16102.

Numerous authors cited in appendix C have used this capability to provide a synoptic look at circulation patterns and have often calibrated the observed turbidity with simultaneous sampling for actual suspended-sediment concentrations.

Finley and Baumgardner (1977) related turbidity concentrations, seen as varying shades of gray on band 5 images of the Aransas Pass area, to the wind and tidal conditions before and during the time of the image. On band 5 data, (fig. 29) the lightest gray correlates with the greatest amounts of suspended material, while relatively clear water appears black.

### WETLAND

Tonal variation on Landsat image products suggests that marshes can be divided into two categories which appear to differ primarily in water content and in reflectivity of the vegetation. Other investigators (Erb, 1974), using computer classification of Landsat digital data, have found a transition between the reflectivity of low, wet marsh areas and higher, drier zones which is related to the percentage of open water and soil-moisture variations rather than to changes in vegetation type. These same factors play a role in optical-image interpretation.

The two marsh categories described do not correlate with a particular assemblage of species throughout the Texas coastal region. Plant species are listed only as examples of those found within the areas illustrated in plate 1. Field checking has shown that localized variation in floral assemblages can be substantial, especially where river influx creates a fresh- to brackish-water environment or where tidal inlets admit water of full marine salinity.

#### Topographically Low Marshes

Examples of low saline marshes are found along bay margins and the Intracoastal Waterway in the vicinity of Freeport (pl. 1A-7) and at Pass Cavallo (pl. 1C-6). Low marshes are characterized by low reflectance on Landsat imagery; color tones of very dark blue to blue black and

greenish black, tending toward a lighter blue in less densely vegetated areas or when lower water levels expose more bare substrate, are typical. Tidal creeks and ponds within the low marshes and the position of this environmental unit along bay, lagoon, and fluvial margins aid in low-marsh delineation on Landsat imagery. Although seasonal variation in reflectance seems minimal (compare pls. 1A-7 and 1B-4), the intermingling of tidal flat, submerged sea grass, and marsh environments causes difficulty in delineating the boundaries of topographically low marshes. Species typical of low marshes include *Spartina alterniflora* (smooth cordgrass) and *Batis maritima* (maritime saltwort); scattered *Avicennia germinans* (black mangrove) are also present in the Pass Cavallo marshes.

J. R. Anderson and others (1976) include mangrove in their forested wetland category. Because this species does not attain the height and density achieved in areas such as south Florida and its detectability is limited, it was not included as forested wetland in the classification of Texas coastal environments (table 3). Harbor Island (pl. 1F-7) is the only area where *Avicennia germinans* achieves sufficient density to be detected and is also the only area within which a single marsh species could be uniquely identified. The evergreen nature of mangrove, its elliptic to oblong leaves 1.5 to 3 inches (4 to 8 cm) long (Jones, 1975), and its high infrared reflectance result in a deep-red Landsat signature which is consistent throughout the year.

#### Topographically High Marshes

Topographically high marshes appear with reddish-black to dull-red tones indicating greater vegetal reflectance and less response of bare substrate and water (pl. 1A-8) than for topographically low marshes. Species that may be found within this unit, which is subject to less frequent flooding by saltwater, include *Spartina spartinae* (gulf cordgrass), *Borrichia frutescens* (sea oxeye, a shrub), and *Spartina patens* (marsh hay cordgrass). The inner boundary of the high-marsh ecosystem grades laterally into coastal prairie grassland which may be dominated by *S. spartinae*; hence, distinguishing these two environments on the basis of

Landsat imagery alone is difficult. The occurrence of a zone of intermediate infrared reflectance, positioned between low marsh and upland environments, is the best indicator of topographically high marsh, especially in coastal regions north of San Antonio Bay.

### Tidal Flats

Tidal flats are wetlands with sparse or no vegetation that occur on the bay margins of the barrier islands, adjacent to the marshes, and along the mainland margin. Because coastal environments are transitional, the interpreter must make a subjective determination as to where marshes or submerged sea-grass beds end and tidal flats begin. It appears that an area must have approximately 20-percent vegetative cover before vegetation is detected on Landsat imagery (Weisblatt, 1976 and personal communication).

Tidal flats appear light blue to bluish or brownish white (pl. 1F-8) on Landsat false-color composite images. Lighter tones are associated with drier substrates, and a speckled appearance is indicative of clumps of vegetation that are most often too small to map individually. Tide level at the time the image is obtained is the primary determinant of the extent of tidal-flat exposure. The greatest extent of tidal flats follows the northerly winds of winter storms, which lower bay water levels abnormally. During the warmer months, submerged sea grass flourishes on the shallow bay bottoms, such as adjacent to Harbor Island, thereby reducing the apparent extent of the tidal flats.

### Sea Grass and Algal Flats

Sea-grass beds are sparse on the upper Texas coast, whereas south of San Antonio Bay (fig. 26) the area of bay and lagoon bottom covered by sea grass increases greatly. On Landsat imagery these beds appear very dark blue to purplish black with gradational margins, and include lighter blue streaks where the vegetation is less dense. Among the species present within Texas bays and lagoons are *Halodule wrightii* (shoalgrass), *Ruppia maritima* (widgeongrass) and *Syringodium filiforme* (manateeegrass) (Edwards, 1976).

Among the largest sea-grass beds mapped (Finley, 1976) were those within Laguna Madre near Brazos Santiago Pass (pl. 1D-3). Sea grass also occurs along the mainland margin of the lagoon (pl. 1D-4). Within Redfish Bay a very dark greenish-blue color signifies the presence of submerged vegetation.

Algal flats occur as sediment-binding mats on the surface of extensive tidal flats. The algae flourish when the flats are inundated but become desiccated when water leaves the flats, leaving a black crust of organic material. On Landsat imagery these areas show extremely low reflectance and appear a slightly darker blue black than the sea-grass beds (pl. 1D-5). Because algal flats are found on very low gradient lagoon margins which may grade laterally into submerged vegetation, they have not been separated from sea-grass beds in the classification system of table 3. To do so would require the interpreter to attempt this distinction in all instances, and it is generally not appropriate to do so

unless field observations or supplementary data on biologic assemblages are available.

### Vegetated Dredge Spoil

Vegetated dredge spoil (pl. 1B-5) is detectable on Landsat imagery primarily because of its form and position relative to adjacent dredged channels. Linear or circular shapes are common and are sufficiently distinct to indicate that they are not natural features. The infrared reflectance of the vegetated dredged material, and hence the red tones of the imagery, is similar to that of topographically high marsh and grassland. Field checking has shown that the same plant species characteristic of these units colonize the spoil material and therefore account for this similarity. Since the presence of dredge spoil, either vegetated or barren, represents an important alteration of the coastal environment by man, the ability to detect this unit on repetitive satellite imagery is significant for Coastal Zone management purposes.

### BARREN LAND

The barren land categories included in table 3 are all high-reflectance features with the exception of low-reflectance and imprecisely identified units which have been classified as undifferentiated barren land. Several environments from within the national system (table 11) have been deleted and others expanded to reflect the emphasis on coastal environments.

### Beaches

Form, location, and the high reflectance of barren sandy substrate make beaches obvious on Landsat imagery (pl. 1E-3). The usual color is bright white; however, where the beach narrows to less than 80 m only a bright-blue tone may be evident because of the dominant signature of the adjacent water. On low-tide images the exposed wet beachface and the surf zone result in a pale-blue signature which is situated parallel to the white tone of the subaerial beach (pl. 1E-3). Under relatively high (10X) magnification, band 5 images, which were obtained coincident with low-tide conditions, reveal the multiple offshore bars that occur along the Texas coast.

### Dunes

As with beaches, a brilliant white color combined with form and location enables the interpreter to delineate major dune systems, both on the barrier islands (pl. 1E-4) and for the inland dune system (pl. 1E-5). Back-island and fore-island blowout dunes (Brown and others, 1976) can usually be discerned without supplemental data; however, the reflectance from unvegetated portions of the fore-island dune ridge and sandflats with wind-shadow dunes commonly merges with the high reflectance of beach sand. The reflectance of these barren sandy environments is so great that all internal boundaries, whether caused by dune or beach topography or by variations in moisture content, are completely masked on Landsat imagery. Large-scale migra-



tion of inland dunes (500 to 1500 ft or 152 to 457 m) can be determined by comparison of map bases generated 10 to 20 years ago with recent Landsat imagery.

#### **Barren Dredge Spoil**

As with vegetated spoil, linear to circular shapes and position adjacent to a dredged channel are keys to identification of this unit. Additionally, barren spoil has extremely high reflectance as shown by tones of white on the Landsat false-color composite (pl. 1F-9). Light-toned but intensely blue margins of spoil banks adjoining water bodies represent barely subaqueous, reworked dredged material. The exact waterline surrounding these spoil units is best determined using black-and-white band 7 imagery.

#### **Undifferentiated Barren Land**

Incorporated within this unit are miscellaneous, non-vegetated elements of land cover and land use such as transitional zones between tidal flats and aeolian sands, low-reflectance depressions filled with mud and organic matter, burned areas with sparse vegetation, and high-reflectance units of barren sandy substrate. The latter category includes areas of dredged material, industrial locations, aeolian sandflats, dunes, and tidal flats which could not be differentiated with a sufficient degree of confidence. Field checking, study of environmental geologic maps (Brown, coordinator, in preparation), or analysis of aerial photographs would be required to further classify many undifferentiated barren areas.

### **EVALUATING THE MAP PRODUCT**

Accuracy analysis of land cover and land use mapped from Landsat imagery may be accomplished by field checking, comparison with other map data, comparison with aerial photographs, or a combination of these mechanisms. Field checking may involve ground observations and/or observation from an aircraft at minimum altitudes. Within large test

sites, representative sample sites may be selected for checking, such as the 1-percent sample selected by Fitzpatrick (1975) from the 74,712 km<sup>2</sup> Central Atlantic Regional Ecological Test Site. The Landsat investigation of Texas coastal resources included an evaluation of seven 1:125,000 scale maps of land cover and land use (part 1, this volume).

### **CONCLUSIONS**

On the basis of color tone, texture, form, and position, Texas coastal environments may be classified from Landsat imagery into 23 categories of land cover and land use (table 3). This classification scheme, by expanding the category of nonforested wetlands and adding other specialized coastal units, such as dredge spoil, enables the interpreter to obtain the maximum amount of information from Landsat data. The repetitive coverage of an area of interest adds the dimension of time to the interpretive process in that seasonal changes in vegetation, the effects of wind stress on surface-water circulation, and varying tide levels may be detected.

The optical-interpretation procedure utilizes 8X enlargement of Landsat false-color composite images and an existing map base to produce land cover - land use maps at a scale of 1:125,000. Knowledge on the part of the interpreter of coastal geologic processes and biologic assemblages partly compensates for the approximately

80 m resolution and original 1:1,000,000 scale of the imagery. For the Texas coastal region, the *Environmental Geologic Atlas of the Texas Coastal Zone* series is a primary aid in Landsat image interpretation. For all areas, topographic, geologic, and any available specialty maps, such as those depicting land and water resources, should be consulted in conjunction with interpretation procedures. Indeed, J. R. Anderson and others (1972) describe the second classification level as including the use of topographic maps as a supplemental data source.

The examples presented here provide an introduction to Landsat image characteristics (table 12) as a starting point in image interpretation and map preparation. Within the context of remote sensing technology available today, the methods outlined are relatively simple, yet they allow the user to take full advantage of the repetitive multiband coverage, synoptic view, and relatively low direct-purchase cost to the user of Landsat.

### **ACKNOWLEDGMENTS**

Funds for this research were provided by the Texas General Land Office through Contract NAS5-20986 with the National Aeronautics and Space Administration. Peggy Harwood coordinated the project for the

General Land Office and Robert W. Baumgardner, Jr., served as project research assistant. The manuscript was reviewed by W. E. Galloway, W. A. White, and E. G. Wermund.

Table 12

---

Summary of characteristics for recognition of coastal land cover–land use classes from  
Landsat false-color composite imagery.

	COLOR TONE	TEXTURE (within class area)	SHAPE (of class boundaries)	ASSOCIATED FEATURES	COMMENTS
<b>URBAN AND BUILT-UP LAND</b> Industrial	white to bluish white	not distinctive	variable; often bounded by water bodies or artificial reservoirs	holding ponds, spoil mounds, roads, and dredged channels	high reflectance results from metal structures, concrete, and shell and sand fill
Extractive-hydrocarbons	pale white for cleared areas and access route, merges with surrounding area	small patches distinct from surrounding area	circular where production located over a salt dome	holding ponds, roads	generally not distinguishable unless the circular pattern of salt dome production is evident
Transportation	white to grayish white pale blue, pale red, and dark blue (dredged channels)	not distinctive	linear and reticulate pattern; spoil mounds adjoin dredged channels	other urban and built-up land categories; patches of roadside development in more built-up areas	detectability varies with road material, width, contrast with surrounding environment; narrow channels not detectable in marshes
Mixed urban	pale blue (densely developed) to dull reddish pink and white	pebbly or patchy pattern where vegetation is mixed with structures	variable, sometimes with blocky boundaries	industrial and transportation features	difficult to detect unless natural vegetation is largely displaced; supplementary information often needed
<b>AGRICULTURAL LAND</b> Cropland	with crops: deep, intense red; barren field: gray to black where muddy, becoming lighter with increasing sand content	uniform within a field, but with field-by-field variations due to soil moisture or crop maturity differences	regular geometric boundaries	roads along field boundaries	comparison of summer and winter imagery aids mapping of croplands
<b>GRASSLAND/ RANGELAND</b> Range-pasture	dull red, brownish red to reddish pink	finely divided pattern of patches and irregular blocks of color where unimproved; uniform texture where improved	variable	includes relatively large areas surrounding other land units	season and variations in plant growth strongly affect color tone and intensity
Vegetated dunes	red, brownish red to blackish red; darker in swales	not distinctive	linear pattern of dune ridges and swales is key to identification	barrier island or nearshore environment	vegetated dunes difficult to detect unless linear or arcuate pattern evident; supplementary information usually needed
Vegetated barrier flat	red, brownish red dull blackish red	uneven to patchy pattern on winter imagery; more uniform during growing season	conforms to shape of barrier island	beaches, dunes, and other barrier island environments	designation dependent on recognizing the range-pasture grassland signature in the barrier island environment
Brushland	red to brownish red, may be a more intense tone than range-pasture, but less intense than woodland	variable depending on vegetation density	variable	not distinctive	very difficult to delineate without ground or low-altitude aircraft observation; color tone merges with that of range-pasture grassland

<b>FOREST LAND</b> Woodland or dense chaparral	intense red to purplish red (during growing season); usually the purest red tone in a scene (for broadleaf trees)	very uniform	dependent on extent of the stand of trees	not distinctive	live oak easily detected on winter imagery; comparison of summer and winter imagery helpful in detecting deciduous woodland
<b>WATER</b> Nonturbid Slightly turbid Moderately turbid Highly turbid/ very shallow	varies from dark navy blue to light whitish blue or pale turquoise as turbidity increases; very shallow water has the lightest blue tone	relatively uniform within a single turbidity category, otherwise streaky	distribution of turbid water is indicative of surface- water circulation patterns	not distinctive; holding ponds at industrial loca- tions may have unique coloration, especially yellowish green if iron oxides are present	precise shorelines are difficult to determine over tidal flats
<b>WETLAND</b> Topographically low marsh	dark blue, blue black and greenish black with minor amounts of red; lighter blue where more bare substrate exposed	uneven to slightly patchy on a fine scale due to plant-density variations	related to shoreline or water-body configuration	bay and lagoon shoreline, tidal flats, tidal creeks, and streams	mangroves have an intense red signature if present in sufficient numbers (see text for typical plant species)
Topographically high marsh	reddish black to dull red with less dark tones than the topographically low marsh	uniform to uneven due to plant-density variations	related to shoreline or water-body configuration	bay and lagoon shorelines, tidal creeks and streams, topographically low marsh, range-pasture grassland	boundaries with adjacent grassland or low marsh are often indistinct because of gradation of environments
Tidal flat	light blue to bluish or brownish impure white	uneven to patchy due to varying water content and small amounts of vegetation	related to bay or lagoon shoreline configuration and tide level at image time	marshes, sea grass, and algal flats; other bay margin environments	tide level and wind condi- tions at image time influence extent of exposed flat
Sea grasses and algal flats	sea grass appears dark blue to purplish black; algal flats appear relatively darker blue black	uniform where vegetation is dense with enclosed or marginal areas of lighter tone	often elongate parallel to lagoon margin or area of greatest depth	within or adjacent to bay and lagoon tidal flats and marshes	supplementary map data or field observations often needed to reliably dis- tinguish these units
Vegetated dredge spoil	similar to high marsh and grassland	variable; from uneven and patchy to uniform depend- ing on vegetation density	linear or circular shapes, often aligned parallel to a channel	dredged channels	shape is a key factor in mapping this unit
<b>BARREN LAND</b> Beaches	bright white grading to bright blue near the waterline	textural variations not detectable because of high reflectance	linear to arcuate, depend- ing on local shoreline configuration	barrier and bay shore- line environments	shell berms in bay environ- ments are included in this unit
Dunes	bright white	textural variations not detectable because of high reflectance	linear belts to elongate or arcuate groups or individuals	beach, vegetation barrier flat or range-pasture grasslands (inland dunes)	boundaries between dunes and beach and within dunes are not detectable
Dredge spoil— barren	bright white	textural variations usually not detectable because of high reflectance	linear or circular shapes often aligned parallel to a channel	dredged channels	light blue to bluish white tones indicate areas of greater water content
Undifferentiated barren land	white (sandy substrate) to gray and black (muddy sub- strates and burned areas)	variable	variable	not distinctive	includes nonvegetated areas, many of which are in above categories, but which cannot be classified further from only Landsat data



## REFERENCES

- Anderson, J. R., Hardy, E. E., and Roach, J. T., 1972, A land-use classification system for use with remote sensor data: U. S. Geological Survey Circ. 671, 16 p.
- Anderson, J. R., Hardy, E. E., Roach, J. T., and Witmer, R. E., 1976, A land use and land cover classification system for use with remote sensor data: U. S. Geol. Survey Prof. Paper 964, 18 p.
- Anderson, R. R., Alsid, L., and Carter, V., 1975a, Applicability of SKYLAB orbital photography to coastal wetland mapping: Proc. Am. Soc. Photogrammetry, 41st Ann. Mtg., p. 371-377.
- 1975b, Comparative utility of Landsat-1 and SKYLAB data for coastal wetland mapping and ecological studies, *in* Smistad and others, coord., NASA Earth Resources Survey Symposium: Houston, Johnson Space Center, NASA TM Z-58168, p. 469-478.
- Anderson, R. R., Carter, V. P., and McGinness, J. W., 1973a, Mapping northern Atlantic coastal marshlands, Maryland-Virginia, using ERTS-1 imagery, *in* Shahrokhi, F., ed., Remote sensing of earth resources: Univ. Tenn., Tullahoma, v. 2, p. 1011-1020.
- 1973b, Applications of ERTS data to coastal wetland ecology with special reference to plant community mapping and typing and impact of man, *in* Freden and others, eds., Third Earth Resources Technology Satellite Symposium, v. 2: Washington, D. C., NASA, p. 1225-1242.
- Avery, T. E., 1968, Interpretation of aerial photographs, 2d ed., Minneapolis, Minn., Burgess, 324 p.
- Bartlett, D., Klemas, V., and Rogers, R., 1975, Investigations of coastal land use and vegetation with ERTS-1 and SKYLAB-EREP: Proc. Am. Soc. Photogrammetry, 41st Ann. Mtg., p. 378-389.
- Berry, B. J., and Baker, A. M., 1968, Geographic sampling *in* Berry, B. J., and Marble, D. F., eds., Spatial analysis—A reader in statistical geography: Englewood Cliffs, N.J., Prentice-Hall, p. 91-100.
- Brown, L. F., Jr., project coordinator, in progress, Environmental geologic atlas of the Texas Coastal Zone: seven volumes, Univ. Texas, Austin, Bur. Econ. Geology.
- Brown, L. F., Jr., Brewton, J. L., Evans, T. J., McGowen, J. H., Groat, C. G., and Fisher, W. L., in preparation, Environmental geologic atlas of the Texas Coastal Zone—Brownsville - Harlingen area: Univ. Texas, Austin, Bur. Econ. Geology.
- Brown, L. F., Jr., Brewton, J. L., McGowen, J. H., Evans, T. J., Fisher, W. L., and Groat, C. G., 1976, Environmental geologic atlas of the Texas Coastal Zone—Corpus Christi area: Univ. Texas, Austin, Bur. Econ. Geology, 123 p.
- Carter, V., and Schubert, J., 1974, Coastal wetlands analysis from ERTS MSS digital data and field spectral measurements: Ann Arbor, Michigan, Proc. 9th Inter. Symp. on Remote Sensing Environ., p. 1241-1260.
- Clark, J., 1974, Coastal Ecosystems: Washington, D. C., The Conservation Foundation, 178 p.
- Clements, G., 1976, Landsat field investigation summary: Austin, Texas Parks and Wildlife Dept., unpub. report to the Texas General Land Office, 7 p. and attachments.
- Edwards, P., 1976, An illustrated guide to the seaweeds and sea grasses in the vicinity of Port Aransas, Texas: Austin, Univ. Texas Press, 128 p.
- Erb, R. B., 1974, The ERTS-1 investigation, Vol. II-ERTS-1 Coastal/estuarine analysis: Houston, Johnson Space Center, JSC-08457, 284 p.
- Finley, R. J., 1976, Interpretation of enhanced Landsat imagery for wetland and land use delineation in the Texas Coastal Zone: Gulf Coast Assoc. Geol. Soc. Trans., v. 26, p. 279-297.
- Finley, R. J., and Baumgardner, R. W., Jr., 1977, A Landsat study of nearshore circulation off Aransas Pass, Texas: (Abs.) Soc. Econ. Paleontologists and Mineralogists, 51st Annual Meeting, Washington, D. C., June 1977, AAPG Bull., v. 61, no. 5, p. 783.
- Fisher, W. L., McGowen, J. H., Brown, L. F., Jr., and Groat, C. G., 1972, Environmental geologic atlas of the Texas Coastal Zone—Galveston - Houston area: Univ. Texas, Austin, Bur. Econ. Geology, 91 p.
- Fitzpatrick, K., 1975, Cost accuracy and consistency comparisons of land use maps made from high-altitude aircraft photography and ERTS imagery: Greenbelt, Md., Goddard Space Flight Center, Final Report., v. 6, CARETS Project, 61 p.
- Jones, F. B., 1975, Flora of the Texas Coastal Bend: Sinton, Tx., Welder Wildlife Found., 262 p.
- Klemas, V., Daiber, F. C., Bartlett, D., Crichton, O. W., and Fornes, A. O., 1974, Inventory of Delaware's wetlands: Photogramm. Eng., v. 40, p. 433-439.
- McGowen, J. H., Proctor, C. V., Jr., Brown, L. F., Jr., Evans, T. J., Fisher, W. L., and Groat, C. G., 1976, Environmental geologic atlas of the Texas Coastal Zone—Port Lavaca area: Univ. Texas, Austin, Bur. Econ. Geology, 107 p.
- National Aeronautics and Space Administration, 1976, Landsat data users handbook, Doc. No. 76SDS4258: Goddard Space Flight Center, Greenbelt, Md.
- Reeves, R. G., Anson, A., and Landen, D., eds., 1975, Manual of remote sensing: Falls Church, Virginia, Am. Soc. Photogrammetry, 2144 p.
- Weisblatt, E. A., 1975, Regional applications project supporting research and technology: Johnson Space Center, Houston, LEC-6647.
- 1976, Satellite inventories of coastal zone environments (abs.), *in* Symposium on Research Techniques in Coastal Environments: Baton Rouge, Louisiana State Univ., March 18-19, 1976, p. 42.
- Wood, W. F., 1955, Use of stratified random samples in a land use study: Annals Assoc. Am. Geographers, v. 45, p. 350-376.

## APPENDIX C

### ANNOTATED BIBLIOGRAPHY ON THE APPLICATION OF AERIAL PHOTOGRAPHS AND LANDSAT IMAGERY TO THE STUDY OF COASTAL REGIONS<sup>1</sup>

Alexander, R. H., 1973, ERTS regional-scale overview linking land use and environmental processes in CARETS: Symposium, Significant Results Obtained from ERTS-1, p. 931-937.

The pattern of tones and textures of ERTS-1 images was found to correspond most closely to land use maps when compared with preexisting maps of various types for the same area.

Anderson, D. M., Gatto, L. W., McKim, H. L., and Petrone, A., 1973, Sediment distribution and coastal processes in Cook Inlet, Alaska: Symposium, Significant Results Obtained from ERTS-1, p. 1323-1339.

Bands 6 and 7 allowed determination of the coastline of Cook Inlet, and bands 4 and 5 showed the suspended sediment and current patterns in the estuary. Circulation was seen to be primarily counterclockwise. Previously unmapped tidal flats and certain cultural features were identified.

Anderson, R. R., Alsid, L., and Carter, V., 1975, Applicability of Skylab orbital photography to coastal wetland mapping: Proc. American Soc. Photogrammetry, 41st Ann. Mtg., March 9-14, 1975, p. 371-377.

Skylab S190A color-infrared photographs were enlarged to a scale of 1:125,000, allowing transparent overlays to be used in mapping wetland features directly from the imagery. The study area was divided into five mappable units: (1) fresh estuarine river marsh, (2) brackish estuarine river marsh, (3) fresh estuarine bay marsh, (4) brackish estuarine bay marsh, and (5) near-saline marsh.

Anderson, R. R., Carter, V., and McGinness, J., 1973, Applications of ERTS data to coastal wetland ecology with special reference to plant community mapping and typing and impact of man: 3d ERTS-1 Symposium, p. 1225-1242.

Imagery from ERTS-1 was shown to be useful in wetland studies for test areas in North Carolina and Georgia. The authors explain why different data-enhancement techniques were used and how each type aided the program.

Anderson, R. R., Carter, V., and McGinness, J., 1973, Mapping Atlantic coastal marshlands, Maryland, Georgia, using ERTS-1 imagery: Symposium, Significant Results Obtained from ERTS-1, p. 603-608.

Data from ERTS-1 were used as an inexpensive source of information for mapping the extensive coastal marshes of the eastern United States. This paper is a report on the feasibility of this approach. The study found that the following information could be derived from Landsat: (1) upper wetland boundary, (2) drainage pattern in wetland, (3) plant communities, (4) ditching activities associated with agriculture, and (5) lagooning for water-side housing developments.

Anderson, R. R., and Wobber, F. J., 1973, Wetlands mapping in New Jersey: Photogramm. Eng., v. 39, p. 353-358.

Color and color-infrared aerial photographs were shown to be a practical way to map or inventory wetlands. Determinable features include the mean high-water mark, the upper wetland boundary, and species associations in the area.

Barrell, E. C., and Curtis, L. F., eds., 1974, Coastal vegetation surveys, in *Environmental remote sensing: Applications and achievements*: Edward Arnold, publisher, p. 127-143.

Ecological zones in the coastal region have distinct vegetation coverage which is discernible on aerial photographs. The vegetation assemblages in six zones are discussed; these are intertidal, mudflat, salt marsh, shingle beach, sand dunes, and cliffs. The examples given are for the English coast.

Bartlett, D., Klemas, V., and Rogers, R., 1975, Investigation of coastal land use and vegetation with ERTS-1 and Skylab-EREP: Proc. American Soc. Photogrammetry, 41st Ann. Mtg., March 9-14, 1975, p. 378-389.

Machine-assisted analysis of ERTS-1 MSS scanner data was compared to manual interpretation of Skylab EREP S190B photographs to determine their usefulness in wetlands management. Skylab S190B was found to be superior in resolution but had the disadvantage of limited coverage. The authors conclude that either type of data is useful for the inventory of land cover types on a regional basis.

Bowker, D. E., Fleischer, P., Gosink, T. A., Hanna, W. J., and Ludwick, J., 1973, Correlation of ERTS multi-spectral imagery with suspended matter and chlorophyll in lower Chesapeake Bay: Symposium, Significant Results Obtained from ERTS-1, p. 1291-1297.

Data from ERTS were shown to be useful in monitoring estuarine waters for the assessment of siltation, produc-

<sup>1</sup>Two references which appear repeatedly are

(1) Symposium, Significant Results obtained from ERTS-1, referring to Freden, S. C., Mercanti, E. P., and Becker, M. A., eds., 1973a, Symposium on significant results obtained from the Earth Resources Technology Satellite-1, Vol. I, Technical presentations, Sections A and B: Washington, D. C., Goddard Space Flight Center, NASA SP-327, March 5-9, 1973, 1730 p.

(2) 3d ERTS-1 Symposium, referring to Freden, S. C., Mercanti, E. P., and Becker, M. A., eds., 1973b, Third Earth Resources Technology Satellite-1 Symposium, Vol. I, Technical presentations, Sections A and B: Washington, D. C., Goddard Space Flight Center, NASA SP-351, December 10-14, 1973, 1974 p.

tivity, and water type. Major areas of suspensate concentrations have been determined for Chesapeake Bay.

- Carter, V., and Schubert, J., 1974, Coastal wetlands analysis from ERTS MSS digital data and field spectral measurements: Ann Arbor, Michigan, Proc. 9th Internat. Symposium, Remote Sensing of Environment, p. 1241-1260.

In utilizing vegetation distribution in the coastal area to map wetlands, signature analysis of vegetation types and physical features found in the zone has been tabulated. Also, seasonal variation and its effects are discussed. The system utilized computer analysis of the digital data.

- Clark, D. K., Zaitzeff, J. B., Strees, L. V., and Glidden, W. S., 1974, Computer derived coastal water classifications via spectral signatures: Ann Arbor, Michigan, Proc. 9th Internat. Symposium, Remote Sensing of Environment, p. 1213-1239.

Data from ERTS-1 MSS were shown to be highly effective in the detection, classification, and delineation of water masses. Technical details of the processing of the color and black-and-white photographs are given, along with good definitions of terms. The enhancement and color slicing techniques used in the study are explained.

- DeBlieux, C., 1962, Photogeology in Louisiana coastal marsh and swamp: Gulf Coast Assoc. Geol. Soc., Trans., 12th Ann. Mtg., Oct. - Nov. 1962, p. 231-241.

Aerial photographs of the Louisiana coastal zone show several structural features which exhibit surface expressions. This method may be useful in the search for stratigraphic and structural traps for oil and gas.

- Denathieu, P. G., and Verger, F. H., 1973, The utilization of ERTS-1 data for the study of the French Atlantic Littoral: 3d ERTS-1 Symposium, p. 1447-1450.

The direction of transport of sediments from rivers emptying into the Atlantic Ocean along the southwest coast of France could be accurately determined using ERTS-1 data. Ocean currents and a turbidity front at a depth of about 50 m were observed.

- Dolan, R., and Vincent, L., 1973, Coastal processes: Photogramm. Eng., v. 39, p. 255-260.

High-altitude aircraft photographs were used in conjunction with ground observations to study the crescentic forms seen on long, sandy coasts. These features indicate where overwash may occur during storms.

- Dolan, R., and Vincent, L., 1973, Evaluation of land use mapping from ERTS in the shore zone of CARETS: Symposium, Significant Results Obtained from ERTS-1, p. 939-948.

Data from ERTS-1 provided a basis for land cover and land use mapping within the shore zone. Bands 4, 5, 6, and 7 are compared for their respective utility in

delineating various features. Problems in mapping are discussed for urban and built-up areas, forest areas, water, nonforested wetland, and barren land.

- El-ashry, M. R., and Wanless, H. R., 1967, Shoreline features and their changes: Photogramm. Eng., v. 33, p. 184-189.

Sequential aerial photographs are shown to be essential in understanding long-term changes in shoreline geomorphology. Through the use of sequential photographs, net changes and the rate of change can be determined.

- Estes, J. E., Thaman, R. R., and Senger, L. W., 1973, Applications of ERTS-1 satellite imagery for land use mapping and resource inventories in the central coastal region of California: 3d ERTS-1 Symposium, p. 457-490.

Data from ERTS-1 were used to construct land use, landform, drainage, and vegetation maps of central California. Kelp distribution offshore was also mapped. The appendix lists the various categories mapped from the ERTS data.

- Feinberg, E. B., Yunghans, R. S., Stitt, J., and Mairs, R. L., 1973, Impact of ERTS-1 images on management of New Jersey's coastal zone: 3d ERTS-1 Symposium, p. 497-503.

The New Jersey Department of Environmental Protection has used ERTS data to monitor and manage that State's coastal zone. Primary uses of ERTS are to: (1) detect land use changes, (2) monitor offshore waste disposal, (3) pick sites for outfalls of sewage treatment plants, and (4) allocate funds for shore protection.

- Fezer, F., 1971, Photo interpretation applied to geomorphology—A review: Photogrammetria, v. 27, n. 1, p. 1-50.

The majority of the previous literature on the use of aerial photographs in geomorphology is reviewed. Most examples (and literature subjects) are for regions outside the United States. The paper includes a section on coastal landforms (p. 21-22) and a small section on deltas (p. 20).

- Flores, L. M., Reeves, C. A., Hixon, S. B., and Paris, J. F., 1973, Unsupervised classification and areal measurement of land and water coastal features on the Texas coast: Symposium, Significant Results Obtained from ERTS-1, p. 1675-1681.

With two classification algorithms with digital ERTS data, from 17 to 30 different classes could be determined representing mixtures of water, land, and vegetation. The two areas studied were the Trinity River delta and the Galveston area.

- Fontanel, A., Guillenot, J., and Guy, M., 1973, First ERTS-1 results in southeastern France: Geology, sedimentology, pollution at sea: Symposium, Significant Results Obtained from ERTS-1, p. 1483-1511.

There are four parts to this paper: (1) Linear Trends Observed in the Western French Alps; (2) Some Results



from the Study of the Dynamic Behavior of Coastal Sedimentation in the Gulf of Lions; (3) Study of Pollution at Sea in the Western Mediterranean; and (4) Processing of ERTS Imagery.

In part 2 (p. 1492-1499), ERTS-1 data clearly showed past shorelines of the Rhone River delta and allowed them to be accurately mapped. Many of these shorelines had not been known prior to ERTS data usage. Fault control is also indicated in the area of ERTS data coverage.

Gallagher, J. L., Reimold, R. J., and Thompson, D. E., 1972. A comparison of four remote sensing media for assessing salt marsh primary productivity: Ann Arbor, Michigan, Proc. 8th Internat. Symposium, Remote Sensing of Environment, 2-6 Oct. 1972, p. 1287-1296.

Four types of imagery from fixed-wing aircraft were compared: Kodak Aerochrome Infrared, Ektachrome MS Aerographic, Kodak Infrared Aerographic, and imagery from a Bendix thermal mapper. Imagery interpretation was done with and without enhancement, and ground observation was used to evaluate results.

Grimes, B. H., and Hubbard, J. C. E., 1971, A comparison of film type and the importance of season for interpretation of coastal marshland vegetation: Photogramm. Rec., v. 7, p. 213-222.

Color aerial photographs were found to be the best film type to use in England for the determination of coastal marshland vegetation. October was found to be the best time of the year for determination of vegetation, whereas February was best for mapping topographic features. Mudflats were best seen on false-color imagery.

Guss, P., 1972, Tidelands management mapping for the coastal plains region: Washington, D. C., American Soc. Photogrammetry, Proc. Coastal Mapping Symposium, June 5-8, 1972, p. 243-262.

The author describes a pilot project conducted for the State of South Carolina to determine the feasibility of using aerial photographs to produce multipurpose maps for tidelands management. Requirements of the project are discussed as well as limitations of the data.

Heath, G. R., and Parker, H. D., 1973, Forest and range mapping in the Houston area with ERTS-1 data: Symposium, Significant Results Obtained from ERTS-1, p. 167-172.

The paper discusses procedures and results for two types of investigations using ERTS-1 data: forestry studies in which species content and condition of timber stands were determined, and a range investigation concerned with vegetation mapping in the Gulf Coastal marsh. Species of *Spartina* could be differentiated with or without computer-aided analytical techniques. The boundary between *S. patens* and *S. spartina* in the area closely coincides with the wetlands inner boundary.

Hunter, R. E., 1973, Distribution and movement of suspended sediment in the Gulf of Mexico off the Texas

coast: Symposium, Significant Results Obtained from ERTS-1, p. 1341-1348.

Sediment plumes observed on ERTS imagery differ very slightly in amount of suspended sediment. Data along the Texas coast show the extent and form of these plumes, some of which extend for many kilometers parallel to the shoreline. These plumes permit interpretation of nearshore currents.

Kevlin, R. T., 1973, Recognition of beach and nearshore depositional features of Chesapeake Bay: Symposium, Significant Results Obtained from ERTS-1, p. 1269-1274.

ERTS-1 support aircraft imagery was used to map such nearshore features as longshore bars in Chesapeake Bay. Also mapped were welded beach ridges and recurved spits.

Klemas, V., Bartlett, D., Philpot, W., Rogers, R., and Reed, L., 1974, Coastal and estuarine studies with ERTS-1 and Skylab: Remote Sensing of Environment, v. 3, p. 153-174.

The repetitive nature of the ERTS and Skylab imagery covering Delaware Bay allowed detection of changing conditions in and around the bay. Coastal vegetation, land use, current circulation, water turbidity, and ocean waste dispersion were studied. Ground observations allowed correlation of sediment concentration with reflectance on the images. The method used to determine currents from ERTS-1 data is discussed.

Klemas, V., Bartlett, D., Rogers, R., and Reed, L., 1974, Inventories of Delaware coastal vegetation and land-use utilizing digital processing of ERTS-1 imagery: Ann Arbor, Michigan, Proc. 9th Internat. Symposium, Remote Sensing of Environment, p. 1399-1410.

Computer analysis of digital ERTS-1 data produced maps of various vegetative types with accuracies of 83 to 90 percent when compared with previous, conventional vegetation maps. The investigators plan to update and refine the system until higher accuracies are attained.

Klemas, V., Daiber, F., and Bartlett, D., 1973, Identification of marsh vegetation and coastal land use in ERTS-1 imagery: Symposium, Significant Results Obtained from ERTS-1; p. 615-627.

ERTS-1 data were used in combination with high- and low-altitude aircraft coverage and ground observation to determine the accuracy of using ERTS-1 data alone to distinguish stands of vegetation. Plant communities can be discriminated, but problems were encountered owing to the resolution of the satellite data. Coverage from U-2 and RB-57 was used to map small vegetation communities and the larger stands more accurately.

Klemas, V., Otley, C. W., and Rogers, R., 1973, Monitoring coastal water properties and current circulation with ERTS-1: 3d ERTS-1 Symposium, p. 1387-1411.

Currents in Delaware Bay detectable from ERTS-1 data coincided with predicted and measured currents in the



- bay. Convergent boundaries between different water masses were detected; some exhibited convergent shear. Waste disposal distribution was mapped. Results from the ERTS study are being used to predict potential oil-slick movement and to estimate sediment transport.
- Klemas, V., Srna, R., Treasure, W., and Otley, M., 1973, Applicability of ERTS-1 imagery to the study of suspended sediment and aquatic fronts: Symposium, Significant Results Obtained from ERTS-1, p. 1275-1290.
- The ERTS images of Delaware Bay were studied and compared with ground observations and aircraft coverage. Suspended-sediment patterns and several types of aquatic interfaces, or fronts, were observed.
- Klemas, V., and others, 1974, Correlation of coastal water turbidity and current circulation with ERTS-1 and Skylab imagery: Ann Arbor, Michigan, Proc. 9th Internat. Symposium, Remote Sensing of Environment, p. 1289-1317.
- Imagery and digital tapes of ERTS-1 data, along with extensive ground observation as to the exact amount of suspended sediment in the water, gave an indication of reflectance signatures for various sediment concentrations. The study of sediment distribution has also allowed determination of circulation patterns in Delaware Bay.
- Klemas, V., and others, 1974, Inventory of Delaware's wetlands: Photogramm. Eng., v. 40, no. 4, p. 433-439.
- Enhanced RB-57 color-infrared imagery was used to map five categories in the wetlands of Delaware: (1) salt-marsh cordgrass, (2) salt-marsh hay and spikegrass, (3) reedgrass, (4) high-tide bush and sea myrtle, and (5) freshwater species in impounded areas. These units were characterized by (1) *Spartina alterniflora*, (2) *Spartina patens* and *Distichlis spicata*, (3) *Phragmites communis*, and (4) *Iva frutescens* and *Baccharis halimifolia*.
- Magoon, O. T., Berg, D. W., and Hallermeier, R. J., 1973, Application of ERTS-1 imagery in coastal studies: Symposium, Significant Results Obtained from ERTS-1, p. 1697-1698.
- Use of MSS ERTS images has permitted more accurate determination of tidal inlet configuration (as well as information on longshore transport), updating of navigation charts in uninhabited, remote areas, and the nearshore water-movement patterns. No enhancement techniques were used.
- Mairs, R. L., Wobber, F. J., Garefalo, D., and Yunghans, R., 1973, Application of ERTS-1 data to the protection and management of the New Jersey coastal environment: Symposium, Significant Results Obtained from ERTS-1, p. 629-633.
- With MSS bands 4 and 5, it was possible to detect the extent, drift, and dispersion of waste disposed in coastal waters.
- Moore, G. K., and North, G. W., 1974, Flood inundation in the southeastern United States from aircraft and satellite imagery: Ann Arbor, Michigan, Proc. 9th Internat. Symposium, Remote Sensing of Environment, p. 607-620.
- Data from ERTS-1 are useful in flood mapping if satellite passage coincides with the exact time of flooding. Otherwise, color-infrared photographs are the most useful for determining the extent of flooding in forested areas during winter months.
- Orr, D. G., and Quick, J. R., 1971, Construction materials in delta areas: Photogramm. Eng., v. 37, no. 4, p. 337-351.
- Black-and-white, color, and color-infrared aerial photographs were used to locate depositional features on the Mississippi River delta. This method is shown to be a practical way of locating new sand, gravel, and clay deposits in this area.
- Pestrong, R., 1969, Multiband photos for a tidal marsh: Photogramm. Eng., v. 35, p. 453-470.
- The author compares various wavelength-sensitive films used in aerial photography to determine their usefulness in delineating vegetation zones within tidal marshes. Ektachrome infrared was superior for vegetation-type determination, and Ektachrome color transparencies were the most useful for general interpretation.
- Pirie, D. M., and Stellar, D. D., 1973, California coastal processes study: 3d ERTS-1 Symposium, p. 1413-1446.
- Data from ERTS-1 were used to analyze nearshore currents, sediment transport, and river discharge along the California coast. Seasonal patterns in sediment transport were found to be related to current systems and coastal morphology. Sediment plumes at times extended much farther offshore than previously thought. Sediment distribution was determined by using computer enhancement of the data.
- Polcyn, F. C., and Lyzenga, D. R., 1973, Updating coastal and navigational charts using ERTS-1 data: 3d ERTS-1 Symposium, p. 1333-1346.
- Fairly accurate water depth data, up to 30 ft in the Bahamas and up to 200 m in Lake Michigan, were obtained from ERTS-1 data. Processing of original ERTS data for depth information costs approximately \$1.50 per square mile. Details of the process were not given.
- Reimold, R. J., Gallagher, J. L., and Thompson, D. E., 1972, Coastal mapping with remote sensors: Washington, D. C., Am. Soc. Photogrammetry, Proc., Coastal Mapping Symposium, p. 99-112.
- Color and color-infrared films and a Bendix Thermal Mapper were used in conjunction with biomass figures to estimate yield ( $\text{g/m}^2$ ) in a Georgia salt marsh. Results were categorized by individual marsh species.
- Short, N. M., Lowman, P. D., Jr., Freden, S. C., and Finch, W. A., Jr., 1976, Mission to Earth: Landsat views the world: Washington, D. C., NASA SP-360, 459 p.

This volume includes an introduction to Landsat and a survey of Landsat applications, followed by 400 color Landsat plates with an explanation of the features evident on each. The coverage is worldwide, and a glossary of technical terms is included.

Slaughter, T. H., 1973, Seasonal changes of littoral transport and beach width and resulting effect on protective structures: Symposium, Significant Results Obtained from ERTS-1, p. 1259-1267.

The direction of littoral transport and resulting beach width along the Maryland shoreline changes seasonally. This change makes erosion rates difficult to determine. Ground observation combined with ERTS-1 coverage points out the need for a year-long study to see a complete seasonal cycle. This would aid in protective structure design along waterfront properties, because the full potential for erosion would be shown.

Sonu, C. J., 1964, Study of shore processes with aid of aerial photogrammetry: *Photogramm. Eng.*, v. 30, p. 932-941.

Ways in which aerial photographs may be used to better understand coastal environments are discussed. A lengthy bibliography lists the majority of papers printed on the subject prior to this paper.

Stafford, D. B., and Langfelder, J., 1971, Air-photo study of coastal erosion: *Photogramm. Eng.*, v. 37, no. 6, p. 565-575.

Aerial photographs taken in successive years permit accurate determination of erosion in coastal areas. Only horizontal distances can be measured, making volumetric measurements of erosion difficult. These data are shown to be necessary for development of urban areas or industry in coastal regions.

Steller, D., Lewis, L. V., and Phillips, D. M., 1972, Southern California coastal processes as analyzed from multisensor data: Ann Arbor, Michigan, Proc. 8th Internat. Symposium, Remote Sensing of Environment, p. 983-998.

Airborne imagery was used to detect and measure suspended sediment and tracer dyes in the nearshore zone off southern California. The methods discussed were developed to study sediment transport and coastal effluent distribution in the area.

Steller, D. D., and Pirie, D. M., 1974, California nearshore processes: Ann Arbor, Michigan, Proc. 9th Internat. Symposium, Remote Sensing of Environment, p. 1261-1278.

The suspended sediment present in turbulent nearshore waters, along with the repetition of ERTS-1 data over a year-long period, have allowed the oceanic circulation patterns near the California coast to be determined.

Tuyahov, A. J., and Holz, R. K., 1973, Remote sensing of a barrier island: *Photogramm. Eng.*, v. 39, p. 177-188.

Three types of imagery are compared for their effective-

ness in determining the environments of Padre Island, Texas. Color, color-infrared, and thermal infrared are compared in delineating vegetation stands, vegetated versus nonvegetated dunes, tidal flats, and hurricane washover channels.

Williams, R. S., Jr., 1973, Coastal and submarine features on MSS imagery of southeastern Massachusetts: Comparison with conventional maps: Symposium, Significant Results Obtained from ERTS-1, p. 1413-1422.

Data from ERTS-1 provided the necessary geologic and hydrographic information to update conventional maps of coastal areas where conditions vary rapidly. The data obtained through ERTS are both accurate and relatively inexpensive and provide a constant update.

Williams, R. S., Jr., and Carter, W. D., eds., 1976, ERTS-1: A new window on our planet: U. S. Geol. Survey Prof. Paper 929, 362 p.

This volume consists of a series of short articles including numerous color illustrations on the application of Landsat imagery. Examples relating to coastal activities are in chapter 3, "Applications to Water Resources"; chapter 6, "Applications to Environmental Monitoring"; and chapter 8, "Applications to Oceanography."

Williamson, A. N., and Grabau, W. E., 1973, Sediment concentration mapping in tidal estuaries: 3d ERTS-1 Symposium, p. 1347.

Methods are discussed for the determination of the amount of suspended sediment in water and of ways ERTS data may be used to exactly locate and delineate surface-water turbidity.

Wobber, F. J., and Anderson, R. R., 1973, Simulated ERTS data for coastal management: *Photogramm. Eng.*, v. 39, p. 593-598.

Data from ERTS are shown to be potentially useful in mapping wetland boundaries, monitoring land use changes in wetlands, studying offshore currents, and in planning dredge-spoil disposal.

Wright, F. F., Sharma, G. D., and Burbank, D. C., 1973, ERTS-1 observations of sea surface circulation and sediment transport, Cook Inlet, Alaska: Symposium, Significant Results Obtained from ERTS-1, p. 1315-1322.

Suspended sediment, visible on MSS bands 4 and 5, allowed the determination of sediment and pollutant trajectories, areas of probable commercial fish concentration, and the circulation regime.

Yost, E., Hollman, R., Alexander, J., and Nuzzi, R., 1973, An interdisciplinary study of the estuarine and coastal oceanography of Block Island and adjacent New York coastal waters: 3d ERTS-1 Symposium, p. 1067.

Water samples were taken to correspond with the timing of ERTS-1 coverage. This procedure allowed reflectance to be "quantified" in terms of the amount of suspended sediment present in the water.



## GLOSSARY

The definitions included here have been adapted primarily from Reeves, Anson, and Landen, eds., (1975) to aid the reader in understanding remote sensing terminology.

**angle of elevation:** The angle of the sun above the horizon. Used here to refer specifically to the sun angle elevation at the time a Landsat image is obtained.

**azimuth:** The bearing or direction of a line usually referenced to geographic north. Used here to refer specifically to the sun's azimuth at the time a Landsat image is obtained.

**band:** A particular group of wavelengths of electromagnetic radiation. (See table 9 in text for examples.)

**electromagnetic radiation:** Energy propagated through space or through material media which include X-rays, visible light, infrared radiation, and radio waves.

**image:** The recorded presentation of the Earth's surface by optical, electro-optical, or electronic means. This term is preferred over the word photograph when a record is not made directly on film.

**infrared:** Pertaining to electromagnetic radiation with wavelengths just beyond (or longer than) the red end of the visible spectrum. The infrared wavelengths listed in table 9 for bands 6 and 7 are in the near infrared, a term emphasizing the radiation reflected by plant materials (which peaks at an intensity of 0.85 micron).

**micron:** Equivalent to micrometer and designating a length equal to 0.000001 m. A size unit used in measuring the wavelength of light. (See table 9.)

**multispectral scanner:** A remote sensing device which uses a mirror to direct incoming electromagnetic radiation to a detector for conversion into an electrical signal and, later, an image. Detectors in the ultraviolet, visible, and infrared portions are among those which may be used.

**reflectance:** The ratio of the radiant energy reflected by a body to that incident upon it. High reflectance objects appear the brightest on Landsat imagery.

**remote sensing:** The measurement or acquisition of information on some property of an object or the Earth's surface by a recording device not in contact with the object or surface under study.

**resolution:** The ability of an entire remote sensing system to render a sharply defined image. Sometimes given as the size of the smallest area from which electromagnetic radiation is being recorded at any one instant.

**scene:** With respect to Landsat data, each scene corresponds to area framed on the Earth's surface, for which an image is available in each of several spectral bands.

**signature:** Any characteristic or series of characteristics by which a material may be recognized. Used in the sense of all tonal and textural characteristics by which land cover and land use classes may be discriminated.

**spectrum:** A series of energies arranged according to wavelength, such as the visible spectrum which includes (from shorter to longer wavelengths) violet, indigo, blue, green, yellow, and red light.

**texture:** The frequency of change and arrangement of tones in a photograph or image. Some descriptive adjectives for texture are fine, medium, coarse, stippled or mottled.

**tonal response:** A particular shade or tint of color observed on an image or photograph which is correlated with a particular Earth material.



